Feasibility Study of Using PDMS as an Alternate Transmittance Cell Kit in an FTIR

Spectrometer

Harish Krishnan

A Thesis

In

The Department

of

Mechanical and Industrial Engineering

Presented in Partial Fulfillment of the Requirements

For the Degree of Master of Applied Science (Mechanical Engineering) at

Concordia University

Montreal, Quebec, Canada

April 2012

CONCORDIA UNIVERSITY

SCHOOL OF GRADUATE STUDIES

This is to certify that the Thesis prepared,

By: **Harish Krishnan**

Entitled: **"Feasibility Study of Using PDMS as an Alternate Transmittance Cell Kit in an FTIR Spectrometer"**

and submitted in partial fulfillment of the requirements for the Degree of

        Master of Applied Science (Mechanical Engineering)

complies with the regulations of this University and meets the accepted standards with respect to originality and quality.

Signed by the Final Examining Committee:

_____ Chair
Dr. C-Y. Su

_____ Examiner
Dr. M. Packirisamy

_____ Examiner
Dr. M. Z. Kabir   External

_____ Supervisor
Dr. S. Narayanswamy

Approved by: _____
Dr. A.K.W. Ahmed, MASc Program Director
Department of Mechanical and Industrial Engineering

_____
Dean Robin Drew
Faculty of Engineering & Computer Science

Date: _____

ABSTRACT

Feasibility Study of Using PDMS as an Alternate Transmittance Cell Kit in an FTIR Spectrometer

Harish Krishnan

Polydimethylsiloxane (PDMS) based microdevices have bought revolutionary change in the chemical analysis. Suitable mechanical properties of PDMS make it amenable for soft lithography and certain optical properties like transparency in Near InfraRed (NIR) make it a yet unexplored option for use as a window material in Fourier Transform InfraRed (FTIR) Spectrometers. In our work, we investigate the utility of PDMS as a transmittance cell kit in FTIR Spectrometer replacing the CaF_2 windows that are currently in use.

In this work, the spectral characteristics of PDMS in NIR and MIR have been thoroughly investigated. A set of design parameters were extracted through experiments and a preliminary design for a PDMS based cell kit has been suggested. PDMS Cell kit was fabricated using a SU-8 coated silicon wafer mold using soft lithography. Experiments by varying the base to curing agent ratio of PDMS pre polymer as well as selected heat treatment protocols were conducted, to improve the transmittance of PDMS in the MIR region. Due to the variation in base transmittances of PDMS across different samples and also due to inherent variations introduced by the FTIR spectrometer, there has not been an appreciable change in the optical characteristics of PDMS.

Further, to prove the utility of PDMS as a window material in the NIR region, Samples of Extra Virgin Olive Oil (EVOO) were analyzed with the PDMS cell kit and the results

were compared with the spectral analysis on same samples with a CaF_2 kit. Even though PDMS does introduce its own artifacts, if a critical sample volume is used for the analysis, the performance of the PDMS kit is comparable to that of CaF_2 cell kit. This volume which is dependent on the ratio of the thickness of a particular sample to that of the PDMS slabs, and the Critical Volume Ratio (CVR) of EVOO have been identified through this work. Once the CVR for a particular test sample is known, a PDMS based cell kit can effectively replace a CaF_2 kit and hence will prove as a less expensive option. This opens up multiple opportunities for enabling low cost and rapid liquid sample analyses using PDMS based microfluidic devices directly as window material in an FTIR spectrometer.

ACKNOWLEDGEMENTS

Last but not the least, I bow to God Almighty for arranging everything and keeping me in company of good people and being merciful and kind although I am the most undeserving.

"Therefore, Arjuna, you should always think of Me in the form of Kṛṣṇa and at the same time continue your prescribed duty of fighting. With your activities dedicated to Me and your mind and intelligence fixed on Me, you will attain Me without doubt."

Bhagavad Gita 8.7

TABLE OF CONTENTS

LIST OF FIGURES

LIST OF TABLES

LIST OF ABBREVIATIONS

ANN	Artificial Neural Networks
A.U	Absorbance Units
BaF_2	Barium Fluoride
Bio MEMS	Bio Micro Electro Mechanical System
BHK-21	Baby Hamster Kidney Cells-21
BT-20	Breast Cancer Cells-20
CaF_2	Calcium Fluoride
CMOS	Complementary Symmetry Metal Oxide Semiconductor
CVR	Critical Volume Ratio
DAQ	Data Acquisition
DIW	De Ionized Water
DTGS	Deuterated TriGlycine Sulphate
dpi	dots per inch
EVOO	Extra Virgin Olive Oil
FBS	Fetal Bovine Serum
FTIR	Fourier Transform Infra Red
FT-NIR	Fourier Transform Infra Red- Near Infra Red
FT-MIR	Fourier Transform Infra Red- Mid Infra Red
GC	Gas Chromatography
Ge	Germanium
HCA	Hierarchical Cluster Analysis
HF	Hydrogen Fluoride

HPLC	High Performance Liquid Chromatography
He Ne	Helium Neon
IR	InfraRed
KBr	Potassium Bromide
KRS-5	Thallium bromoiodide
LED	Light Emitting Diode
LDA	Linear Discriminate Analysis
$LiTaO_3$	Lithium Tantalite
Mid IR, MIR	Mid Infra Red
MCT	Mercury Cadmium Telluride
mW	milliWatt
NaCl	Sodium Chloride
Near IR, NIR	Near Infra Red
NIST	National Institute of Standards and Technology
NMR	Nuclear Magnetic Resonance
PEB	Post Exposure baking
PCA	Principal Component Analysis
PDMS	Poly-Di-Methyl-Siloxane
PLS	Partial Least Square
RPMI	Roswell Park Memorial Institute
RMS	Root Mean Square
SNR	Signal to Noise Ratio
ZnSe	Zinc Selenide

CHAPTER 1.   INTRODUCTION

Various methods are used in analytical chemistry for the qualitative as well as quantitative analysis of chemical species. Spectrometric techniques which involve the emission or absorption of electromagnetic radiation over a range of wavelengths are widely used for enabling qualitative as well as quantitative analysis. Qualitative analysis reveals information only about the presence or absence of a chemical in question without estimating its concentration.

1.1   Introduction to Spectroscopy

Spectroscopy is the study of interaction of light with matter and Infrared spectroscopy in turn, is the study of interaction of infrared light with matter [1]. Infrared is the light radiation falling in the range of 14000 cm^{-1} (714 nm) to 100 cm^{-1} (0.1cm) wave number (wavelength) where wave number = 1/wavelength (Figure 1.1) [2]. The basis for infrared spectrometry is that molecular absorption of infrared radiation, causes vibration of the chemical bonds and the resultant spectrum can be used to identify a chemical species. Different chemical species leave characteristic signature on the spectrum because of their unique vibration pattern, which in turn can be used for the qualitative and quantitative analysis(3-5). The region from 4cm^{-1} (0.25 cm)to 400 cm^{-1} (25μm)is called the *far infrared*, the region between 400 cm^{-1}(25μm) to 4000 cm^{-1}(250 μm) is called the *mid infrared* and the region between 4000 cm^{-1}(250 μm) to 14,000 cm^{-1}(714 nm) is the *near infrared region.* The region between 14,000 cm^{-1} (714 nm) and 40,000 cm^{-1} (250nm) is referred to as UV-Vis, which encompasses the Ultraviolet and Visible region.
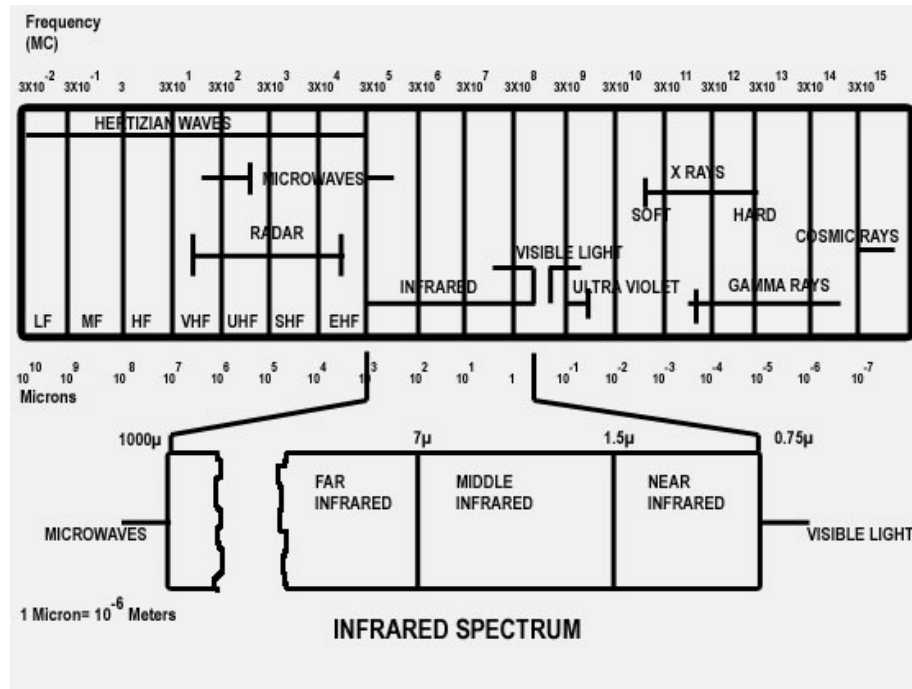
Figure 1.1 The Infrared spectrum [2]

Far infrared radiation absorbencies are low in energy and are therefore limited in use. *Mid infrared* absorbencies are of a higher energy compared to the *far infrared* radiation, as proved by experiments. As *mid infrared* absorbencies are intense, a wide range of molecules including solids, liquids, gases, polymers and semi solids can give a usable *mid infrared* spectrum. A notable drawback of the process is that sometimes the sample may absorb all the radiation falling on it making it difficult to obtain a spectrum. This is called the thickness problem and in order to avoid this difficulty care has to be exercised in estimating the proper concentration and thickness of the sample [3]. More details about this would be discussed in the second chapter of this work.

The *near infrared* radiation causes the sample to vibrate at an even higher energy compared to the *mid infrared* region [6]. But the absorbencies are 10-100 times weaker than the *mid infrared* absorbencies. But because of the absence of the thickness problem as in the previous case, there has been a tremendous growth in the quantitative

2

applications of *near infrared* spectroscopy with the advent of high performance spectrometers. Further details are discussed in Section 1.3

1.2   Fourier Transform InfraRed Spectroscopy

Fourier Transform InfraRed (FTIR) spectroscopy uses a Fourier Transform to convert raw data produced by the spectrometer in to a spectrum which is generally a plot of the absorbance or % transmittance of the sample versus the wave number. FTIR spectroscopy has proven to be a versatile tool in analytical chemistry for quantitative and qualitative assessment of known and unknown chemical species. The earlier dispersive instruments were less efficient and time consuming and hence were not very popular, but with the introduction of microcomputers and interference spectroscopy, FTIR spectrometers [7], as shown in Figure 1.2 have practically proved to have advantages over the dispersive or filter methods of infrared spectrometric analysis and hence become a fixture in laboratories [3].
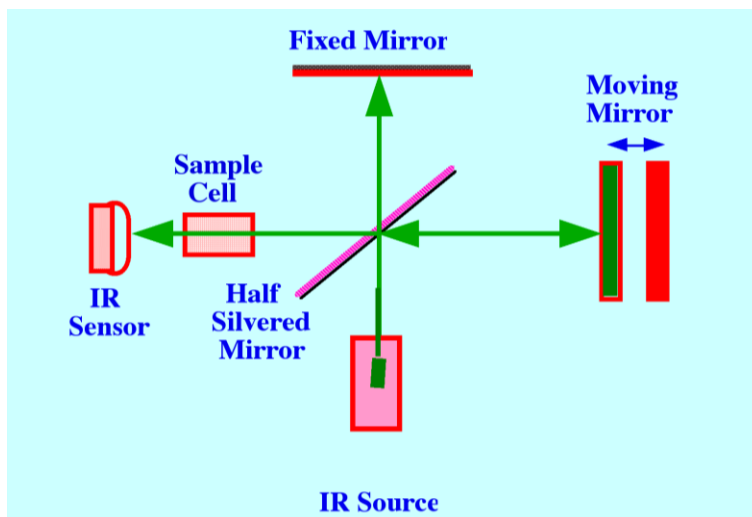
Figure 1.2 The general layout of an FTIR spectrometer [3]

Many studies on the applications of FTIR spectroscopy have been reported in the literature. Traditionally, FTIR spectrometers have been Mid IR spectrometers, but more recently NIR spectrometers have been widely used for analysis. The published literature carry wide ranging information on different analyses carried out, and in this work, focus has been on applications in the food processing industry as well as biological sample analysis.

NIR spectroscopy plays a key role in the analysis of product quality and authenticity in the olive oil industry of which details are discussed in the section 1.3.3. Advancement in analysis protocols and chemo metric data treatment methodologies have enabled rapid analysis of desired parameters which has helped in understanding quality and detecting adulterants in Olive oil. On the other hand, MIR spectroscopy is being increasingly used in biological sample analysis, of which details are provided in section 1.4. In continuation with these discussions, details of experiments conducted to understand cell proliferation by analyzing cell growth medium, which are being currently carried out in our group are provided. In order to provide consistent results, some modifications of the current FTIR transmittance cell kit accessories are necessary, which could be enabled by a PDMS based micro device. Published work in PDMS based Bio MEMS devices have been studied and it is concluded that fabricating a PDMS device could enable a low cost and rapid micro volume analysis in a FTIR spectrometer . However, to the best of our knowledge IR transmittance of PDMS and the effectiveness of PDMS as an IR analysis window in an FTIR set up have not been studied yet. The motivation for the current work is derived from the potential applications of a PDMS based micro device to replace the

transmittance cell kits made from alkaline halides. This could bring a drastic reduction in the cost of the accessories as well as speed up the spectrometric analyses.

1.3   Applications of NIR spectroscopy

NIR spectroscopy has been reported widely in literature but most of the applications can be classified mainly in to three groups, industrial chemicals, pharmaceuticals and in food and agriculture industry [6].

1.3.1   Applications in Pharmaceutical and Chemical Industries

The existence of infrared radiation was discovered by Herschel in the 1800's following which the first infrared spectra were recorded by Abney and Festing in 1881[6].Following this several applications were reported throughout the 19th and 20th century. However, with the advent of NMR spectroscopy in 1950's, the growth of applications stagnated for a while, only to grow after the advent of NIR reflection instrumentation and data treatment protocols. Now NIR spectroscopy is being widely used for process control applications, rapid laboratory measurements and real-time online analyses Applications in Pharmaceuticals [8, 9] and in chemical industries [10-16] have been widely reported.

1.3.2   Applications in Food and Agriculture Industry

Karl Norris [6] is generally regarded as the pioneer in applications for NIR in the food and Agriculture Industry. Norris et al reported their first results in 1962, which was the determination of moisture in methanol extracts of seeds. Initially the applications were focused on estimating the moisture content in grain products as the economic value of these products were dependent on the dry weight as well as protein content[17].

5

Gradually, applications have been reported in processed foods such as meat and dairy products etc. [18-25].

1.3.3 *Applications of NIR in Olive Oil industry*

The applications of NIR spectroscopy in the Olive oil Industry [26-29] can be summarized as in the figure 1.4 from the work of S. Armenta *et. al.* [30]. NIR spectrometry proves as a useful tool in (a) Fruit Reception section for initial characterization (b) paste preparation process (c) analysis of the olive oil pomace and (d) Olive oil characterization. With the combination of NIR spectrometry and chemo metric data characterization methods accurate estimation of the fatty acid and moisture content of the olive oil specimen can be achieved. In the literature, different chemo metric data treatment methods like PLS, HCA, PCA, Artificial neural network , multivariate analysis have been used in the to estimate the oil content, moisture and fat content as well as composition and estimation oleic and linoleic acids. Many methodologies like reflectance and transmittance spectroscopy [31] exist to carry out the analysis, however the methods by which the liquid sample has been physically carried on to the instrument where the sample is studied with the help of a transmittance kit has been the focus of the literature review.
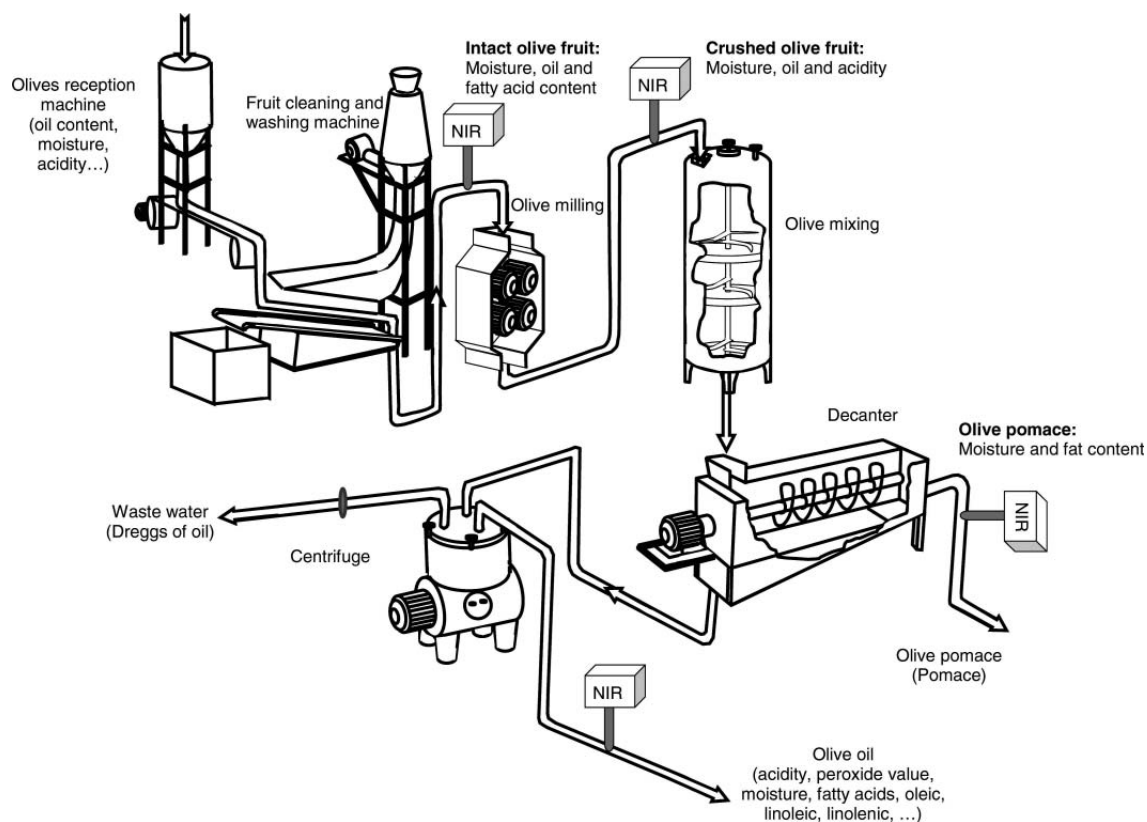
Figure 1.3: Different applications of NIR spectroscopy in Olive Oil Industry [30]

In analyzing the olive oil liquid samples, mostly approaches exist to enable classification of origin of the sample, authentication of the sample as well as locating the adulterants in the sample. Based on these requirements, a suitable spectroscopic as well as chemo metric treatment protocol is suggested. There is published work both in NIR as well as in MIR spectroscopy to understand the authenticity of Olive Oil.

Lerma Garcia *et. al.* [32] studied the origin classification and authenticity of olive oil by using the normalized absorbance peaks of their samples as predictors for the LDA (Linear discriminate analysis) data treatment method. The characteristic peaks of Extra Virgin Olive Oil (EVOO) have been considered along with the normalized absorbencies of the adulterants in the MIR region. This analysis was enabled by a 2µl sample in a

FTIR spectrometer pointing in the direction of micro volume analysis. Irudayaraj and Yang [33] studied the effectiveness of FTIR, FTNIR and FT-Raman spectroscopy for discriminate analysis of ten different olive oil samples. The analyses have proved these methods to be rapid and efficient in EVOO classification and authenticity experiments. FTIR has been found more suitable in the qualitative analysis of EVOO because of its strong absorbencies, while FTNIR has been found effective in quantitative analysis.

Ismail Kavdir *et. al.* [31] have worked on the comparison of using reflectance as well as transmittance spectroscopy as a tool in qualitative and quantitative analysis of the EVOO samples. The reflectance methods were used in the region of 750-2500 nm and the transmittance methods were used in the 800-1725 nm range and both of them were found to be effective methods in the external and internal quality measurements of EVOO. Galtier *et. al.* [34]have used a combination of NIR spectroscopy, referenced in figure 1.4, and PLS chemo metric data treatments to study the geographic origins and composition of virgin olive oil which proved to be more efficient than conventional time consuming methods like Gas Chromatography(GC) and High Performance Liquid Chromatography(HPLC). S Armenta *et. al.* [26] have developed a new chemo metric data treatment protocol using PLS method to accurately determine the olive oil parameters and identification of adulterants, (Figure 1.5). Sinelli *et. al.* [29] have used a combination of chemo metric data treatment in combination with NIR and MIR spectroscopy to classify EVOO based on fruity attribute intensity.
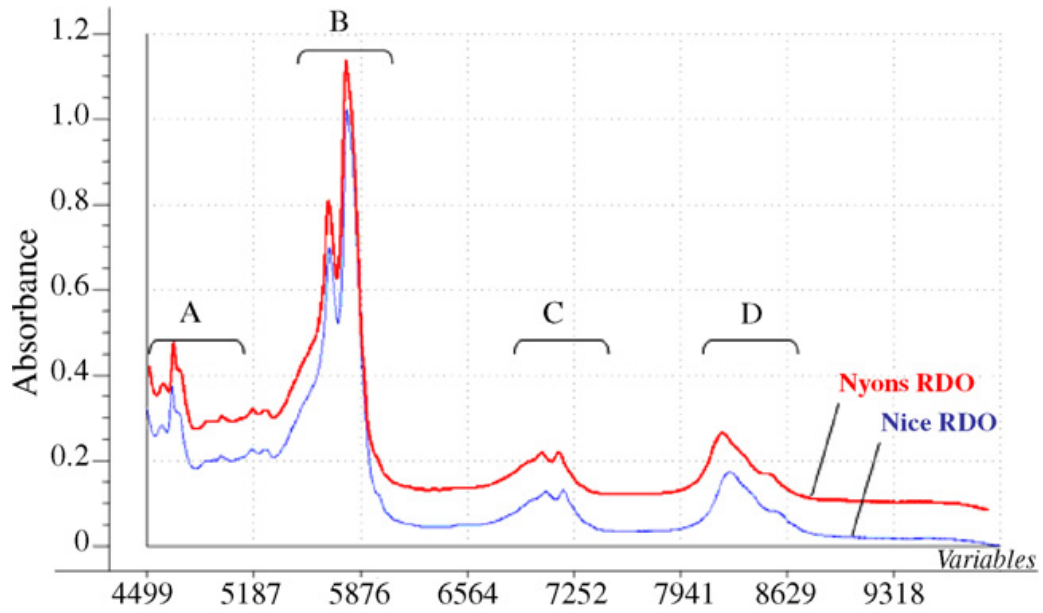
Figure 1.5 Analysis of EVOO based on its Geographic Origin [34]
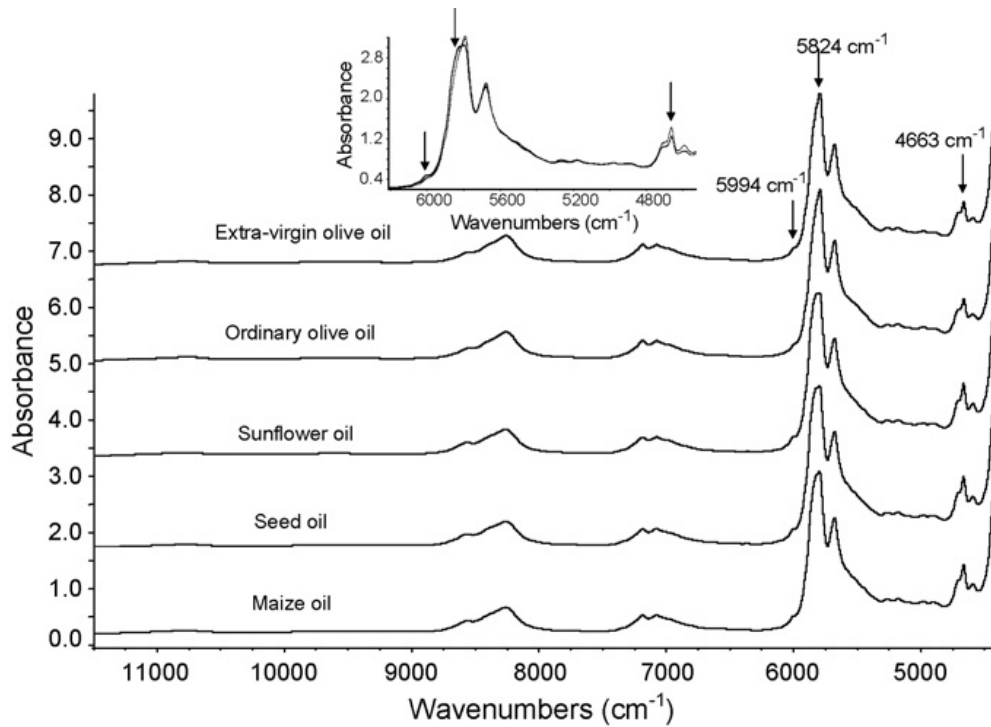
Figure 1.4 Identification of Adulterants in EVOO [26]

Somaporn Kasemsumron *et. al.* [35] have used a combination of PLS and NIR spectroscopy to identify about 280 adulterants in the olive oil in 12,000 cm^{-1} to 4500 cm^{-1} region. Three different fatty acid groups, saturated, monounsaturated and poly unsaturated present in most of the oils were classified and identified based on the spectral information in the NIR region as shown in figure 1.6.

Overall, NIR spectroscopy has proven to be a very rapid and cost effective method in the Olive oil industry for qualitative and quantitative analysis and further a PDMS based micro device would certainly help in reducing the overall time and cost of analysis.
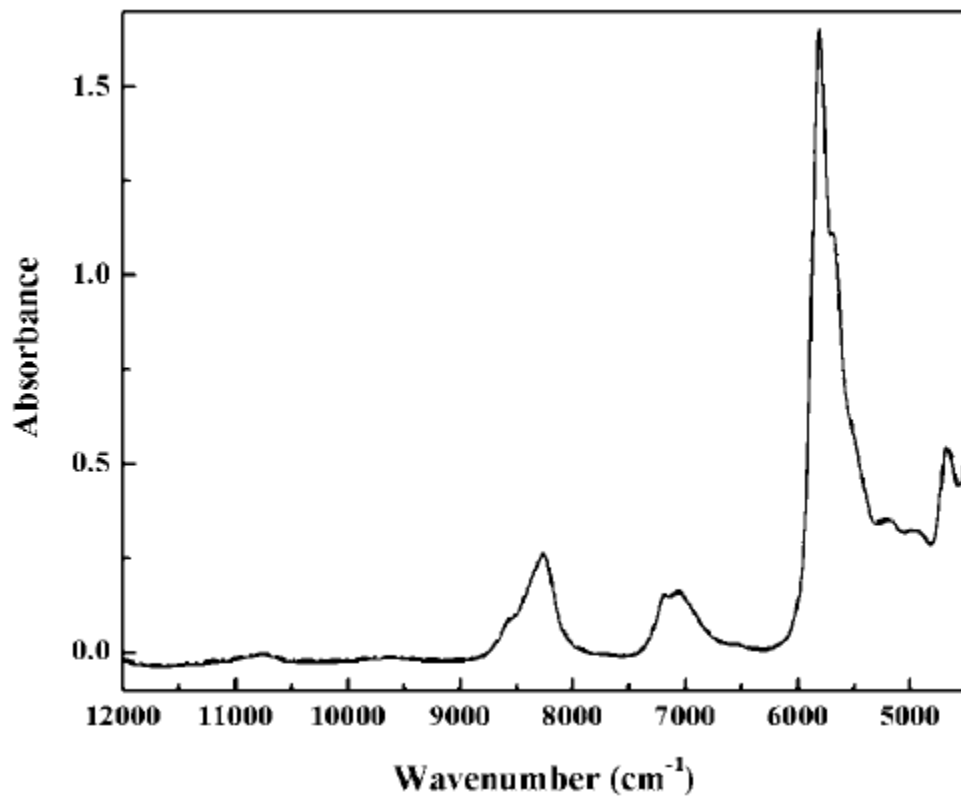
Figure 1.6 FT-NIR Spectrum for Identifying Adulterants in EVOO [35]

1.4 Applications of MIR Spectroscopy

MIR spectroscopy has been reported widely in literature but most of the applications can be classified mainly in biomedical industries primarily because of the sensitivity of Mid IR radiation to biological specimens [36]. The review of literature pertaining to applications in medical diagnostics and in cellular characterization is discussed briefly in the following sections.

1.4.1 Mid IR in Medical Diagnostics

FTIR spectroscopy has proved to be a very effective tool in medical diagnostics including cancer detection. Bayden *et. al.* [37] have demonstrated the use of FT-MIR spectroscopy in combination with PCA analysis for the study of exfoliated cervical cancer cells as shown in figure 1.7.
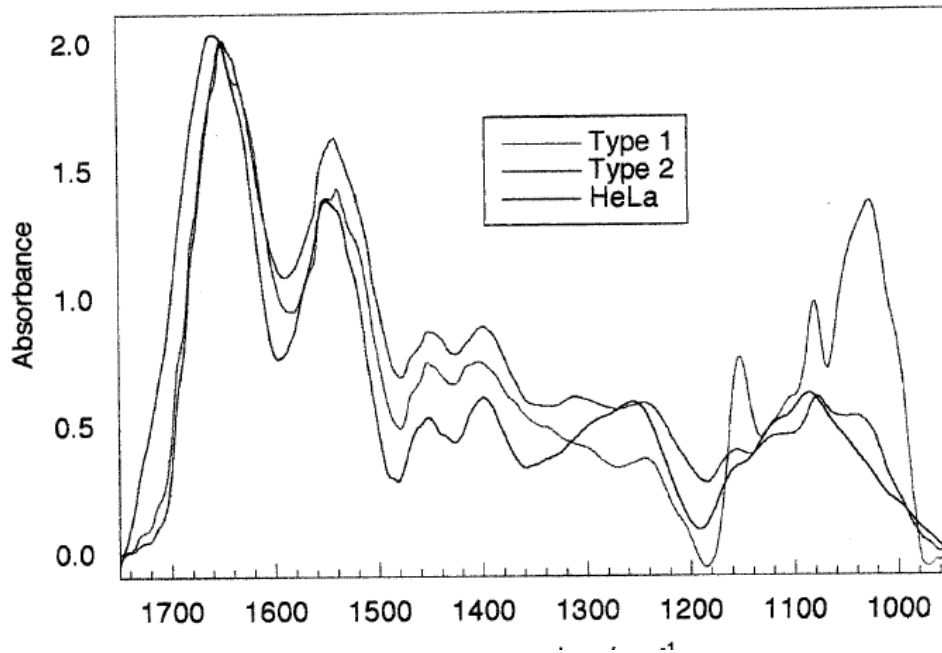
Figure 1.7 FT-MIR Spectroscopy for Cancer Detection [37]

Parvez *et. al.* [38] have demonstrated the application of FTIR spectroscopy in structural characterization of protein molecules in aqueous and non-aqueous media which is shown in figure 1.8. Mariey *et. al.* [39] have reviewed the applications of FTIR spectroscopy in combination with PCA discriminate analysis, HCA and ANN chemo metric analysis methods to identify and classify microorganisms. Schmitt *et. al.* [40] have used FTIR in combination with ANN to detect scrapie infection from blood serum.

Overall, significant amount of applications of MIR spectroscopy in bio fluid analysis
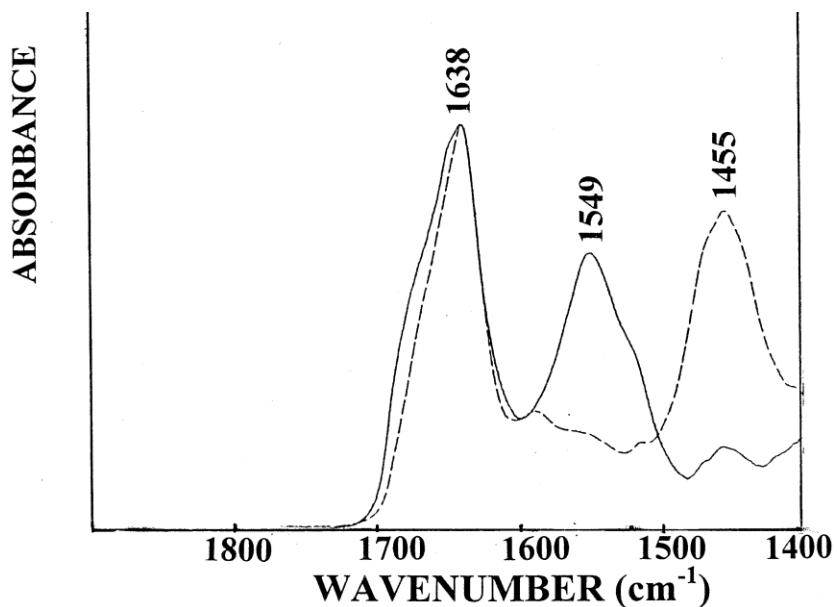
Figure 1.8 FTIR spectroscopy in structural characterization of protein molecules [38]

have been reported in the literature. Work in this direction, currently underway in our group is briefly summarized in the next section.

1.4.2 Mid IR in Bio Fluid Characterization

Fabian *et. al.* [41] have demonstrated the use of FT-MIR spectroscopy and chemo metric data analysis methods for understanding the contents of biofluids in aqueous media.

Current experiments within our group have used HeLa Cells as well as BT20, BT20-E6/E7 cells for proliferation assessment [42]. The Cells were cultured in RPMI-1640 medium (Gibco, Grand Island, NY) supplemented with 5% FBS (Fetal Bovine Serum). Cells were grown either as Cluster of 1 million cells or 500 thousand cells in 100 ml dishes with 6 ml growth medium and 2 ml growth medium respectively and then were incubated for 37ºC in 5 % CO_2 in traditional incubator. From the culture wells, the sample, in this case the cellular medium was drawn and analyzed in the FTIR spectrometer with a CaF_2 window. The results for BT20 (breast cancer cell line) is shown in figure 1.9, and HeLa (Human Melanoma cell line) in figure 1.10.
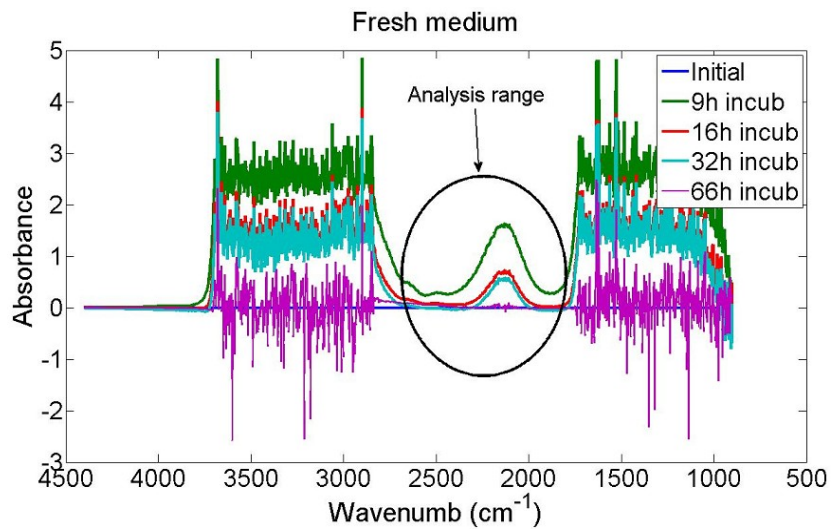
Figure 1.9: Absorbance spectrum for BT20 cells after different exposure times [42]
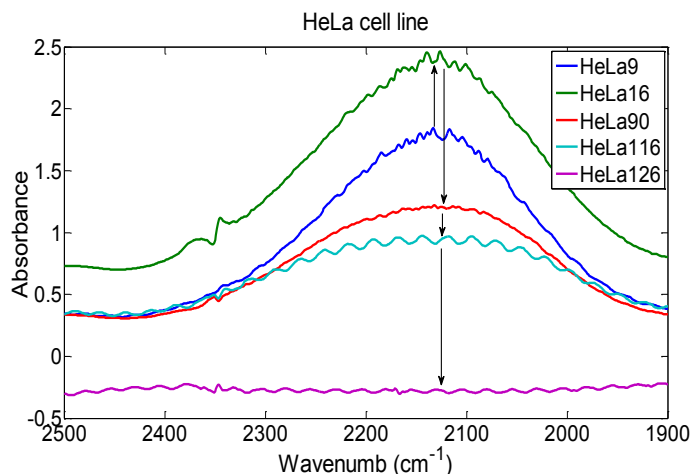
Figure 1.10: Region of Interest of absorbance spectrum- HeLa Cells [42]

However in the present analysis it can be noted that invariably statistical variance has been introduced due to the fact that growth medium for analyses at different time intervals are drawn from different culture wells. The Cell kit in its present form is also not amenable for real time spectral analysis of the growth medium as the cells cannot be cultured in the kit nor can the kit be placed in a traditional incubator. In order to counter this present challenge, a device has to be designed which is amenable to the requirements of the said IR analysis. Considering the facts mentioned above, and the fact that PDMS based Bio MEMS devices are being used in the last few years, a PDMS based FTIR spectrometer analysis window is proposed in this work; and the following section briefly reviews the state of the art in the area of PDMS based bio micro devices.

1.5   Use of PDMS in Bio MEMS systems

PDMS based Bio MEMS devices have proven to be a revolutionary development resulting out of the integration of Micro systems technology and biomedical science [43-48]. The resulting application areas in the Bio MEMS industry can be briefed as in the

14

figure 1.11[43]. Bio MEMS devices which use optical detection methods for different applications can be broadly termed as Optical Bio MEMS systems. Optical Bio systems have generally focused on the use of fluorescence or chemiluminescence in which specific fluorescence markers which emit light at specific wavelengths and initiated by a chemical reaction.
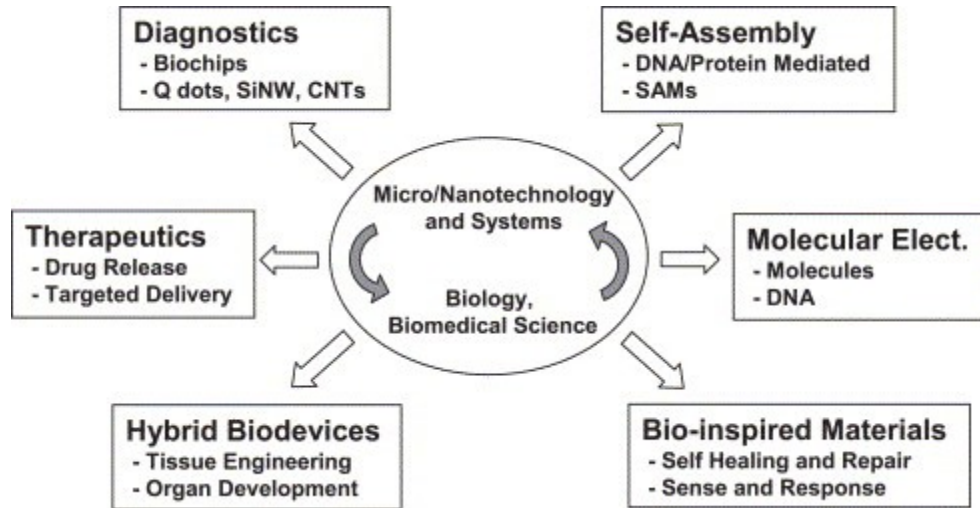
Figure 1.11 Integration of Micro technology to Biomedical Sciences – Applications [43]

Changchun Liu [49] has discussed a novel PDMS- CMOS integrated device which uses a blue LED based optical detection method for amino acid detection. A landmark in advancement in cell culture technique was the integration of CMOS technology used in the electronics industry with PDMS soft lithography techniques to fabrication a micro incubator for standalone cell culture [50]. The traditional cell culture set up consists of a cell incubator which maintains a temperature of 37ºC, 5% CO_2 for a stable pH and 100% relative humidity for maintaining the consistency of the cell culture medium. By the integration of a silicon CMOS die for temperature control through an interface DAQ (data acquisition module), and a disposable PDMS microfluidic device, a standalone cell

incubator was fabricated to holding BHK-21 cells over a three day period in ambient environment. The micro incubator is shown in figure 1.12. The cross sectional perspective of the PDMS device is displayed in figure 1.13, which has a multilevel system which integrates the temperature control system, cell culture vessel, fluidic channels and fluidic ports for enabling fluid transport.

The design parameters have been optimized to enable optimum cell culture conditions
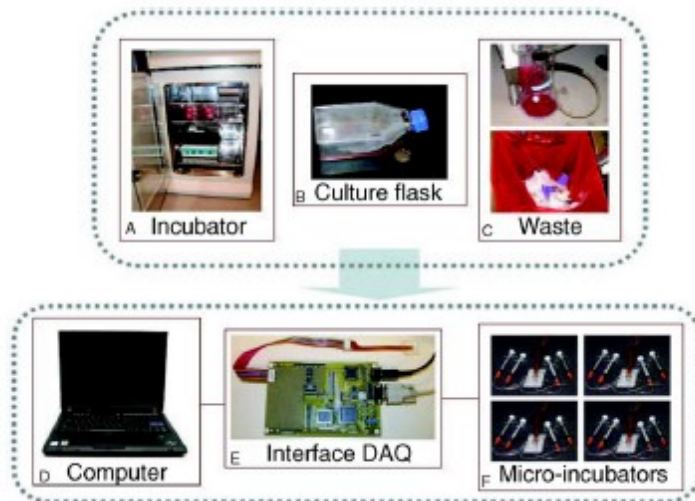
Figure 1.12: Traditional cell culture set up and the new set up created with integration of Silicon die by CMOS and diposible PDMS microfluidic device [48]

and fluid exchange for the cell culture medium as the dimensions of the cell culture well are in the range of cellular dimensions. CMOS die is connected to a computer through an interface DAQ which enables remote monitoring and control of the variables like temperature and humidity. However, with this advancement, the potential to integrate an FTIR analysis system for analyzing the cellular fluid components open up, on understanding the transmittance characteristics of PDMS.
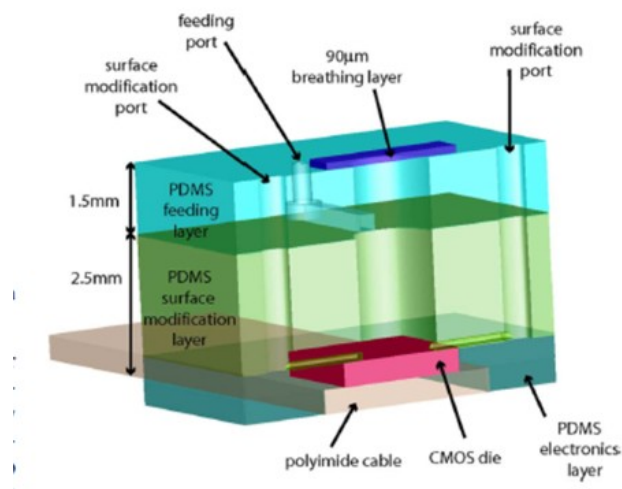
Figure 1.13: Cross sectional perspective of a micro incubator with different features [48]

1.6   Thesis Motivation

As it has been summarized from the literature review, tremendous potential exists for NIR as well as MIR spectroscopy for chemical analysis in many varied applications including industrial chemicals, food processing, pharmaceuticals, medical diagnostics and other related industries. FTIR spectroscopy for understanding the chemical composition of cell culture medium as a result of cell proliferation is in progress currently as described in section 1.4.2.

However due to the inherent limitations introduced by the Perkin Elmer™ CaF$_2$ cell kit, currently micro volume analysis of the said cell culture medium from a single well cannot be carried out at desired time intervals. As a result, currently media drawn from multiple wells are used for the chemo metric analysis which introduces unavoidable statistical variability in the results. There seems to be a pertinent need for a device which would enable real-time online analysis of cell culture media to avoid the statistical imbalance.

17

It has been established that a PDMS based micro device is successfully able to culture cells independently as a cell incubator. If a PDMS based cell kit can be fabricated it will open up new opportunities for integrating the current cell incubator with the cell kit for analyzing the cell culture medium, enabling rapid, real-time, online, non-invasive and a relatively inexpensive technique for cellular biologists and biochemists in furthering their studies.

The current work has been motivated by the potential of the above applications. Fabricating a device in this fashion is an extensive endeavor and would necessitate a multidisciplinary approach. However, understanding the suitability of PDMS as a window material to replace the currently used alkaline halide cell kits would be central to the success of the approaches in this direction.

1.7   Thesis Objective

The objective of the thesis can be defined as the *"study of the feasibility of replacing PDMS as an analysis window material instead of the current alkaline halide (CaF$_2$) cell Kit"*. In order to achieve this objective, fabrication of a PDMS based micro device to replace the current transmittance cell kit is considered. The tasks involved include

- To understand the design constraints of the proposed micro device through suitable experiments

- To arrive at the preliminary design, fabrication protocols and testing of the device

- To undertake experiments for a possible optical property enhancement of device in the Mid IR region

- To arrive at a proof of concept of the device in the Near IR region

1.8   Thesis Outline

The details of the tasks undertaken as well as the discussion of the results have been dealt with in the subsequent chapters in this thesis.

- Understanding the design constraints introduced by the material selection (PDMS) and the inherent design as well as layout of the specific spectrometer (Spectrum BX^{TM}). The results of the experiments designed to extract these constraints will eventually be used as design parameters for the desired PDMS Cell kit. (Chapter-2)

- Subsequent to identifying the design constraints, design of the device and the protocol for device fabrication were established. Further, the device was fabricated and subjected to preliminary testing. Study of the results to understand the performance of the device with respect to CaF_2 cell kit. (Chapter-3)

- In order to improve the performance of the device in the MIR region, curing agent ratio modification and heat treatment in inert atmosphere have been performed to effect a desired optical property modification of PDMS polymer. (Chapter-4)

- In order to understand the feasibility of using PDMS as a replacement window material in the NIR region, a proof of concept study with EVOO sample has been pursued. Results have been compared to understand the optical transmittance characteristics of EVOO in PDMS cell kit vis a vis a CaF_2 cell kit.(Chapter-5)

Each of the chapters in this work has been designed to revolve around the tasks described above and the results achieved. The contribution of the results to the objective has been evaluated in the conclusion section. The final chapter thoroughly summarizes the work and shows the possibilities for direction of future work.

CHAPTER 2. DESIGN CONSTRAINTS FOR ALTERNATE CELL KIT

In section 1.8, it has already been discussed that understanding the design constraints and extracting the design parameters for the alternate cell kit would be the first step in the direction of replacing the current transmittance cell kit or that which is simply referred to as cell kit further in this work, and this task would be addressed in this chapter. More details on the current cell kit are discussed in section 2.3.5.

Broadly speaking, two sets of constraints that have to be considered are a) *Constraints introduced by the choice of the material for the alternate cell kit* and b) *Constraints introduced by the instrument*. The first set of constraints are introduced because of the choice of a material which needs to have multiple attributes like being transparent in the IR range, amenable to rapid prototyping and mass production and less expensive when compared to the existing alkaline halide cell window. The second set of constraints is introduced because of the equipment specifications of the FTIR spectrometer in which the window is to be used.

In this chapter, details of the experiments designed and conducted for enabling the understanding of the above constraints have been elaborated upon. The results have been discussed and finally preliminary set of design parameters have been identified. These parameters form the input for the design of an alternate cell kit.

2.1   Choice of Material for Replacing Cell Kit Window

There are mainly two sets of constraints which have to be considered for a preliminary understanding of the design parameters of the proposed cell Kit, which will replace the existing alkaline halide kit. The required attributes for the choice of the material could be summarized as below:

a)   It has to be bio compatible for handling biological samples

b)   It has to be transparent to IR radiation

c)   It has to be relatively inexpensive and be easily available

d)   The choice of material has to be amenable to micro fabrication for analysis of micro volumes of sample.

     i.   It has to be useful in a rapid prototyping environment and the cost for fabrication per device is low once the master mold is manufactured

    ii.   It has to be disposable so the use and throw principle can be followed in order to avoid cross contamination as multiple types of samples need to be subjected to analysis

From the published literature, glass, silicon and elastomers including PDMS [51] have exhibited most of the above characteristics including biocompatibility and IR transmittance. However, after taking in to account the constraint which necessitates a material suitable for rapid prototyping, elastomers amenable to soft lithography has been considered ideal materials to achieve all the above objectives. The materials that have been used in the previous work are generally elastomers like polyurethanes, polyimides and cross linked Novolac™ resins [52]. Polydimethylsiloxane (PDMS) is considered to

be the best choice meeting all these above conditions, considering its favorable mechanical and optical properties. PDMS is a polymer which has increasingly found applications in the laboratory environment in fabricating micro devices. It is relatively inexpensive and through the process of soft lithography can be easily fabricated with desired features in the laboratory. In the following sections, the properties of PDMS are considered in detail.

2.2 Optical Properties of PDMS

2.2.1 Chemical Nature

Polydimethylsiloxane also, dimethylpolysiloxane or dimethylsilicon fluid and dimethyl silicone oil consists of a fully methylated linear siloxane polymers containing repeating units of formula $(CH_3)_2SiO$, with trimethylsiloxy end blocking units of the formula $(CH_3)_3SiO$- and the chemical structure of the polymer is shown in figure 2.1[53].
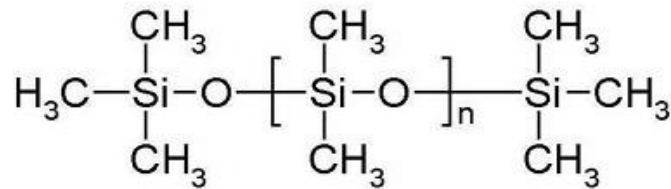
Figure 2.1 Chemical Structure of the polymer PDMS- Monomer Units [53]

It is insoluble in water and has a refractive index of 1.4 which is very close to the refractive index of the CaF_2 cell kit. It can be rendered biocompatible through plasma

treatment and can be used safely for analysis of bodily fluids. It can be also easily fabricated in the lab environment and so is a natural choice of material for the replacement of CaF_2 window. However as the bonds are covalent in nature, PDMS has strong IR absorbance in the Mid IR region. It has also certain overtone bands in the NIR region because of its artifacts in the Mid IR and so its transmittance is lesser compared to the original cell Kit. The characteristic absorptions from aliphatic CH stretching (3000-2840 cm^{-1}), methyl group bending (1375-1450 cm^{-1}), methyl group stretching at (2692 and 2872 cm^{-1}) and CH_3Si stretching at (1300-1280 cm^{-1}) and (875 -750 cm^{-1}) makes these regions opaque (54). So the useful spectral regions in PDMS are 7800- 3035, 2768-1470, 1408-1289, 958-906,745-714, and 658-523 cm^{-1}.

2.2.2   *Experiments to Understand the Transmittance Bands in PDMS*

While in the literature, studies are mostly for thin films of PDMS ranging from 50-150μm, the optical absorption characteristics of thicker samples (1-4mm), similar to the features sizes of proposed micro fabricated device need to be investigated.

A set of experiments were designed to understand the transmittance characteristics of PDMS. PDMS is generally obtained under the trade name SYLGARD 184™ (Dow corning®) in a non- cross linked from as a two-part resin and cross linker. The setting of the elastomer can be achieved by mixing the two components in a 10:1 ratio. The properties of the cured polymer are going to depend on the curing temperature, curing time and the curing agent ratio. The mechanical properties are going to depend on these parameters [55]. The optical properties are influenced by the mechanical properties and

so the curing time, curing temperature and curing agent ratio have to be carefully adjusted to get the desired optical properties.

2.2.2.1 PDMS Fabrication

SYLGARD 184™ (Dow corning®) was procured and the polymer was carefully weighed and mixed at 10:1 base: curing agent ratio. It was spread to about 4mm thick layer over a 4 in. silicon wafer and degassed to remove the gas bubbles. The PDMS fabrication assembly is arranged as in figure 2.2. The curing time and temperatures were determined
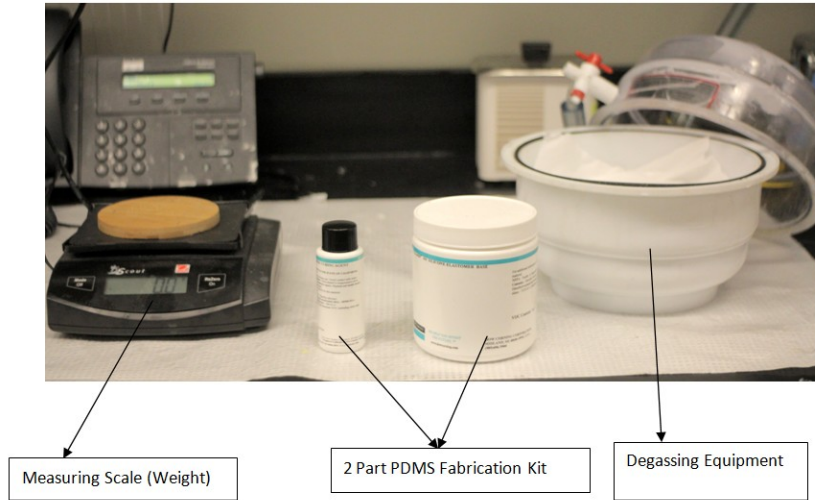
Figure 2.2: PDMS Fabrication Equipment Assembly

from table 2.1. The polymer mix was cured at a convection oven at about 60ºC for 8 hours.

Sample	Curing Temperature(º C)	Curing Period
1	25(room temperature)	48 hours
2	60	8 hours
3	100	45 min
4	125	20 min
5	150	10 min

Table 2.1: Curing time and curing temperature for PDMS

2.2.2.2 FTIR Spectrometer Examination of PDMS

A 4mm thick slab was cut out with the dimensions 38.5mm X 19.5mm X 4mm, assembled in the sample cell kit as shown in figure 2.3 and was subjected to spectral analysis totaling 8 scans @ 4 cm^{-1} resolution between 7800 cm^{-1} and 1000 cm^{-1}. The experiments were repeated three times to get conformance on the absorbance peaks The results are as shown in the figure 2.4, where PDMS shows high transmittance in the NIR region (7800 cm^{-1} to 4500 cm^{-1}).
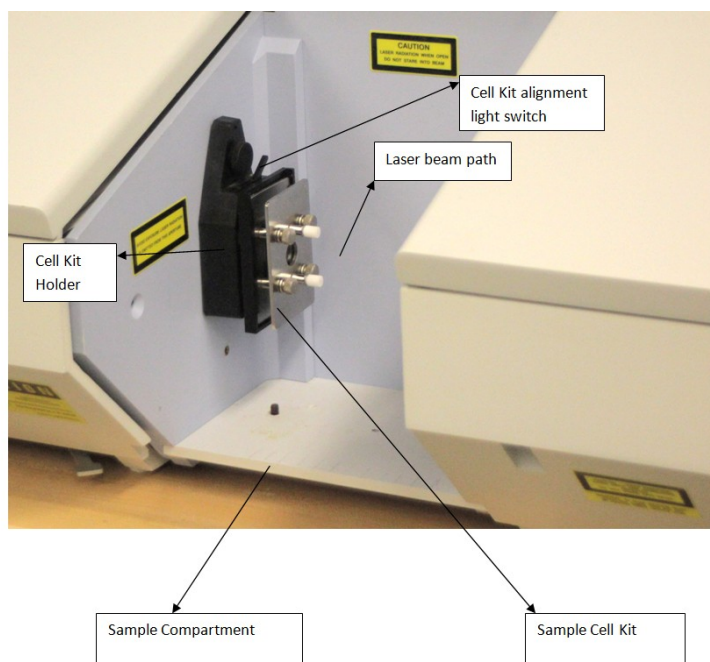
Figure 2.3: FTIR Spectrometer Cell kit Set up
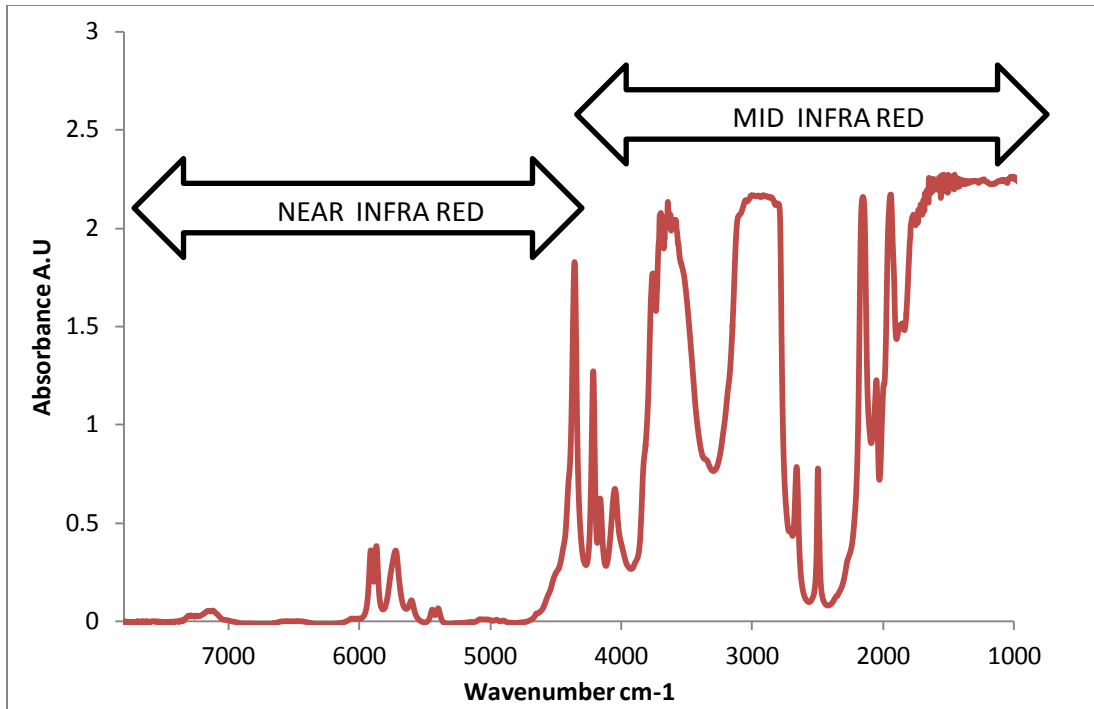
Figure 2.4: Optical Transmittance bands in Mid IR and NIR for PDMS

Within the NIR region, PDMS shows absorbance in the area 5900 cm^{-1} to 5600 cm^{-1} due to overtones presented by the C-H bonds. While in most of the NIR region, except that 300cm^{-1} band mentioned above, PDMS is transparent, it has high bands of absorbance in the Mid IR area as seen in the spectral profile.

Figures 2.5 and 2.6 show the mid infrared and the near infrared spectrum of a 100 μm thick PDMS film [56]. While comparing the results with the experimental data from figure 2.4., although a good correspondence with the published work can be seen in the NIR region, MIR region is largely masked by the artifacts introduced by PDMS. As the IR absorbance of PDMS in the MIR is much higher compared to NIR, the thickness of PDMS plays an important role in the analysis and could be the cause of discrepancy in the results.
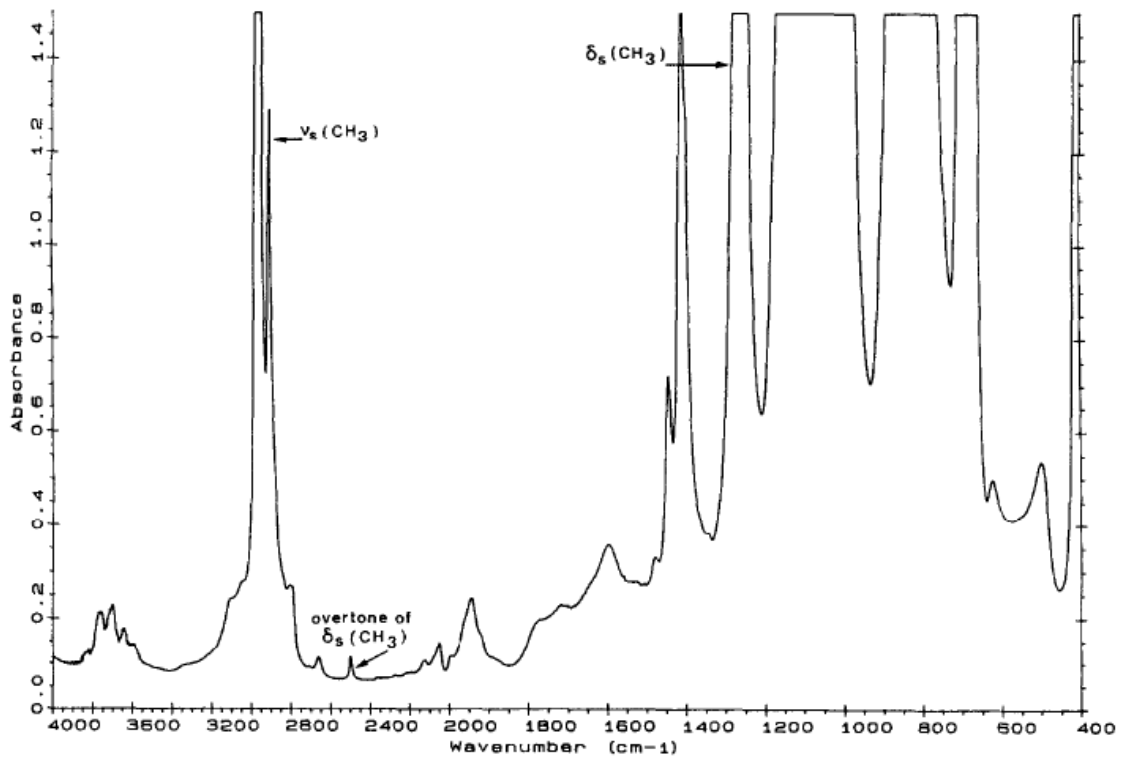
Figure 2.5: Mid Infrared spectrum of PDMS [56]
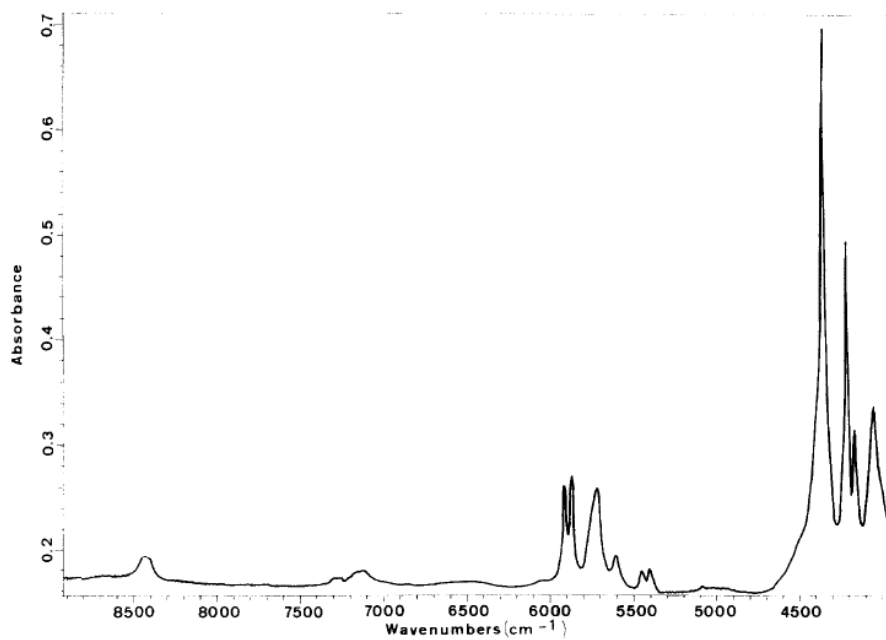
Figure 2.6 Near Infrared spectrum of PDMS [56]

2.2.3   Effect of Thickness of PDMS on its IR Transmittance

As seen in the previous section, thickness of PDMS plays an important role in its spectral characteristics in MIR region. In order to understand the effect of thickness, a set of experiments have been designed with slabs of varying PDMS thickness taking in to account the minimum feature size required for the device. A quantitative analysis can be carried out with the application of the Beer's Law which provides the relationship between absorbance of a sample and its concentration/path length or thickness.
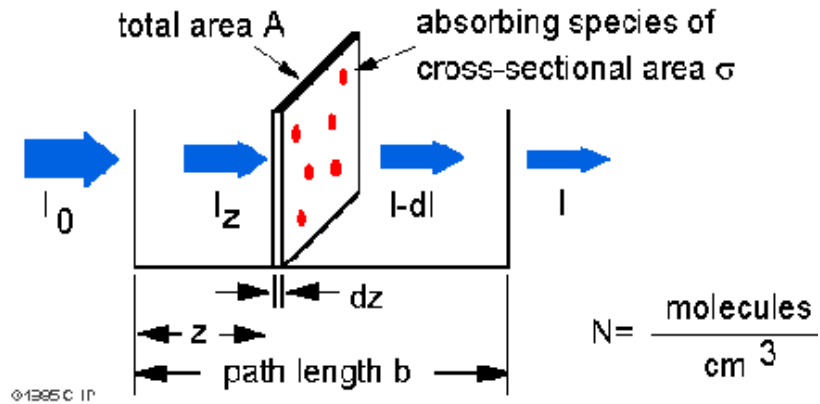
Figure 2.7: Representation of Beer-Lamberts Law for absorbance calculations

Beer- Lamberts law (1) can be summarized from the equation 2.1 below

$$\ln (I_0/I) = \varepsilon\, c\, L \quad \ldots\ldots\ldots\ldots\ldots\ldots\ldots\ldots\ldots\ldots\ldots\ldots\ldots\ldots\ldots\ldots\ldots\ldots\ldots\ldots\ldots (2.1)$$

Where I_0 = Incident Radiation, I= Transmitted Radiation, ε= absorptivity of the sample, L= path length in cm, c= concentration, and $\ln (I_0/I) = A$= Absorbance. As the absorbance is directly proportional to L, which is the path length or the thickness of PDMS slab, the absorbance of PDMS increases with its thickness.
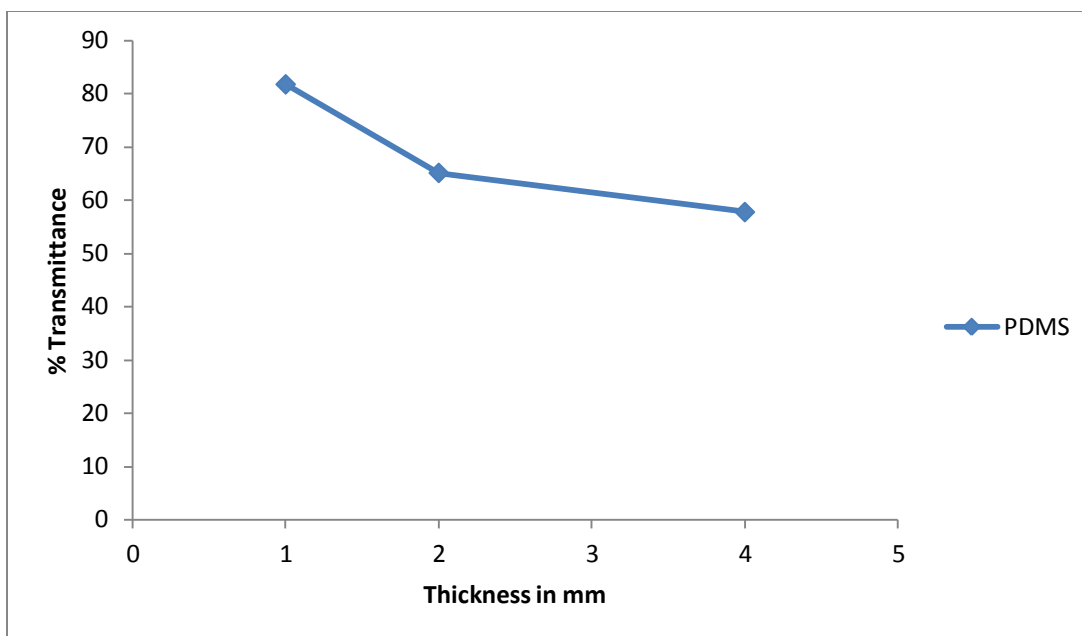
Figure 2.8: Variation of IR transmittance of PDMS at different thicknesses @ 2400 cm-1

PDMS slabs of varying thickness (1, 2 & 4mm) has been fabricated as detailed in section 2.2.2 and subjected to IR analysis and the transmittances were plotted at 2400 cm^{-1}. Figure 2.8 shows the variation in transmittance with thickness and it shows a decreasing trend with respect to thickness where 1 mm shows the highest transmittance.

2.2.4 Biocompatibility

In order to use PDMS for cell culture applications, its surface can be rendered biocompatible using techniques like plasma treatment which makes the surface hydrophilic. Cell culture has shown preferential growth in plasma treated surfaces on PDMS [57]. However, effects introduced by these treatments are reversible in nature.

2.3   Constraints Introduced by the Instrument

Subsequent to the study of the constraints imposed by the selected material for a window, additional set of constraints are imposed by the equipment in which the window material will be placed. In order to understand the constraints imposed by the equipment on the design of the window material, the study of the spectrometer, in which the window is planned to be installed, is proposed in the following sections. A spectrometer has the following basic components (a) Michelson Interferometer (b) Infrared Sources(c) Beam Splitters (d) Infrared Detectors (e) The laser (f) The cell kit.

2.3.1   FTIR Instrument Spectrum BX™

The spectrum BX™ is a bench top integrated self contained unit (Figure 2.9) [58] which has a single beam purge able sample compartment with a holder for the demountable cell
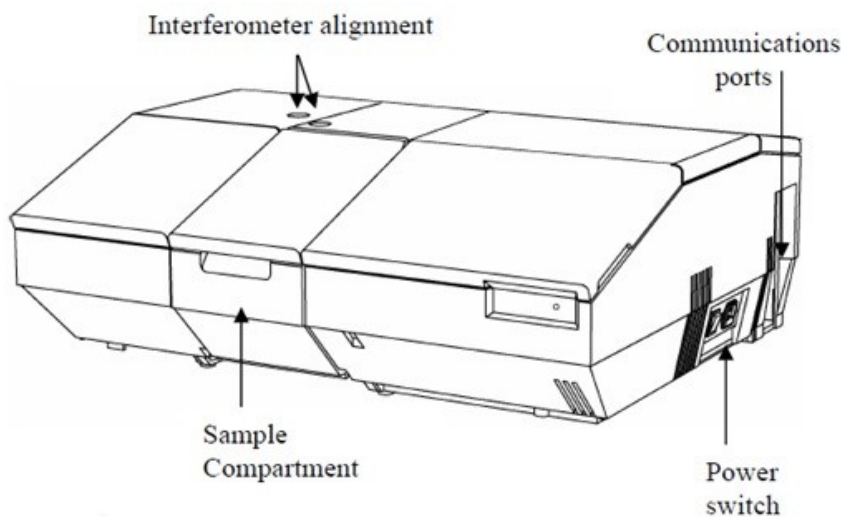
Figure 2.9: FTIR Spectrum BX spectrometer™ -Perkin Elmer® [58]

kit. The spectrum BX™ can work in single beam, ratio and interferogram mode. An optical analysis range of about 7800 cm^{-1} to 100 cm^{-1} is available using a Ge coated Potassium Bromide (KBr) beam splitter and a maximum Optical Path Difference(OPD) of 1 cm^{-1}. The mid infrared detector like Deuterated Triglycine Sulphate (DTGS) or Lithium tantalite ($LiTaO_3$) as standard equipment and Mercury Cadmium Telluride (MCT) as optional, with MOTOROLA 68340 Processor based electronic processing system are factory standard. Signal to Noise ratio (SNR) specifications for BXII are 15,000/1 Root Mean Square (RMS), 3000/1 peak-to-peak for a five second measurement & 60,000/1 RMS, 12,000 peak–to–peak for one minute. The measurement time for a spectrum includes total scan time and signal processing. The SNR improves with the increase in the number of scans, but as the number of scans increase, measurement time is greater and so will require a tradeoff for obtaining an optimum result.

2.3.2 Optical System

The optical system floats on vibration proof mounting pads to isolate it from the bench shocks. The entire optical system is purged and factory sealed and a supply of desiccant (mixture of aluminum oxide, magnesium oxide, chemically prepared silicon dioxide and sodium oxide) is placed within system to remove any water vapor or carbon dioxide. The optical layout is detailed on Figure 2.10[58].The instrument contains a Class II He Ne laser which emits visible, continuous radiation at a wavelength of 633 nm and has maximum power o/p density of 1 mW. A portion of this laser radiation is accessed in the sample compartment with a maximum power level of 0.4 mW.

①	HeNe laser	⑦	IR detector	⑬	Adjustable concave mirror
②	Glass window	⑧	Fixed concave mirrors	⑭	Laser fringe detector
③	Purge cover	⑨	Optical stop	⑮	Interferometer flat mirror
④	Shield	⑩	Window	⑯	Beamsplitter
⑤	Source cover	⑪	Sample compartment	⑰	Interferometer scan mirrors (2)
⑥	Adjustable laser mirror	⑫	IR beam focus	——	IR beam
				- - - -	Laser beam
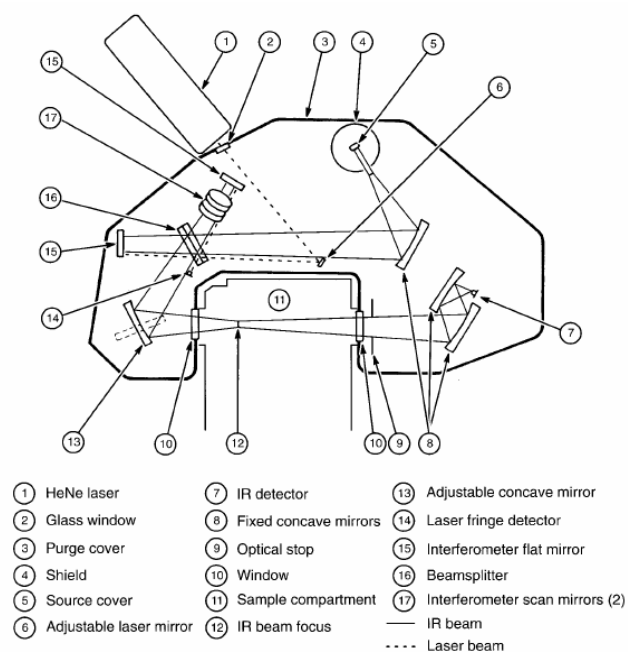
Figure 2.10 Optical Path diagram of FTIR Spectrum BX™ [58]

The beam of He-Ne laser follows the infrared beam through the interferometer. The instrument uses the laser beam to track the Optical Path difference and determines when to measure the data point. The absorbencies in NIR are weaker than in Mid IR and so this will require higher sample size for NIR.

2.3.3 Sample Compartment

The sample compartment is located at the front of the instrument to the left of center and can be accessed by lifting the cover as shown in figure 2.11 [58].

The infrared beam enters the compartment through an aperture on the left behind the sample slide. After passing through the sample, it enters the detector area through an aperture at the right hand side of the compartment. The inlet of the purge gas is on the left side of the compartment. It is connected to a tube that exists at the rear of the spectrum BX™ on the left hand side. The sample slide has an alignment light which can be used to align the accessories. It has to be taken care that the relative humidity of the sample

compartment, if higher than 75% can damage the window of the sample, so if in case the humidity goes above this the moisture content threshold, the sample compartment has to be continually purged or desiccated to control humidity. The maximum space available for movement within the sample compartment is 120mm.
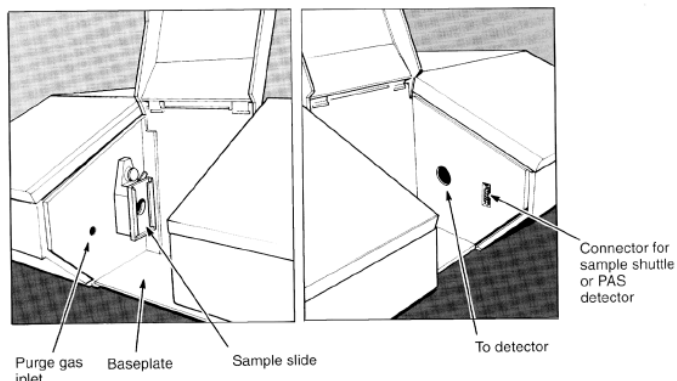
Figure 2.11 LHS & RHS Isometric View of sample compartment and detector [58]

In order to enable a cell kit along with its accessories (for eg: the cell culture vessel) customized for biological analysis, to be placed in the sample compartment, the space for movement in the sample compartment will be a design parameter as the cell kit will have to be placed away from the current holder. Also there is no continuous purging apparatus and the variation in parameters like humidity, temperature etc., could cause an influence in the spectral results.

2.3.4   The Cell Kit

Refer to spectrometer layout is as in Figure 2.11. The emitter is the point from which the infrared radiation emerges from the Michelson interferometer set up and the detector is the point at which the beam emerging from the sample enters infrared detector optics. The sample cell kit or the transmittance cell is the device enabling sample loading and analysis (figure 2.12). Perkin Elmer™ supplies Calcium fluoride (CaF_2) cell kit which is

an alkaline halide demountable cell kit which comes as the standard accessory for the FTIR. CaF_2 is highly insoluble and it resists most acids and alkalis. It has analysis wave number range from 79,500 cm^{-1} to about 1025 cm^{-1}, owing to which CaF_2 is the most widely preferred material in the cell analysis kits.

The cell Kit, shown in figure 2.12 consists of a stainless steel body which is corrosion resistant. The Perkin-Elmer® type cells are generally with 14mm FTIR circular aperture. The stainless steel cell consists of a front plate with two welded "leur-lok™" filling ports and Teflon plugs, a back plate, front gasket, rear gasket and amalgamated window assembly comprised of drilled and undrilled windows. A Teflon gasket is sandwiched to prevent leakage. The general window size for FTIR cell is 38.5mm*19.5mm*4mm. The cells are assembled using the spacers provided to standard path lengths as 0.10mm, 0.20mm, 0.40mm, 1.00mm, and 2.85 mm. The general transmission materials used for the windows are NaCl, KBr, CaF_2, BaF_2, KRS-5 (Thallium bromo Iodide) and ZnSe (Zinc Selenide). As observed above, the window specifically employed in SPECTRUM BX™ was CaF_2. The exploded view of the cell kit and the position of kit in the sample compartment of the spectrometer are shown in figures 2.13 and 2.14.
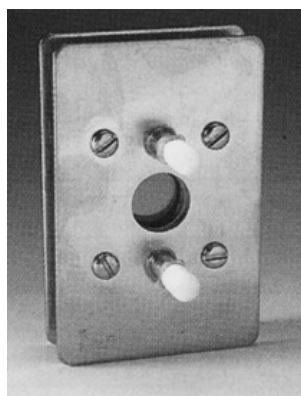
Figure 2.12: Traditional Cell Kit used in an FTIR spectrometer
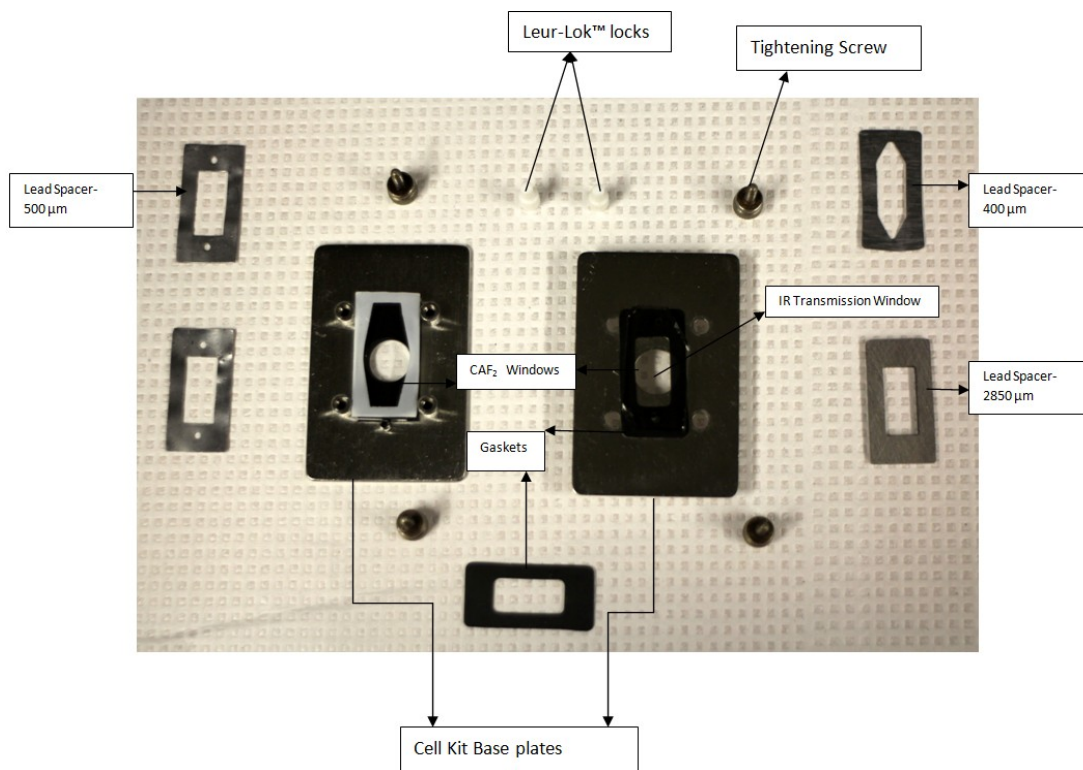
Figure 2.13: Exploded View of the CAF$_2$ transmittance cell kit
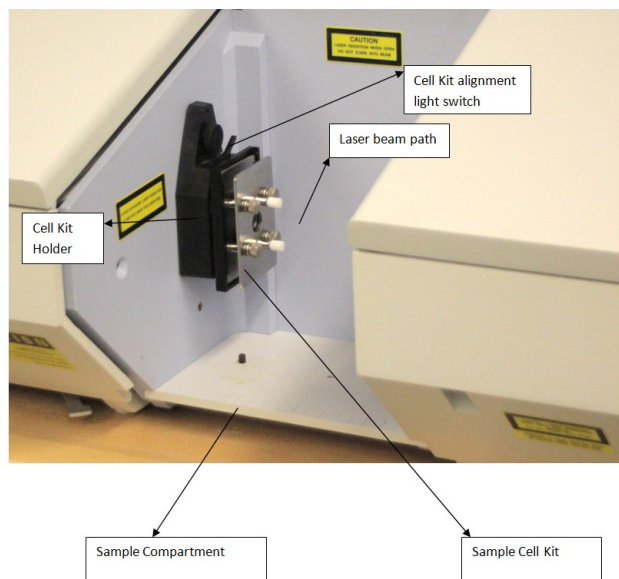
Figure 2.14 Cell kit arrangements in the FTIR spectrometer

CaF_2 is a relatively expensive product and cannot be subjected to design modifications or fabrication in a lab environment. The design parameters for the PDMS window should match the CaF_2 window so that the existing cell window fixtures can be used avoiding design for new fixtures. However, in order to customize the PDMS cell kit for cell incubation applications, following set of experiments have been designed to understand the effect of the distance from the emitter, on IR transmittance of the cell kit.

2.3.5   *Effect of Distance from Emitter on Transmittance*

In order to customize the PDMS cell kit for biological applications, integrating it with a standalone cell incubator is recommended. This necessitates the study of the effect on the performance of the cell kit with respect to its IR transmittance as a function of distance from the emitter. A set of experiments using CaF_2 kit and a PDMS kit has been designed. As described in section 2.2.2; PDMS slabs were fabricated and assembled in the cell kit. The CaF_2 kit and the PDMS kit were loaded with 190 μm of DIW sample and were subjected to spectral analysis at the cell kit holder as well as 30 mm and 60 mm from the emitter position respectively. The top view and the front view of the sample compartment are detailed in figure 2.15-2.16. The top view shows the space for movement of 120 mm for the cell kit within the sample compartment, while the front view shows the elevation at which the cell kit needs to be positioned (60 mm) from the instrument base. The transmittance at 4500 cm^{-1}, where DIW exhibits a peak transmittance is plotted from the results from CaF_2 kit and PDMS kit. The results presented (figure 2.17) show that transmittance decreases with increasing distance from emitter and it drops to about 50% at 60 mm.
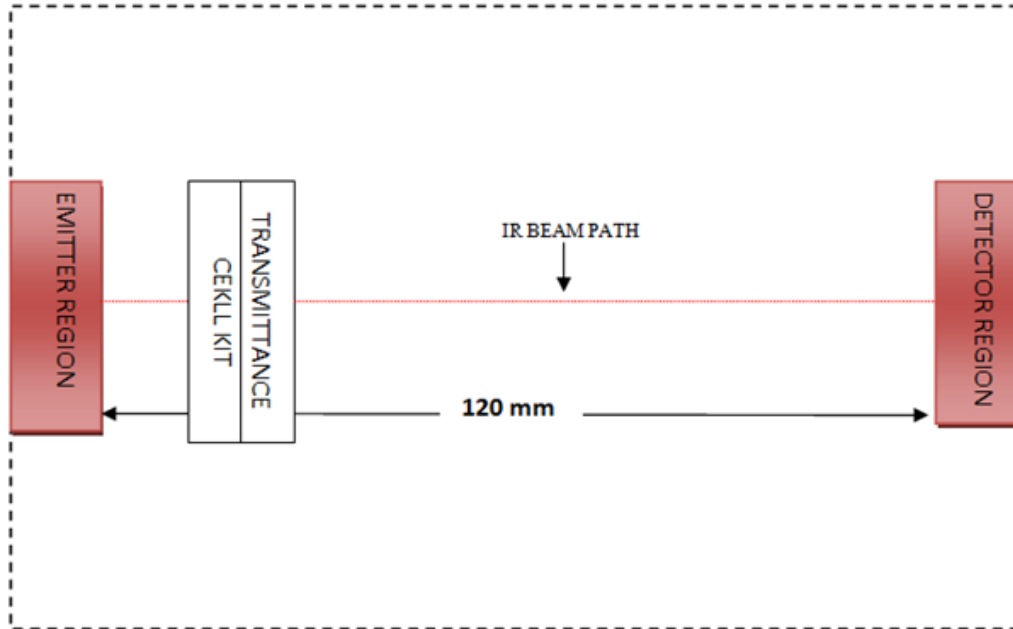
Figure 2.15: SPECTRUM BX™ Sample Compartment Top View
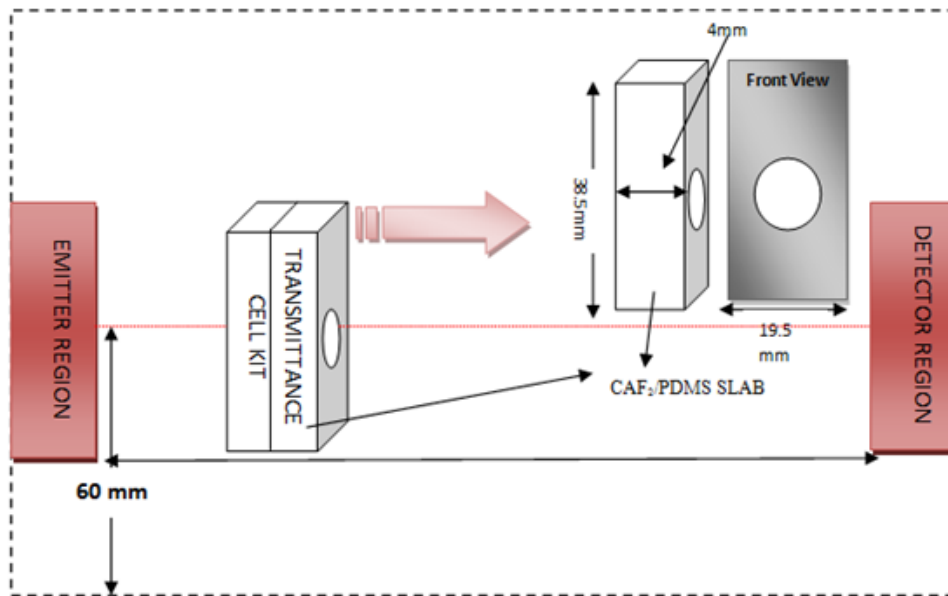
Figure 2.16: SPECTRUM BX™ Sample Compartment Front View
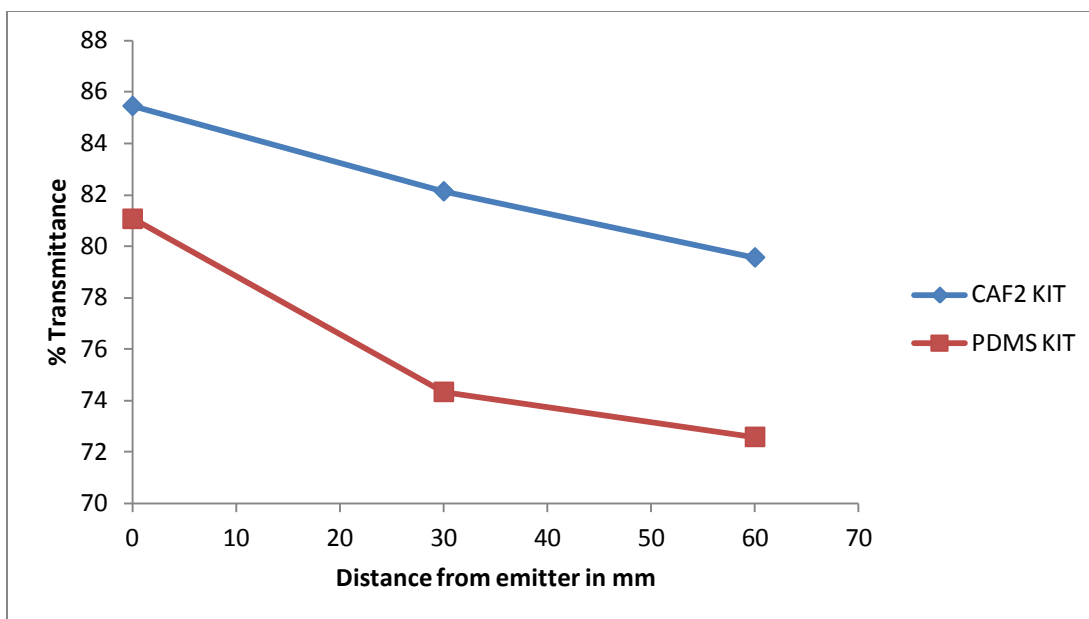
Figure 2.17: Plot of % Transmittance vs. Wave number for PDMSDIW and CaF$_2$DIW at different distances from cell   holder kit at 4500 cm^{-1}

From the experiments it can be concluded that the intensity of the infrared radiation is maximum at the cell kit holder/emitter point and it progressively decreases to about 50% at the midpoint, i.e., 60 mm from the emitter. This decrease could probably be due to the dispersion of the infrared beam in the sample compartment. Hence, it is ideal to use the sample at the cell holder and moving it beyond the emitter decreases its effectiveness.

2.3.6   Other General Precautions

The following constraints in relation to the optimum instrument operating conditions have also to be taken in to consideration in order to fine tune the design parameters.

- ✓ The instrument must be placed in a relatively dust free environment.
- ✓ The work bench should be free of vibrations or mechanical shocks
- ✓ The instrument should not be placed in close proximity to a heating equipment or radiators

✓ The area near the PC for spectra read out should not be subject to strong magnetic fields or heating or cooling units or ducts

✓ Optimum ambient conditions for operation are 15ºC-35ºC and up to 75% Relative Humidity

✓ It can take up to 2 hours for the instrument to reach equilibrium once switched on after being switched off. So it is recommended that the instrument be left ON all the time.

2.4   Summary

In this chapter, all the relevant constraints which will influence the design of the device to replace the CaF_2 cell kit were considered. It can be summarized that the chemical composition of PDMS polymer, its thickness, sample volume, distance of the cell Kit from the cell kit holder and the region of inspection (NIR or Mid IR) are going to be important factors influencing the spectrum results. The transmittance of any sample in FTIR analyses is going to be dependent on the following parameters

a)   The amount of sample (dependent on the spacer thickness)

The spacer thickness has to be adjusted according concentration of the sample and IR region of observation. As the FTIR spectrometer has higher resolution in Mid IR, smaller sample size would be enough to produce the spectrum. But in NIR, a higher sample size is required.

b)   The distance of placement of the cell Kit from the emitter

The transmittance of the sample decreases with increase of sample distance from emitter. It drops to about 50% halfway from the emitter

c)   The Thickness of window material

Mid IR has strong artifacts introduced by PDMS except for the region of 2800 cm^{-1} to 2200 cm^{-1} and so is not a suitable region for analysis in an FTIR spectrometer at higher thicknesses of PDMS.

All these design constraints have to be evaluated to develop a suitable window material for replacing the current CaF_2 cell. Once the design parameters are evaluated, a suitable micro fabrication and testing protocol for the PDMS based device can be finalized. The results have to be compared with the existing CaF_2 kit and in case of non-corroborative results; corrective measures have to be suggested to further refine the above suggested design parameters. This is considered in Chapter 3.

CHAPTER 3.   DESIGN, FABRICATION AND TESTING OF THE DEVICE

In the previous chapter, a detailed study of the design constraints has been conducted. Having taken into account the constraints introduced, a suitable preliminary design of a micro device which can replace the existing window has been suggested in this chapter. Based on this preliminary design of the device, a micro fabrication process has been conceived and executed.

A mask has been designed to create a mold with SU-8 coated on a 4 in. silicon wafer for enabling mass production. Soft lithographic fabrication and bonding techniques have been employed to fabricate and bond the PDMS device. Outlets have been created to enable the flow of analyte through the micro channel for IR irradiation. The device has been subjected to preliminary tests using a sample of DIW. The results have been documented and discussed in comparison with CaF_2 kit.

3.1   Design of the PDMS Cell Kit

From the design constraints established from experiments in the previous chapter, a design of the PDMS micro device based cell kit has been proposed. The dimensional details of the proposed device are shown in figure 3.1. The dimensions have been designed keeping in mind the constraints introduced by the cell holder fixture (refer figure 3.2) which assembles the CaF_2 windows. The micro reservoirs have been centered on the leur locks™ fluid transfer port (see figure 2.12) in the original transmittance cell kit fixture in order to enable smooth transport of the designated analyte into the micro channel.
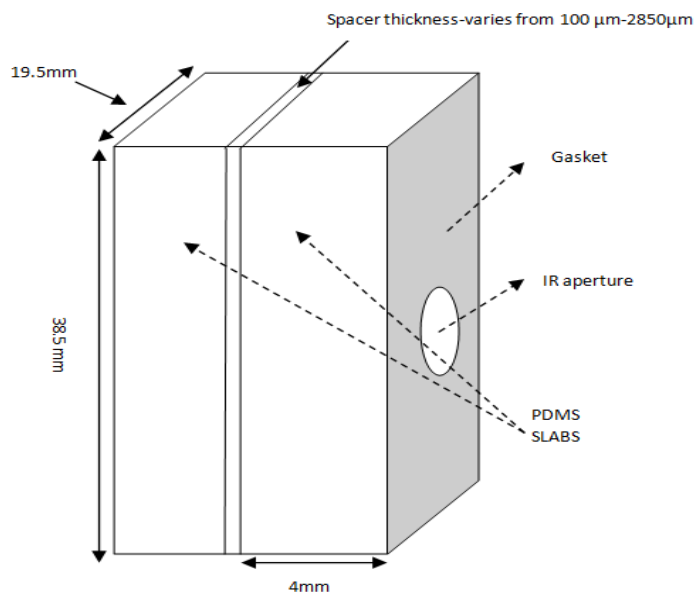
Figure 3.1: Design Parameters for a PDMS cell Kit
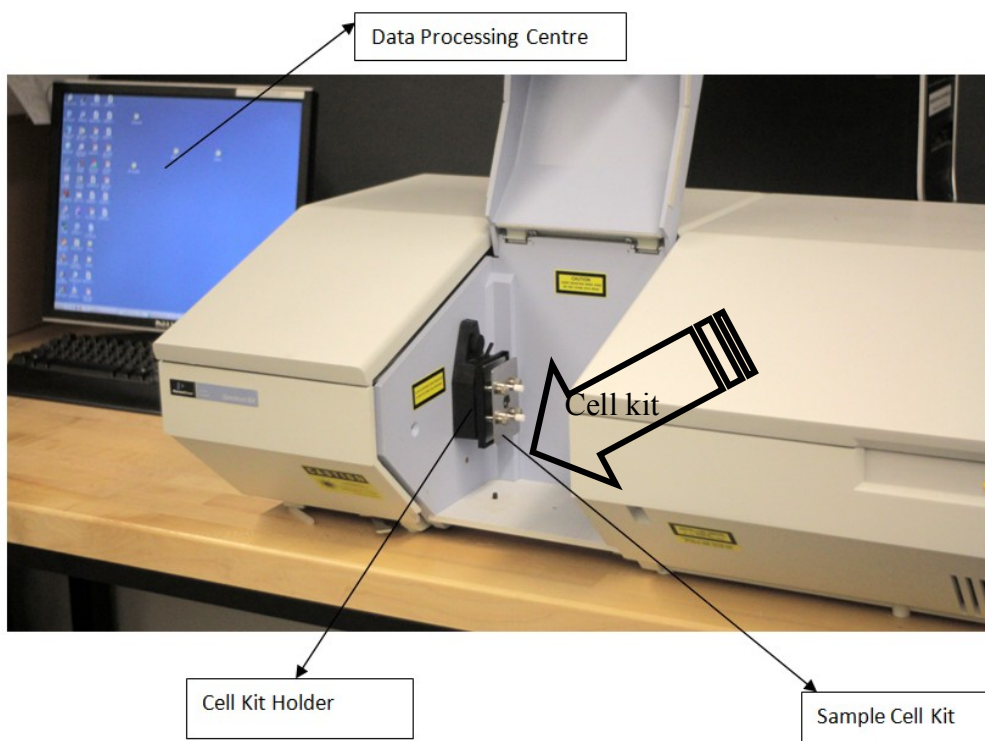
Figure 3.2: Cell kit assembly in an FTIR spectrometer

3.2 Mold Design

PDMS can easily be subjected to soft lithography and so once a Master mold is fabricated large number of devices can be produced. The design for the cell kit master mold is shown in figure 3.3. The mold has the following features.

a. Micro reservoir for fluid storage

b. Micro channel for fluid passage

c. Cell window
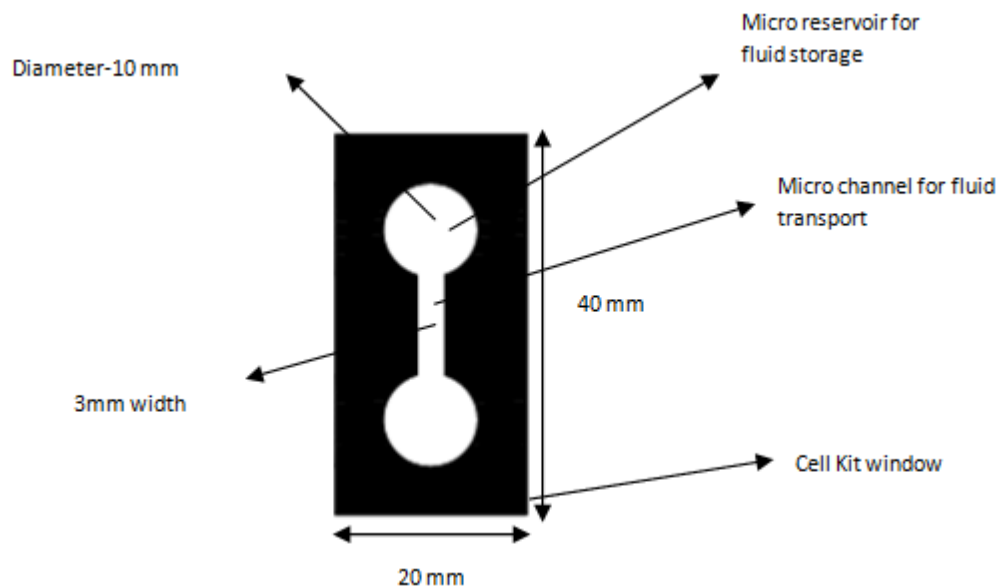
Figure 3.3: Master Mold for the PDMS Window

Micro reservoir for fluid storage is the well that enables extra fluid to be stored at both the terminals of the channel. The reservoir has a diameter of 10mm. Micro channel for fluid passage is the principal channel which is aligned with the beam path and where the spectral analysis occurs. The channel is 10 mm long and 3 mm wide and is positioned in such a way that there is minimum alignment problem with the existing cell kit window and provides sufficient impact area for the infrared beam which has a diameter of about 2

mm. Cell window is boundary feature for the device. Its dimensions are 38.5mm (length) X19.5mm (width) in order to facilitate aligning with the current cell kit fixture.

The depth of the features is basically the spacer thickness provided by Teflon spacers for the CaF$_2$ kit. The minimum spacer thickness has been provided is 100 μm. Two of these slabs will be fabricated and will be bonded together by partial PDMS curing process. In order for the effective micro fabrication using the SU-8 mold and effective bonding using the partial PDMS Curing process , a feature size of 60 μm was found convenient. This would result is a spacer thickness of about 120 μm.

3.3   Micro Fabrication

3.3.1   *Photolithography*

Photolithography is a pioneering process in pattern transfer in micro fabrication that generally involves a set of processes which can be summarized as in figure 3.4[59]

An oxidized silicon wafer is coated to uniform thickness with a photosensitive material
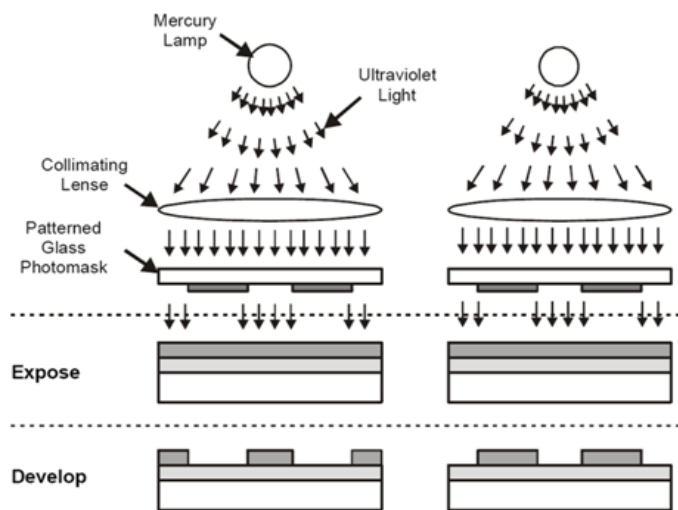
Figure 3.4: Photolithography -Exposure effects on a positive and negative resist [59]

called "photo resist" by spray coating or spinning by holding the wafer on to a vacuum chuck. A glass mask or transparency which has the pattern engraved or printed acts as the master pattern and the resist coated silicon wafer is exposed to controlled UV radiation through the patterned glass mask. The exposed wafer is later treated with a developing solution resulting in the pattern being exposed on the photo resist. A positive photo resist will accept the pattern as it is and a negative one will accept the photographic negative of the master pattern.

The glass masks which are used in the process are generally chrome plated and are expensive to manufacture. A less expensive option is to produce the pattern using a CAD drawing and print it on a transparency using a high resolution printer (3600-4000 dpi). The masks are also classified as dark field and light field masks as shown in figure 3.5.
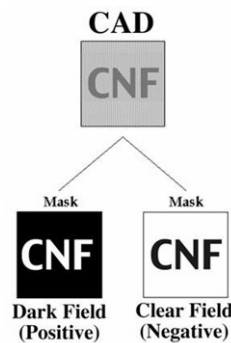
Figure 3.5: Dark Field and Light Field Masks [60]

The dark field is the photographic positive mask in which the patterned areas are transparent to UV radiation and Clear field or light field is that in which the patterned areas are opaque to the UV radiation. The appropriate combination of the mask and the photo resist will determine the pattern which will be transferred on to the surface of the

wafer. A negative photo resist was preferred in the process as it has excellent adhesion capabilities to silicon wafer and is relatively inexpensive.

3.3.2   Mask Fabrication

A drawing was created using AutoCAD® of the mask to be placed in a 4 inch silicon wafer. The mask was created in the scale 1:1. The CAD file was then sent to printer for printing on to a transparency sheet with a high resolution (3600 dpi). The mask created is a dark field mask as shown in figure 3.6.
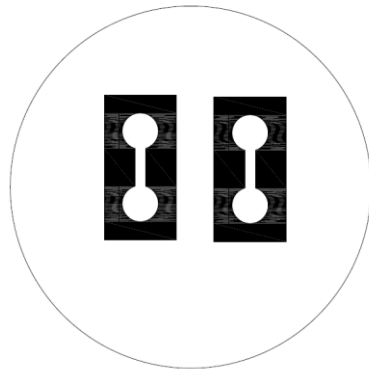
Figure 3.6: Mask for Master Mould Fabrication

3.3.3   Mold Fabrication

SU-8 2000; a permanent epoxy based negative photo resist, has been used as the mold material. The advantages of SU-8 2000 are it is ideal for high aspect ratio imaging and it is good for any feature size from the range of 0.5-200µm. It has faster drying properties and is exposed using UV radiation (350 -400) nm. The SU-8 2035 (figure 3.7) [61] was identified as the best choice for achieving a uniform coat of about 60µm.
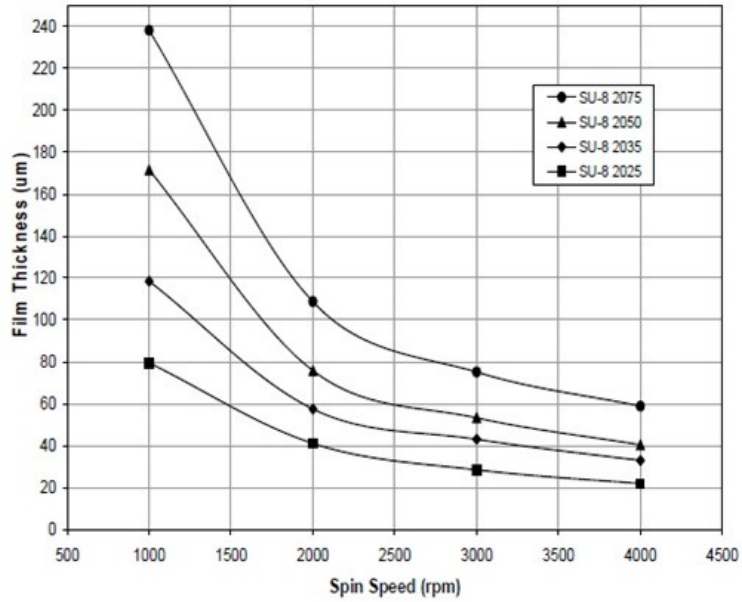
Figure 3.7: SU-8 Spin Speed vs. Film thickness [61]
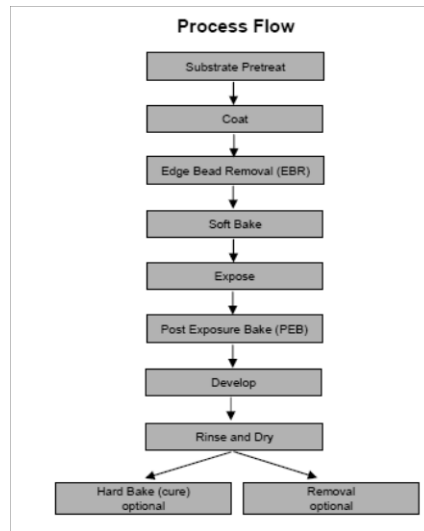
Figure 3.8: Generic process flow for SU-8 Master Mould fabrication [61]

The steps for the recommended fabrication process are shown in the flow diagram figure 3.8[61]. However, generally, the normal steps are spin coating, soft bake, exposure to

UV, Post exposure bake (PEB) and development. The silicon substrate was subjected to an inspection to make sure that it was clean and dry for maximum process efficiency. The recommended cleaning process for removing the SiO_2 layer is with a piranha wet etch ($H_2SO_4 + H_2O_2$) or HF solution in de-ionized water (10:1) followed by de-ionized water rinsing.

3.3.4 Spin Coating

The recommended usage of photo resist is about 1 ml for and 1 inch diameter, and as the wafer used in this process is 4 inches, about 4 ml of SU-8 2035 was required. The chart in Figure 3.7 gives the recommended spinning speeds for achieving the required coating thickness. The spinning was carried out in the vacuum chuck as in Figure 3.9
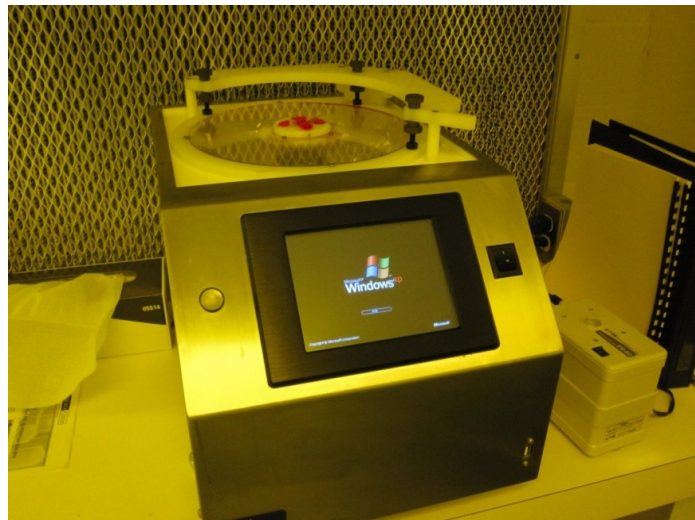
Figure 3.9: Vacuum Chuck for SU-8 spin coating

The first step was to spin at 500 rpm for 7 seconds with an acceleration of 150 rpm/section followed by a step of 2000 rpm spin for 30 seconds with 200 rpm/section acceleration.

3.3.5 Soft Baking

The wafer was then subjected to soft baking which is recommended before exposure as a step for better adhesion to the substrate. The soft bake recipe as shown in the table 3.1

Figure 3.10: High Temperature Oven

provides the recommended times for thicknesses varying from 25-225 µm and since the feature size required for the current fabrication is about 60 µm the soft bake time recommended for 45-80µm features is to be considered.

Thickness (Microns)	Soft Bake time @ 65º C (minutes)	Soft Bake time @ 95º C (minutes)
25-40	0-3	5-6
45-80	0-3	6-9
85-110	5	10-20
115-150	5	20-30
160-225	7	30-45

Table 3.1: SU-8 Thickness and recommended soft baking times

3.3.6 UV Exposure

After the soft bake process the wafer was exposed to UV radiation in a mercury lamp (figure. 3.12). The recommended exposure times have been listed in table 3.2 and the exposure energy for obtaining a feature size of 60 µm is about 215 mJ/cm^2.
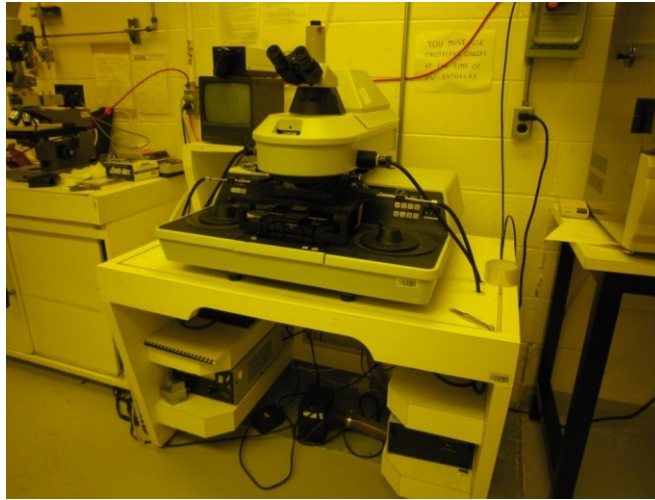
Figure 3.11: UV Exposure -Mercury Lamp

Thickness (Microns)	Exposure Energy mJ/cm^2
25-40	150-160
45-80	150-215
85-110	215-240
115-150	240-260
160-225	260-350

Table 3.2: SU-8 Feature Thickness and recommended exposure energy for UV

3.3.7 Post Exposure Bake

The post exposure bake is done to expose the features as per the recipe for 45-80 µm (ref table 3.3).

Thickness (Microns)	PEB TIME(65ºC) in minutes	PEB TIME(95ºC) in minutes
25-40	1	5-6
45-80	1-2	6-7
85-110	2-5	8-10
115-150	5	10-12
160-225	5	12-15

Table 3.3: Recommended post exposure bake time for attaining SU-8 thickness

3.3.8 Development

The wafer is subjected to developer treatment for about 5 minutes in one container and then shifted to another container having a fresh solution for about 2 minutes. The wafer is then washed in IPA solution to examine if the features have been fully exposed. The wafer is subjected to developer treatment (see table 3.4) to about 5-7 minutes till the features have been exposed fully. Finally, it's ideal to bake the wafer for about 10 minutes at 95ºC for feature stability.

Thickness (Microns)	Development time (in minutes)
25-40	4-5
45-70	5-7
80-110	7-10
115-150	10-15
160-225	15-17

Table 3.4: SU-8 Thickness and development time

3.3.9 Cleaning and Silanization

The wafer is cleaned again with IPA solution and is subjected to drying with a nitrogen gun. The master mold is finalized with the exposure to $CF_3 (CF_2)_6(CH_2)_2SiCl_3$ for about 5hours. 1 ml of xylene is spread on top of the wafer and is covered and subjected to hot plate treatment maintained at 60ºC. The silanization produces a non-adhesive layer on top of the SU-8 for effective peel of PDMS after soft lithography.

3.3.10 Soft Lithography

The soft lithographic process can be summarized as in figure 3.12[52]. PDMS is fabricated as detailed in section 2.2.2.1.The PDMS elastomeric used is SYLGARD 184^{TM} procured from Dow Corning®. It is obtained as a two part kit with a liquid silicone rubber base (vinyl terminated PDMS) and a curing agent (a mixture of platinum complex and copolymers of methyl hydrosiloxane and dimethyl siloxane) which acts as the catalyst for bonding. It is mixed at a ratio of 10:1 and poured over the mold, maintained at 60°C overnight. This result in the liquid mixture undergoing a hydrosilation reaction and transforming in to a solid, cross linked elastomer. The PDMS slabs can then be peeled off from the mold.
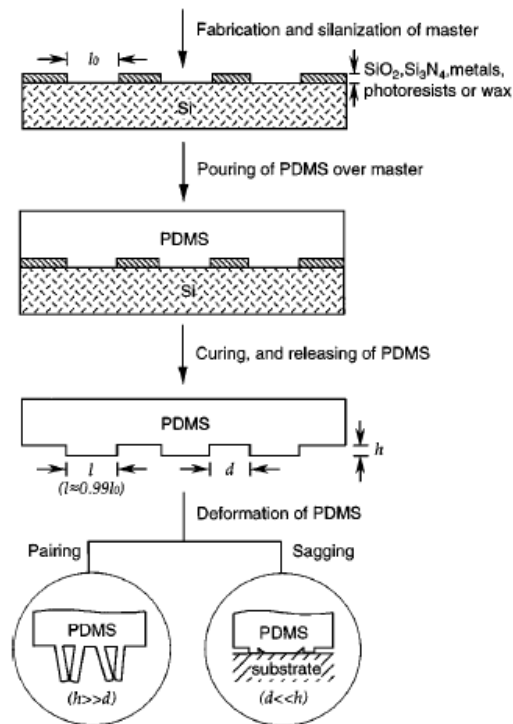
Figure 3.12: Schematic of Soft lithography process for PDMS [52]

3.3.11 PDMS Bonding

Partial curing or uncured PDMS adhesive is preferred over Oxygen plasma or Corona discharge methods as the average bonding strength achieved is higher[62] (see figure 3.17). In partial curing the PDMS is pre-cured for 35 min at 60º C before bonding and left overnight is the oven after bonding. In uncured PDMS adhesive bonding, the PDMS mixture is applied on to the device in suitable proportions across the edge to make sure that mixture doesn't overflow in to the channels. The device is bonded and left for curing in an oven maintained at 60º C for 8 hours.
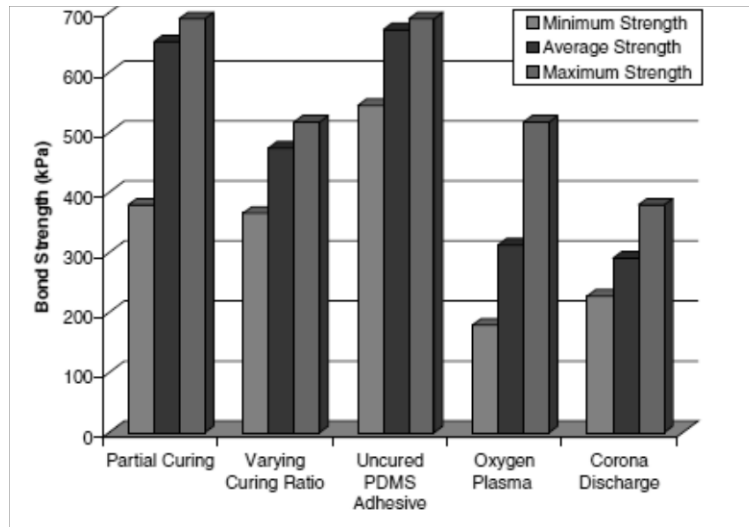
Figure 3.13: Strength Comparisons of PDMS bonding techniques [62]

3.3.12 Device Assembly and Set up

The suggested set up of the current device is shown in figure 3.14 below. The PDMS cell kit windows fit snugly in to the current demountable cell holder (see section 3.2). The Cell kit will have insertions for the fluidic reservoirs to receive fluid from the cell assembly kit and the syringe assembly.
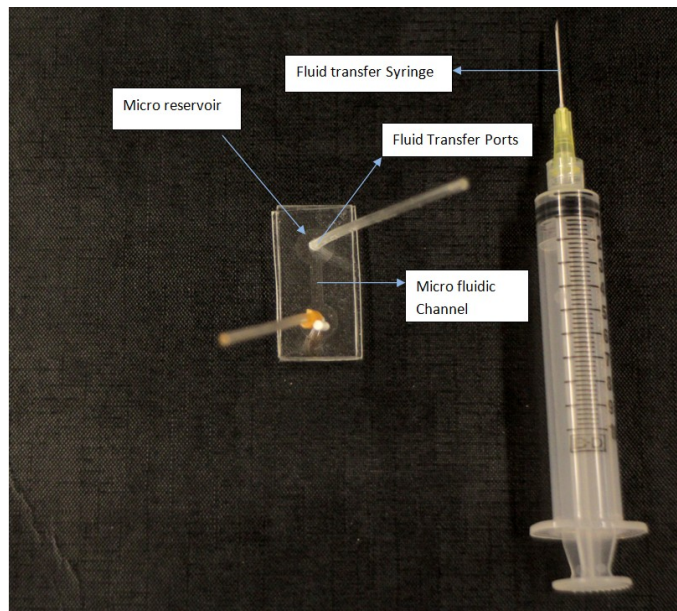
Figure 3.14: Top View of the assembled micro device

3.4   Experiments on the device using DIW (De Ionized Water)

In order to understand the performance of PDMS kit *vis a vis* a CaF_2 kit, experiments with a sample of DIW with a 100 μm spacer in CaF_2 kit and the DIW sample with 120 μm spacer in device (the final bonded device has a channel of 120 μm) were conducted in FTIR spectrometer (section 2.2.2.2 for details of analysis) and the results compared.
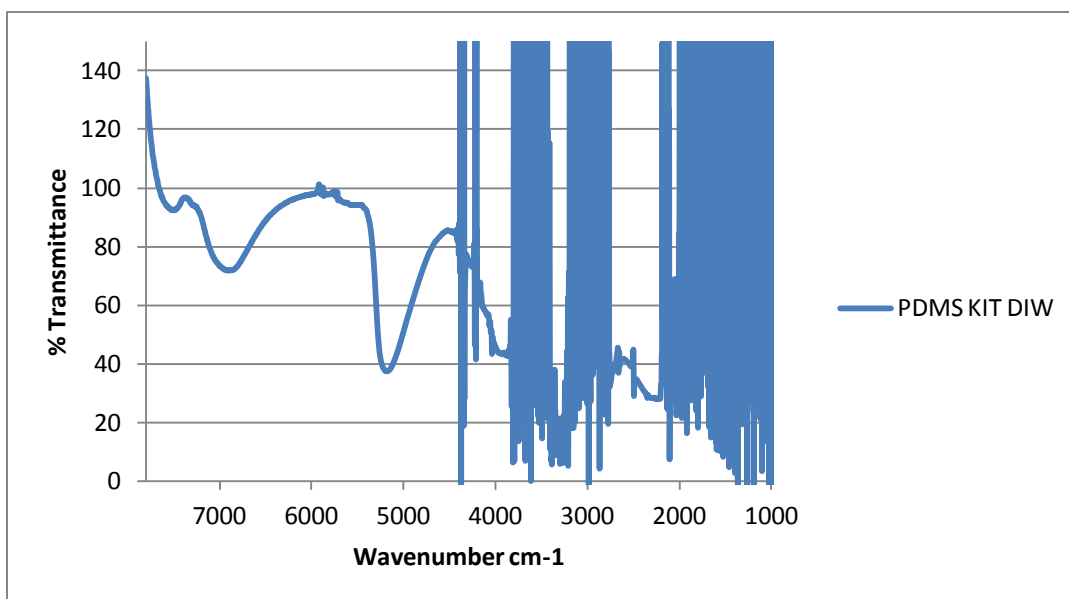
Figure 3.15: The IR Spectra of DIW in a PDMS KIT

54
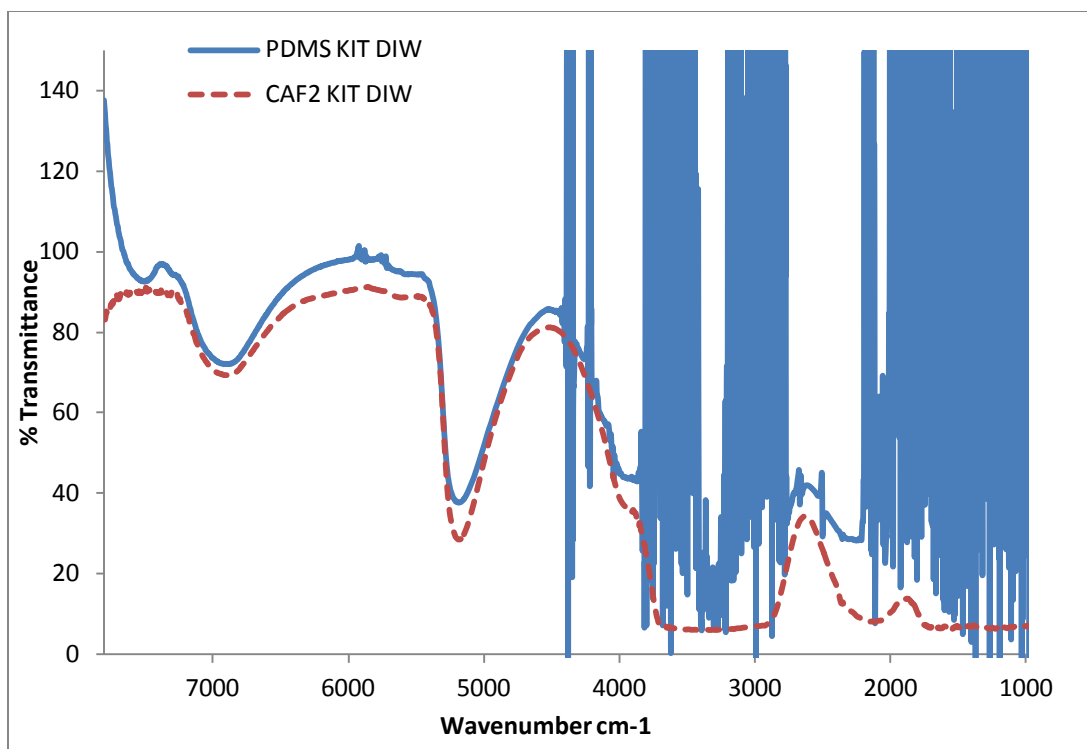
Figure 3.16: Spectra of DIW in a PDMS CELL Kit and CaF$_2$ cell Kit Comparison

The results in the PDMS Kit is presented in figure 3.15.While the experiments show good correspondence between the PDMS and CaF$_2$ kit in the NIR region, the MIR region was masked by the artifacts' introduced by PDMS (figure 3.16).Further, in order to validate the results, the DIW spectra from CaF$_2$ kit have been compared with the water spectra from NIST .As NIST only provides spectra in the MIR region, the results from CaF$_2$ Kit have been normalized in the region of 4000 cm^{-1} to 1000 cm^{-1} (figure 3.18) in order to enable a comparison.

The results show an absorbance peak in the region of 3000 cm^{-1} to 3500 cm^{-1} where the O-H group of water has fundamental vibrations (figure 3.17-3.18) [63]. Hence it can be concluded that there is excellent agreement in the NIR for both the kits while the results in MIR for the PDMS kit were noisy.
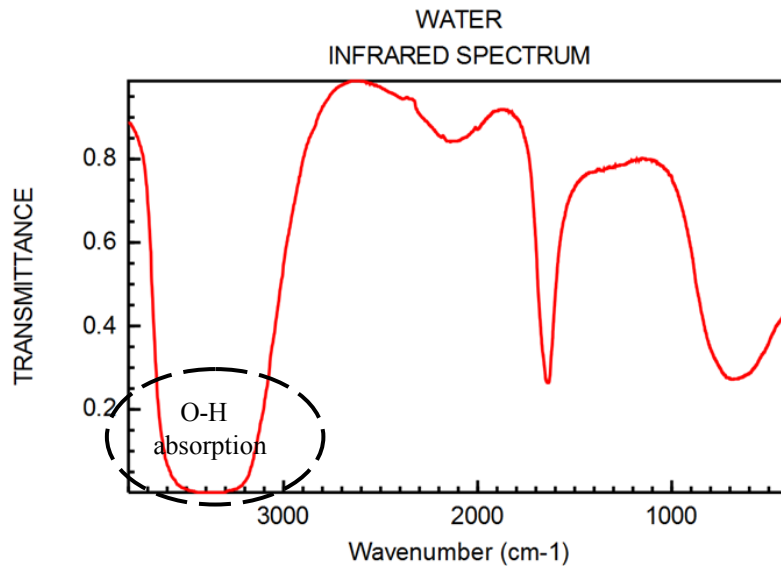
Figure 3.17: Mid IR spectra of DIW (Source: NIST)[63]
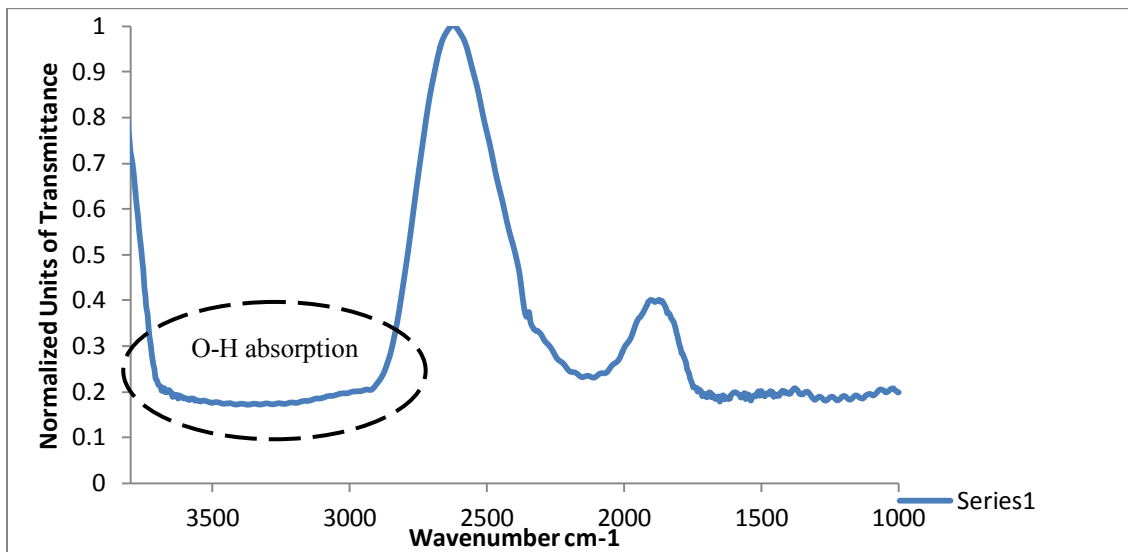
Figure 3.18: Normalized results of DIW from CaF_2 kit in MIR

3.5   Summary

In this chapter, based on the design constraints derived from chapter -2, a device has been

fabricated and tested with DIW. The results show close corroboration of the CaF_2 kit with

the standard spectrum of DIW from NIST in the MIR region from about 3300 cm^{-1} to 3500 cm^{-1}. Also the results from the PDMS Kit match with that of the CaF_2 kit in the NIR region from about 7800 cm^{-1} to about 4500 cm^{-1}. The device which has been fabricated has not proved to be effective in the Mid IR due to the intense absorption of PDMS in this region and the artifacts introduced there forth. In the region of Mid IR from about 4000 cm^{-1} to about 400 cm^{-1} a small region from 2800 cm^{-1} to about 2200 cm^{-1} is the only region in PDMS which has transmittance band that can be used for detection purposes. In order to improve the overall performance of the device, its Mid IR artifacts have to be handled in such a way that more band area is relieved for detection purposes. To this end trials to effect an optical property modification have been undertaken in the next chapter.

CHAPTER 4. OPTICAL PROPERTY MODIFICATION OF PDMS IN MID IR

In the previous chapters, it has been established that the PDMS fabricated device shows a good transmittance profile in the NIR region and has proved to be a viable substitute for CaF_2 kit. However, the PDMS Device introduced its own artifacts in the mid infrared region to a large extent such that the peaks produced by de-ionized water have been masked. Also because water is a high absorber of IR radiation, it introduced its own peaks. Because of the combined effect of an aqueous solution as well as the inherent transmittance characteristics of PDMS device, the mid infrared region has been rendered ineffective for chemical analysis. In this chapter, experimental approaches for modifying the optical properties of PDMS have been considered.

From the literature, it has been established that curing time, curing temperature and curing agent ratio may have an effect on the mechanical properties of PDMS. However, the effects of above factors on the optical transmittance of PDMS in the mid IR range have not been investigated in detail in the published literature to the best of our knowledge. In this chapter, the effect of different curing agent ratios on the IR transmittance is considered. Also, the effect of heat treatment in which a sample of known thickness was subjected to a predetermined temperature in an inert atmosphere for a fixed time period and then quenched in ambient air is being discussed in detail. The samples were subjected to scans in the FTIR spectrometer and spectrum were recorded and studied for a possible modification in the transmittance characteristics.

4.1 Background

From a survey of the literature, experiments have shown that mechanical properties like young's modulus are affected by the variation of the curing agent to base ratio [64]. Also there are few instances where mechanical properties have been linked to change in optical properties in PDMS [65, 66]. However, this has not been studied in detail, to the best of our knowledge. In order to investigate the effects on optical properties, the set of experiments that have been planned could be broadly classified as prefabrication or post fabrication treatments. Prefabrication treatments are the sets of treatments which can be carried out before or during the fabrication phase (curing phase) of the two part PDMS polymer. The treatments carried out have been classified as (1) Curing agent to base ratio variation and (2) Chemical microstructure modification. The variation in transmittance effects due to changes in curing agent ratio have been studied in this work. Post fabrication treatments are those sets of treatments which can be carried out after the fabrication (curing) of the PDMS polymer. The processes reported in the literature have been classified as (1) Heat Treatment and (2) Plasma Treatment [67]. While the effect of heat treatment on mechanical property has been reported in the literature widely, its effect on optical transmittance has not been reported. Hence the study of these effects has been proposed in the next sections.

4.2 Desired Effects on Optical Transmittance of PDMS

The optical transmittance of PDMS in the Mid IR region is shown in figure 4.1, and it can be clearly seen from the figure that PDMS introduces artifacts of its own that will mask the analyte, if we were to use this as a window material. So the desired optical property enhancements can be broadly classified as either opening of a band; increasing

the transmittance of a band; or transition of a band to a different wave number region. Bands are those regions in which PDMS exhibits an artifact or transmittance. Band regions are enclosed by wave numbers , for e.g.: all the wave numbers lying in between 2500 cm^{-1} to 2000 cm^{-1} (Figure 4.1 area 2) which has a % transmittance value above 50% could be classified as a single band, where the desired effects could manifest. The desired effects are discussed in the following section.
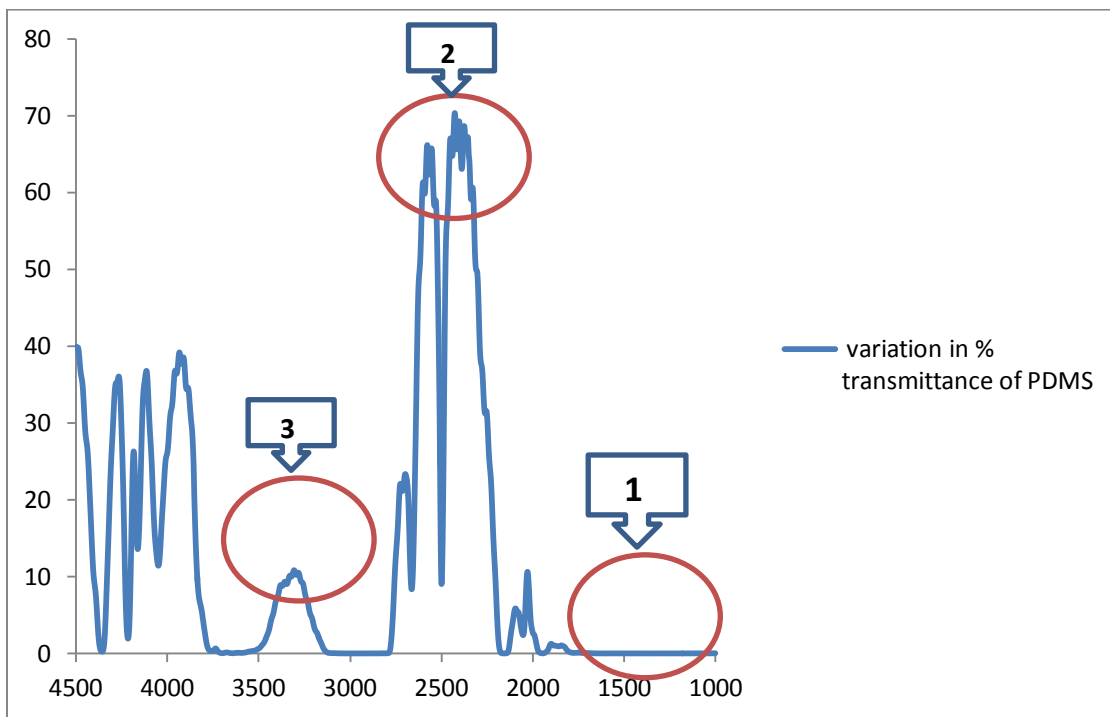
Figure 4.1: Effects on optical transmittance in Mid IR in PDMS

4.2.1 Band Opening

This is the process or effect by which, bands which were closed prior to treatment open up to transmittance post treatment. These are the regions in which PDMS (area 1 figure 4.1), prior to treatment would have traditionally exhibited total absorbance and post treatment its absorbance values decline or it shows a positive % transmittance value.

4.2.2 Band Transition

This is the process or effect by which transmittance bands move their base area to a different band width which might prove more effective in identifying a particular set of samples. This is the case in which the region in which PDMS (area 2 figure 4.1), prior to treatment has exhibited a transmittance in a particular wave band and post treatment the transmittance band shifts to a different wave number region or base area.

4.2.3 Band Enhancement

This is the effect by which within the existing bands of transmittance, the base area or transmittance area expands. In the area which had an existing transmittance pre treatment, either has an improved transmittance in the same wave band or increment in the base area of transmittance band (area 3 figure 4.1).

4.3 Effect of Curing Agent Ratios on the % Transmittance of PDMS

PDMS is commercially obtained as a two part polymer composed of a curing agent and a base. The manufacturer generally recommends a 10:1 base to curing agent ratio for fabrication of PDMS. However the effect of the different curing agent ratios on the optical transmittance of PDMS in the mid IR range has not been widely investigated. In the work presented by Chen *et. al.* [55], a 57 μm PDMS membrane was spun coat and then subjected to FTIR scan. 3 different samples with curing agent ratios of 8:1, 10:1, 12:1 were investigated. It is reported that the specimen with 8:1 ratio had the highest transmittance followed by 10:1 and 12:1 in a region of interest from(2700-2200 cm^{-1}) range. Although, the factors that influence the transmittance results were numerous,

curing agent ratio was found out to be single most dominant reason for the effect of transmittance.

4.3.1 Experiment Description

While in the literature, the reported results have been for a sample thickness of 57 μm, as discussed in the previous section, the specific constraints introduced in the current work due to the instrument as discussed in Chapter-2, and due to constraints of soft lithography process as discussed in Chapter-3, a PDMS slab thickness higher than that reported in the literature need to be considered for analysis. Due to constraints introduced by the current Perkin Elmer™ supplied transmittance cell kit fixture accessory which facilitates the loading of the sample kit, a 4 mm slab of PDMS needs to be considered. Also for stable features of the design as discussed in section 3.1, the minimum PDMS slab thickness needs to at least 1mm. As these results have not been reported in published work, in order to understand the effect of curing agent ratio on transmittance of PDMS in the mid IR, the following experiments were designed.

2 different sample sets, each of curing agent ratio 8:1, 10:1, 12:1, 15:1, 20:1 were fabricated in different beakers and were labeled separately. The base to curing agent ratios lower than 8:1 and higher than 20:1 didn't exhibit full curing and where unstable and hence they were not considered in the present analysis. The fabrication procedures are as described in section 2.2.2.1. Samples of two different thicknesses of 1 mm & 2mm were fabricated in order to understand the influence of thickness. Each of these samples were fabricated in different curing agent ratios and then the spectra were collected in the mid IR (4000 – 400 cm^{-1}) and the results were plotted on the percent transmittance value

at 2400 cm^{-1} as PDMS exhibits the highest transmittance in Mid IR in the bands in vicinity of this wave number.

Finally the device, fabricated as detailed is Section 3.3, with a base: curing agent ratio of 10:1 was also subject to IR analysis. All the slabs were sandwiched in between the existing CaF$_2$ cell kit windows and the samples were subjected to 4 scans per run with a spectral resolution of 4 cm^{-1}. 3 runs were conducted to obtain conformance on peaks. As PDMS exhibits highest transmittance in and around the 2400 cm^{-1} wave number region, the numerical value of % transmittance were noted and were plotted for each sample at different base: curing agent ratio. The results obtained from the 1mm, 2mm and device have been compared to the results obtained from the literature for 57μm as shown in figure 4.2.
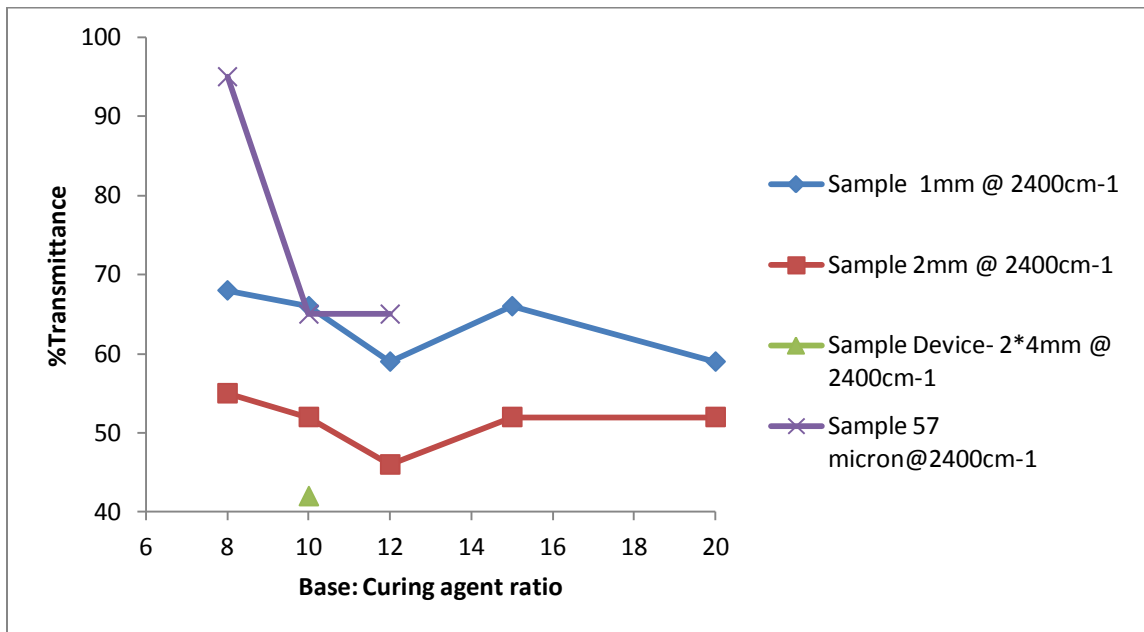
Figure 4.2: Variation in the base transmittance of PDMS samples with thickness at different base: curing agent ratios

It should be noted that in Figure 2.8 a similar transmittance profile has been plotted for PDMS slabs with the 1, 2 and 4mm thickness. In comparison, even though the absolute difference in transmittance in figure 2.8 between samples of varying thickness is exactly the same as in figure 4.2 where the difference in transmittance of 1mm and 2mm thick sample is about 10 %, the numerical values of base transmittances are higher for the samples in figure 2.8. The reason for this apparent discrepancy is that the scans for samples in figure 2.8 have been conducted in the entire spectral region from 7800 cm^{-1} to 1000 cm^{-1} while for the samples in figure 4.2 is in the Mid IR from 4000 cm^{-1} to 400 cm^{-1}. The noise exhibited in the Mid IR of PDMS is comparatively higher compared to the NIR and hence the absolute values of base transmittance tend to be lower when the scans are run only in the Mid IR compared to running scans through the whole spectrum.

4.3.2   Results and Discussion

The following can be noted from the above results.

- A general decrease in the value of % transmittance can be noted with increasing thickness, with the lowest transmittance recorded for the device.

- The maximum transmittance is obtained for 8:1 ratio for 57μm and it decreases with the thickness of the sample with the lowest value being recorded for 2 mm thick sample

- The transmittance values show a decreasing trend from 8:1 to 12:1 ratios for all thicknesses and this is line with the results in the literature

- A relatively sharp drop in transmittance is noted for a 57μm from 8:1 to 10:1 and it remains a constant from 10:1 to 12:1

- The transmittance profile shows a decreasing trend from 8:1 to 12:1 and then shows an increasing trend towards 15:1 and then remains almost a constant till 20:1 for both 1mm and 2 mm thick slabs.

- The lowest transmittance is exhibited by the device at 10:1

- As the variance of the % transmittance for samples of 1 mm and 2 mm are a maximum of about 10% and this is within the limits of the variability introduced by the instrument in its measurements

- A detailed study of the spectra indicate that the peaks of transmittance of PDMS in the Mid IR region do not shift with varying the base: curing agent ratio or does any desired effects as detailed in section 4.2 manifest.

- Because of all the above factors, it cannot be conclusively proved if base: curing agent ratio is a major influencing factor in the IR transmittance characteristics of PDMS

The variation of the mechanical properties of PDMS may have an effect on the optical properties of PDMS. The variation of base: curing agent ratio produces variation in the optical properties; however the results have not shown any manifestation of desired effects (ref section 4.2) in the Mid IR region. In order to further understand the effects of mechanical property modification in the optical properties, experiments with different heat treatment protocols of the sample have been designed.

4.4   Effect of Heat Treatment on the optical transmittance of PDMS in the Mid IR

Heat treatment of PDMS polymer has proven to be affecting the mechanical properties [68, 69].However the effects on optical properties have not been documented. Curing

time and curing temperature have shown to affect the properties of PDMS. The effect of heat treatment post fabrication (curing of polymer) on the optical properties have yet to be investigated, which is the goal of the present set of experiments. The transmittance profile of PDMS in the Mid IR is as shown below in figure 4.3
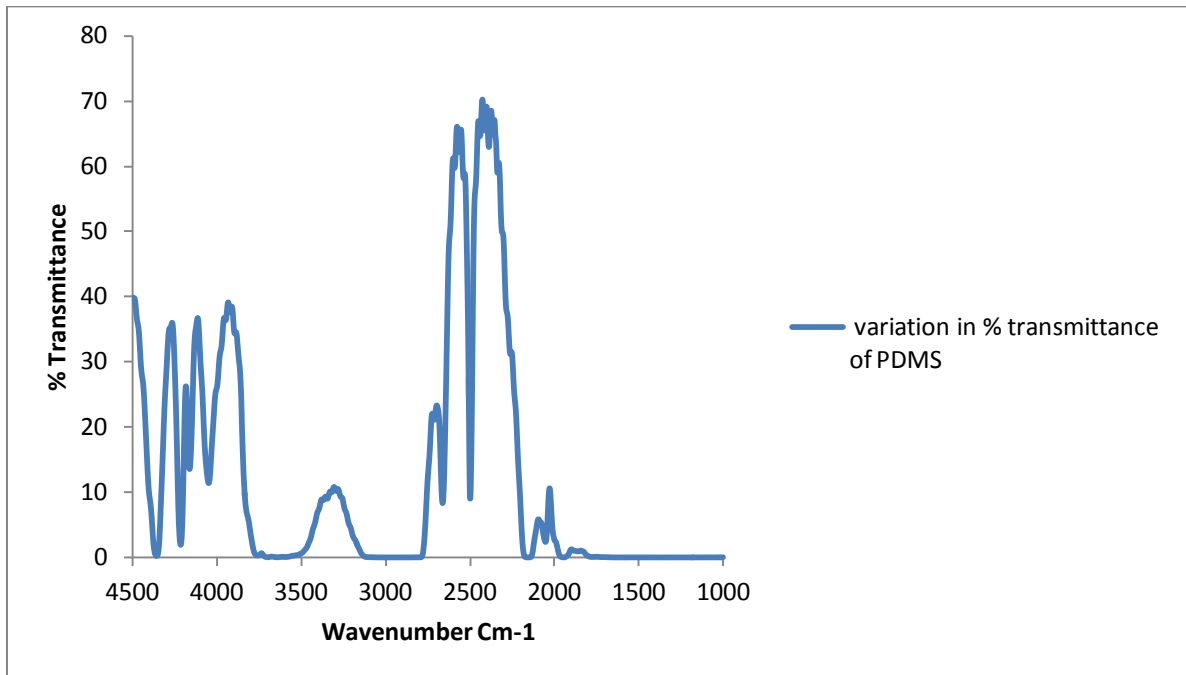
Figure 4.3: Percentage Variation of transmittance of PDMS in the Mid IR region

4.4.1 Materials and Methods

4.4.1.1 Experiment Summary

PDMS was fabricated as detailed in section 2.2.2.1.Sets of samples were cut out from the master plate. A preliminary set of spectra was recorded in the FTIR spectrometer. The sample was immediately taken to the heat-treatment area and subjected to heat treatment to a predefined time and temperature settings. This will be discussed in detail section 4.4.1.2. After the heat-treatment, the sample was immediately taken to the FTIR spectrometer area and subjected to spectral reading. Prior to the spectral analysis the

samples were thoroughly cleaned using IPA solution. After the spectral analysis, the samples were left for about 6hrs and again subjected to FTIR analysis. All the above spectra were recorded in the Mid IR region from 4000 cm^{-1} to 400 cm^{-1}. The difference introduced by these treatments on the base transmittance at 2400 cm^{-1} has been calculated by subtracting the transmittance recorded 6hrs after heat treatment to the base transmittance as in figure 4.5
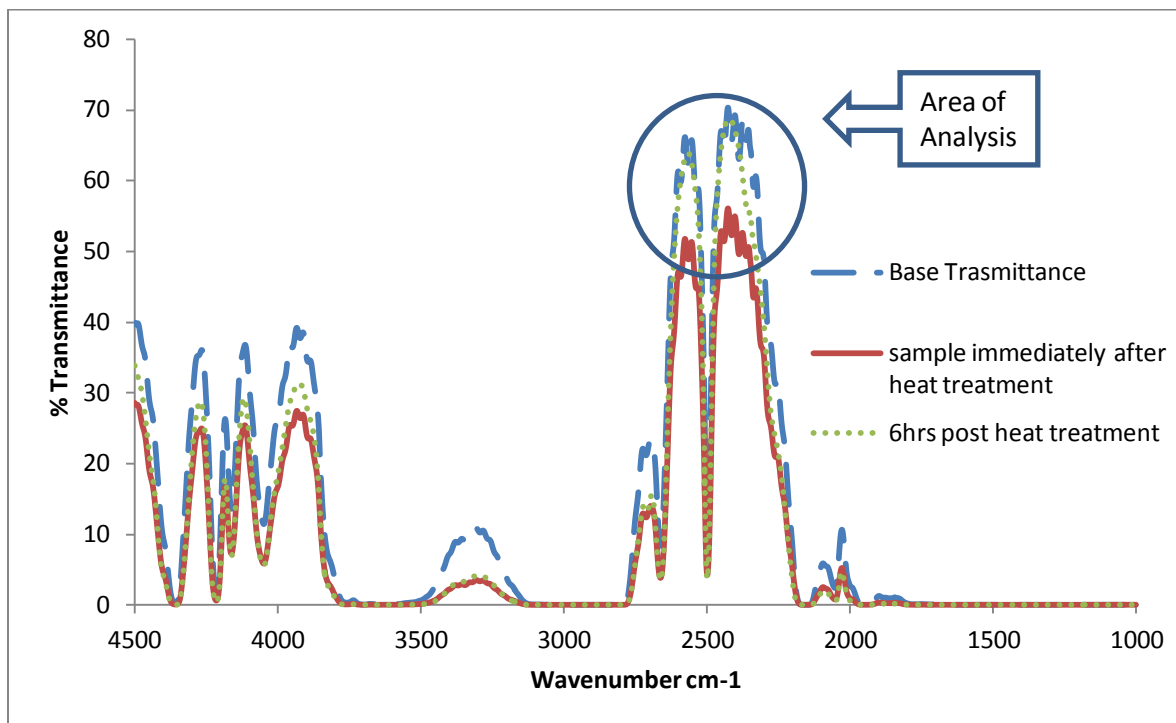
Figure 4.4: Spectral Calculation for the change of base transmittance in PDMS due to heat treatment

4.4.1.2 Heat Treatment Apparatus

The heat treatment apparatus consists of a Convection oven, Temperature control apparatus and Inert gas transfer arrangement. The convection oven has a silicon glass crucible with a sample loading bay for handling multiple variety of samples. The temperature control apparatus will help to set the temperature up to about 1000º C. The inert gas apparatus will help maintain a controlled flow of inert gas in the crucible to

maintain an inert atmosphere and remove the oxygen and water vapor from the crucible atmosphere. The inert gas used in the apparatus in generally nitrogen or argon. The apparatus layout is as detailed in figure 4.5. The samples are loaded and recovered through an iron spoke through the sample loading bay and samples are placed in the heating area in the crucible enclosed within the convection oven.
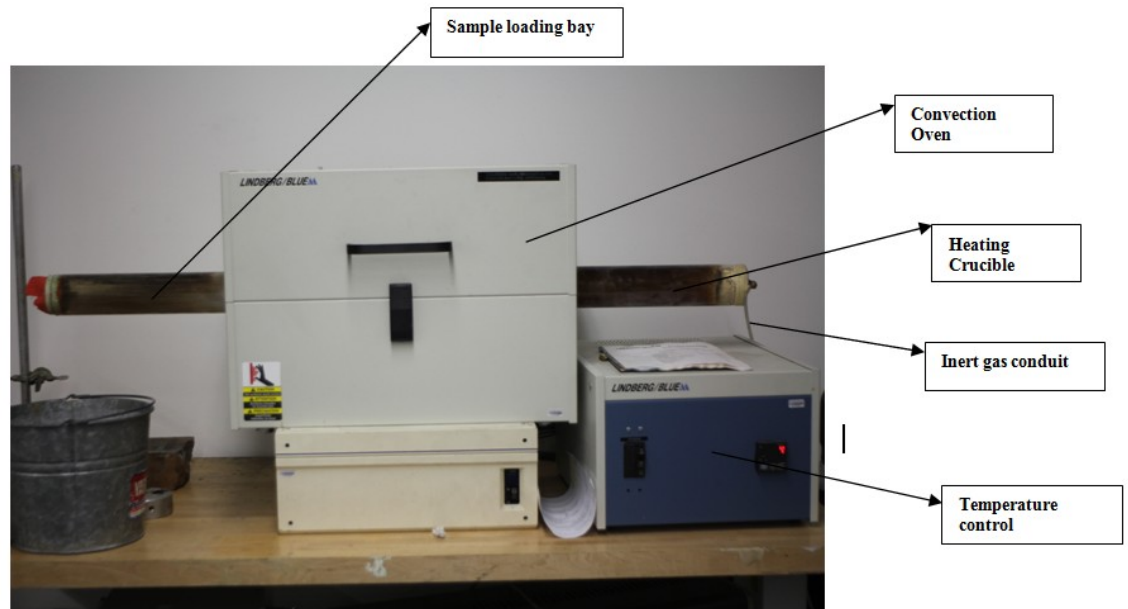
Figure 4.5: General Layout of the Heat Treatment Apparatus

The flow of inert gas is controlled through the flow gauge and the control valve. The flow exits through the sample loading bay.

4.4.2 Preliminary Set of Experiments

PDMS was fabricated as detailed in section 2.2.2 .1. The slabs which were cut out from the culture vessel were about 2 mm (±100 µm) thick. The thickness variations are due to errors introduced during the soft lithographic process. The slabs were subjected to a pre-heat treatment spectral analysis in the FTIR spectrometer. The samples were placed sandwiched between the windows of the CaF_2 cell Kit. The scans were conducted in Mid

IR (4000 cm^{-1} to 400 cm^{-1}) with 8 scans and a 4 cm^{-1} spectral resolution to provide an optimum balance between SNR and analysis time. Each sample was subjected to 3 runs to confirm the peaks. A total of 9 slabs (3 sets of 3 each) were cut out to the same thickness. The slabs were subjected to heat treatment in an inert atmosphere at 3 different temperatures 150º C, 225º C, 300º C .Each set of 3 slabs were loaded in the sample bay in the oven and kept at predetermined temperature (either at 150º C, 225º C, 300º C) for a predetermined time (30 min, 60 min, and 90 min). Each sample was unloaded at the end of its predetermined time and quenched in ambient air. After all the samples were unloaded, they were thoroughly cleaned using IPA solution.

The samples were carried to the FTIR spectrometer area and subjected to the spectral analysis with the same parameters mentioned above. In total all the 9 samples (30 min @150º C, 60 min@150º C and 90 min@150º C, 30 min @ 225º C, 60 min @ 225º C, and 90 min @ 225 º C, 30 min @ 300º C, 60 min @ 300º C and 90 min@ 300º C) were labeled as 3 sets of 3 samples. They were again subjected to a spectral analysis with the same parameters as mentioned above after 6 hrs from the heat treatment. The difference in the % transmittance values of the base spectra and post heat treatment spectra @ wave number 2400 cm^{-1}have been calculated and plotted against the particular sample as shown in figure 4.6.
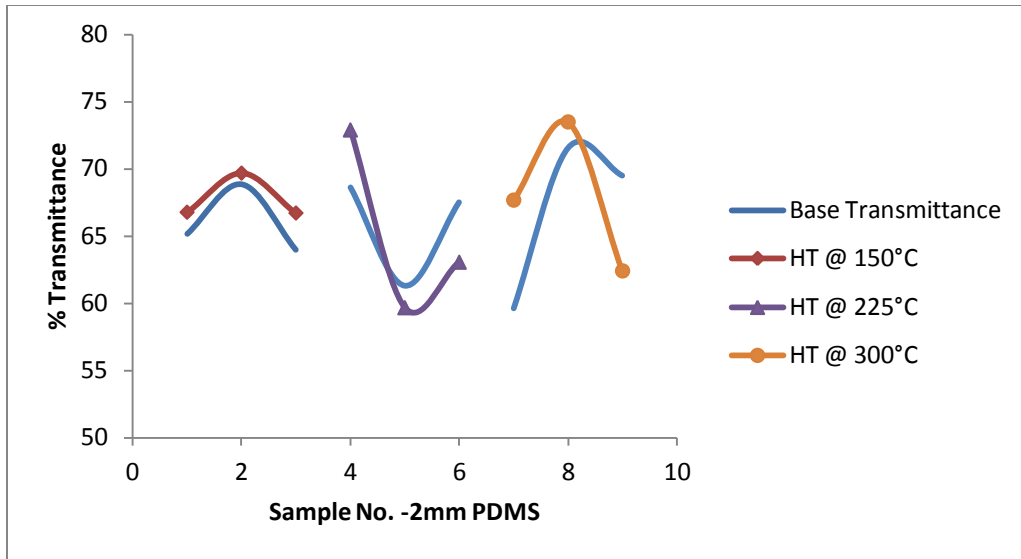
Figure 4.6: Variation in transmittance for a 2mm PDMS slab at different times

4.4.2.1 Results and Discussion

The following could be summarized from the spectral results plotted above in figure 4.6

- The samples show a marginal improvement in 30 minutes of heat treatment plot with increase in temperatures, lowest at 150ºC leading up to 300ºC

- The samples show no appreciable change at any temperature for 60 min of heat treatment

- The samples show a net decrease in the percentage variation of transmittance at 90 min for all temperatures with the largest decrease at the highest temperature 300 ºC

It can be inferred from the results that as 30 minutes of heat treatment at the highest temperature produces as positive variation in transmittance, samples could be tried at lower times with higher temperatures for a possible manifestation of the desired effects (section.4.2) .Also if samples of lower thickness say 1mm were tried, there could be a higher possibility of manifestation of the desired effects.

4.4.3 Second Set of Experiments

Based on the results discussed in section 4.4.2.1, a second set of experiments have been designed with of 3 sets of 4 samples each with a thickness of 1mm (±100 µm) in order to see a possible manifestation of the desired effects. PDMS slabs were fabricated as detailed in previous sections. A total of 12 slabs (4 sets of 3 each) were cut out from the silicon wafer culture vessel. They have been subjected to heat treatment at temperatures (150ºC, 225ºC, 300ºC and 375 ºC) at times 10 min, 20 min, and 30 min.

The samples were spectra analyzed prior to the heat treatment to understand the peaks as described in the previous section. After the heat treatment, the samples were thoroughly cleaned in IPA solution and then again subjected to spectral analysis immediately. The samples were again subjected to a spectral analysis after 6hrs from heat treatment. The samples have been labeled as (10 min@150 ºC, 20 min@150 ºC, 30 min@150 ºC, 10 min@225 ºC, 20 min@225 ºC, 30 min @ 225 ºC , 10 min@300 ºC , 20 min@300 ºC , 30 min@300 ºC, 10 min @ 375 º C, 20 min @ 375 º C, 30 min @ 375 º C) .The difference in the % transmittance values of the base spectra and post heat treatment spectra @ wave number 2400 cm^{-1} (Mid IR), in the vicinity where PDMS shows the highest transmittance in the Mid IR, have been plotted in figure 4.7.
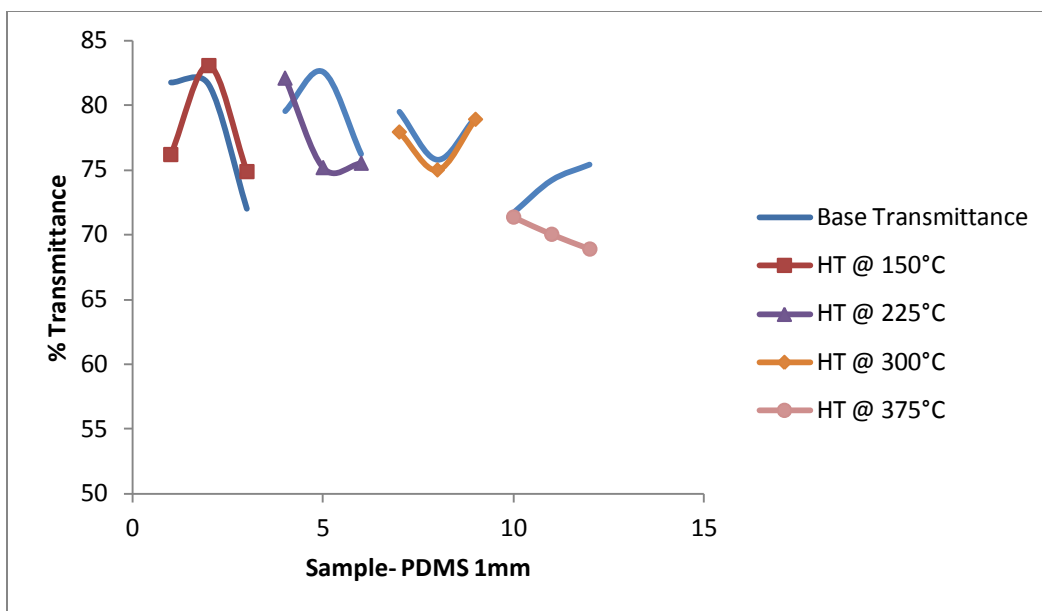
Figure 4.7: Variation in transmittance of 1 mm PDMS slab at different times

4.4.3.1 Results and Discussion

The following can be summarized from the results plotted in figure 4.7

- The results for 1mm have shown inconsistent trends across all times and temperature parameters

- The average variation of % transmittance is about 6 % from peak to peak for the plots at 10 ,20 and 30 minutes

- From the results it can be concluded that heat treatment has not produced any significant variation in base transmittance of the samples

- The desired effects explained in section 4.2 have not been manifested.

In order to understand further the results, the base transmittances of 6 samples of 1mm and 2mm each were plotted (figure 4.8)
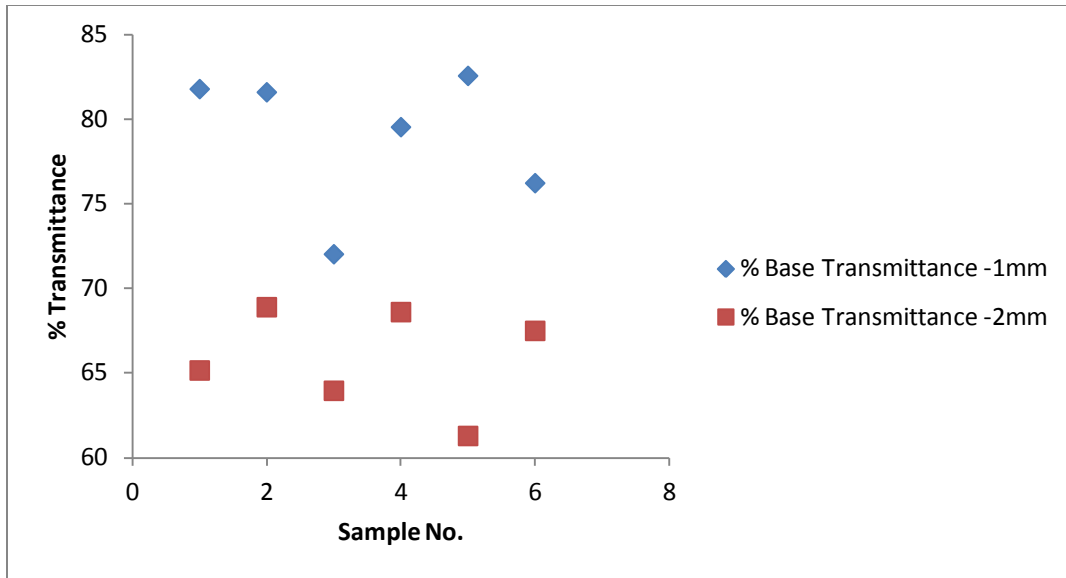
Figure 4.8: Variation in base transmittance across samples in 1mm and 2mm PDMS samples

The results expressed in the plot can be summarized as below

- The base transmittances for 1mm samples show a variation of about 15 % across the 6 samples

- The base transmittances of 2 mm samples show a variation of about 8 % across the 6 samples

- It can be noticed that as the thickness of the samples increase, the % variation of base transmittances reduces, and so thicker samples should produce less variation in base transmittance

- These variations could be due to the errors (± 100 μm) in thickness introduced due to fabrication process of PDMS.

- The effect of these errors on a 1mm thick sample is higher than that in a 2 mm sample and so the inconsistency in results shown by the plot of 1 mm samples in heat treatment is higher than those shown by 2mm.

In order to reduce the impact shown by the variation introduced by thickness, 4mm slabs were fabricated and were subject to heat treatment protocols

4.4.4   Third Set of Experiments

For the third set of experiments total of 6 slabs of 4mm (±100 μm) were cut out from the silicon wafer where PDMS was fabricated(as in section2.2.2.1) .The heat treatment times are set at 30 min and 60 min in order to offset the effects produced by longer times in the first set of experiments. The same protocol as in first set of experiments were followed prior to heat treatment and after heat treatment spectral analysis of the samples. The samples have been labeled as (1 slab of 30 min@150 ºC, 1 slab of 60 min@150 ºC, 1slab of 30 min@225 ºC, 1slab of 60 min@225 ºC, 1slab of 30 min@300 ºC, 1 slab of 60 min@300 ºC).

The samples were subjected to spectral scanning prior to heat treatment to note the base spectra, immediately after heat treatment and after 6hrs of heat treatment and termed as post heat treatment. The difference in the % transmittance values of the base spectra and post heat treatment spectra @ wave number 2400 cm^{-1} (Mid IR), in the vicinity where PDMS shows the highest transmittance in the Mid IR and@ 5900 cm^{-1} (NIR) in the vicinity where PDMS shows the minimum value in NIR have been calculated and plotted against the particular sample. The spectral parameters are as detailed in section 4.5.5. The results have been plotted in figure 4.9-4.10
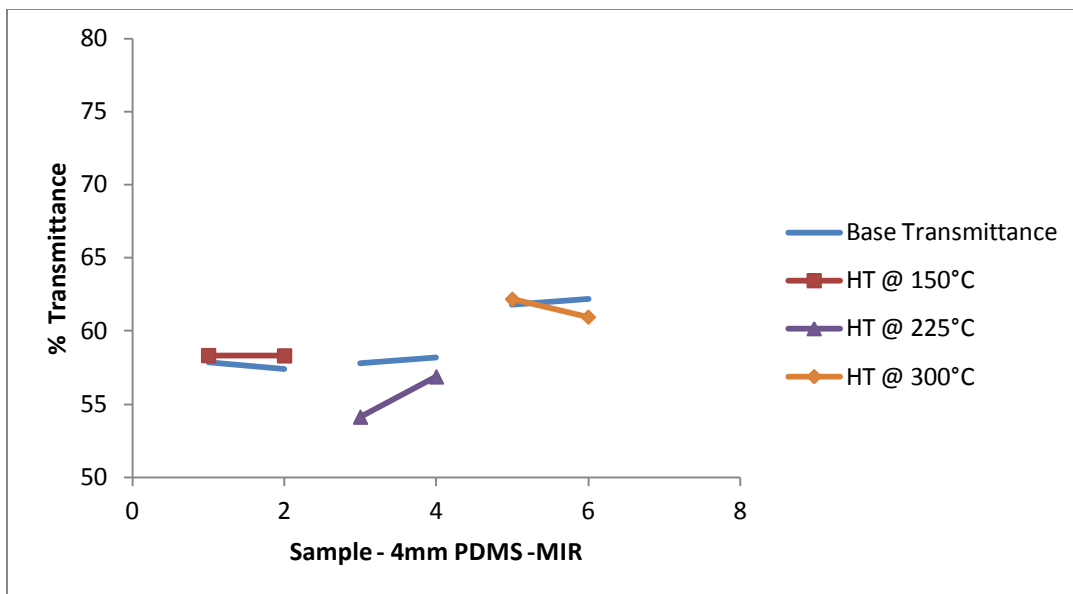
Figure 4.9: Variation in Transmittance for 4 mm PDMS slabs in the MIR region at different times
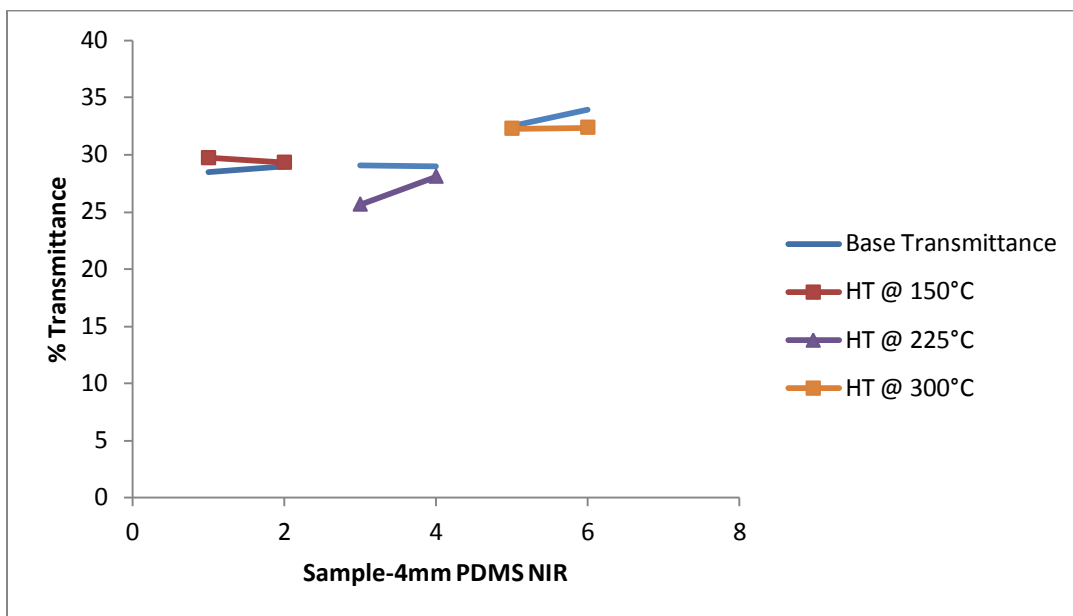
Figure 4.10: Variation in Transmittance of 4mm PDMS slabs in the Near Infrared Region at different times

4.4.4.1   Results and discussion

The following can be summarized from the plots 4.9 and 4.10 below

- The Plots for % variance in transmittance in both Mid IR and NIR show inconsistent results as in previous cases.

- The plots have shown a maximum variance of about 5% which are as a result of the errors introduced due to thickness variation($\pm$ 100 µm) introduced in the PDMS fabrication in the base transmittances as shown in plot 4.11
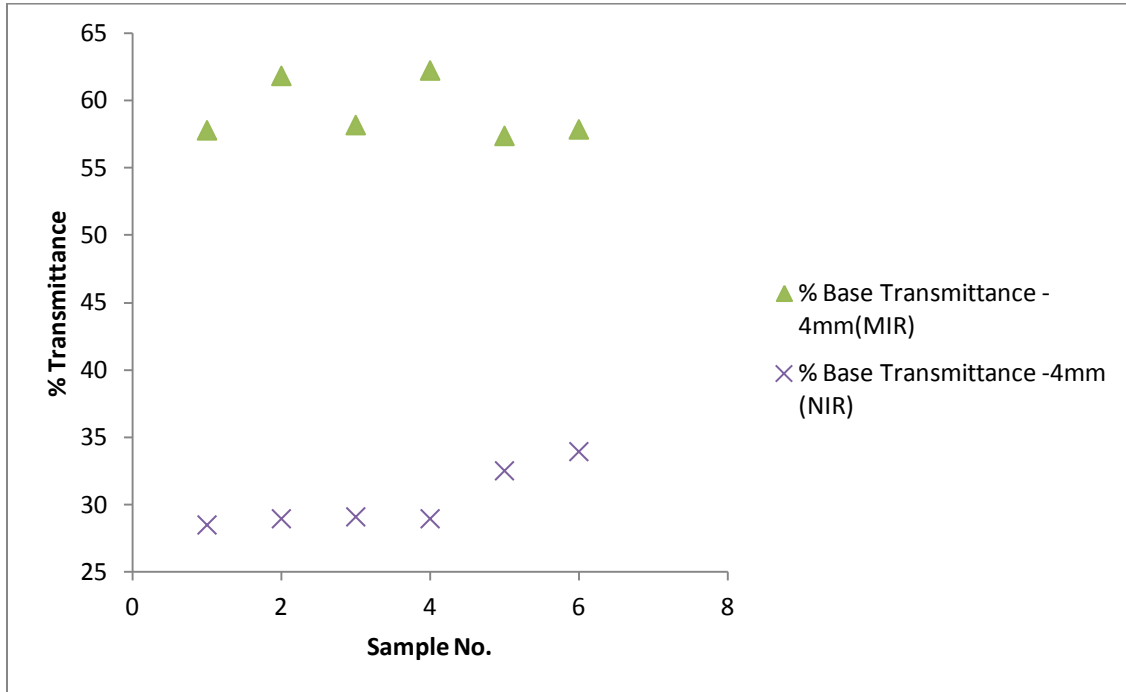
Figure 4.5: Variation in Base Transmittance of 4 mm PDMS slabs at Mid IR and Near IR at different times

4.5   Summary

In this chapter, experiments with varying curing agent ratios were performed to study its effect on the optical property of PDMS in the MIR region. While the results show marginal improvement of transparency for a ratio of 8:1 compared to 10:1, the use of manufacturer recommended 10:1 ratio was found to be suitable at higher thicknesses. Further, different heat treatment protocols with varying temperature and time have been conducted. These treatments have not produced the desired results in improving the MIR

transparency of PDMS. This has been attributed mainly to two factors, (a) base transmittances vary from sample to sample and the variations amount to about 5% in case of 4mm samples to 15% in case of 1mm samples, due to fabrication limitations. (b) at higher thicknesses where the base transmittances have lesser variance, heat treatment did not introduce appreciable change in the transparency in the MIR region. Detailed investigations are needed in other prefabrication treatments like modifying the chemical matrix that can improve the transparency of PDMS in MIR, which is beyond the scope of the current thesis objectives. As the transmittance is higher in NIR for PDMS, trials could be conducted in proving the concept of use of PDMS in that region, which is the objective pursued in the next chapter.

CHAPTER 5.   PDMS AS A WINDOW MATERIAL IN NIR

In the last chapter, attempts were made to effect optical property modification in the Mid IR region by using different curing agent ratios and through heat treatment. It has been observed that more trials need to be conducted to obtain consistent and reliable results by these processes. So, in order to provide a proof of concept for the use of PDMS as a substitute window material, experiments have been conducted in the NIR. As it has been documented in Chapter-2, PDMS shows better transmittance in NIR region compared to the Mid IR region as shown in figure 5.1.
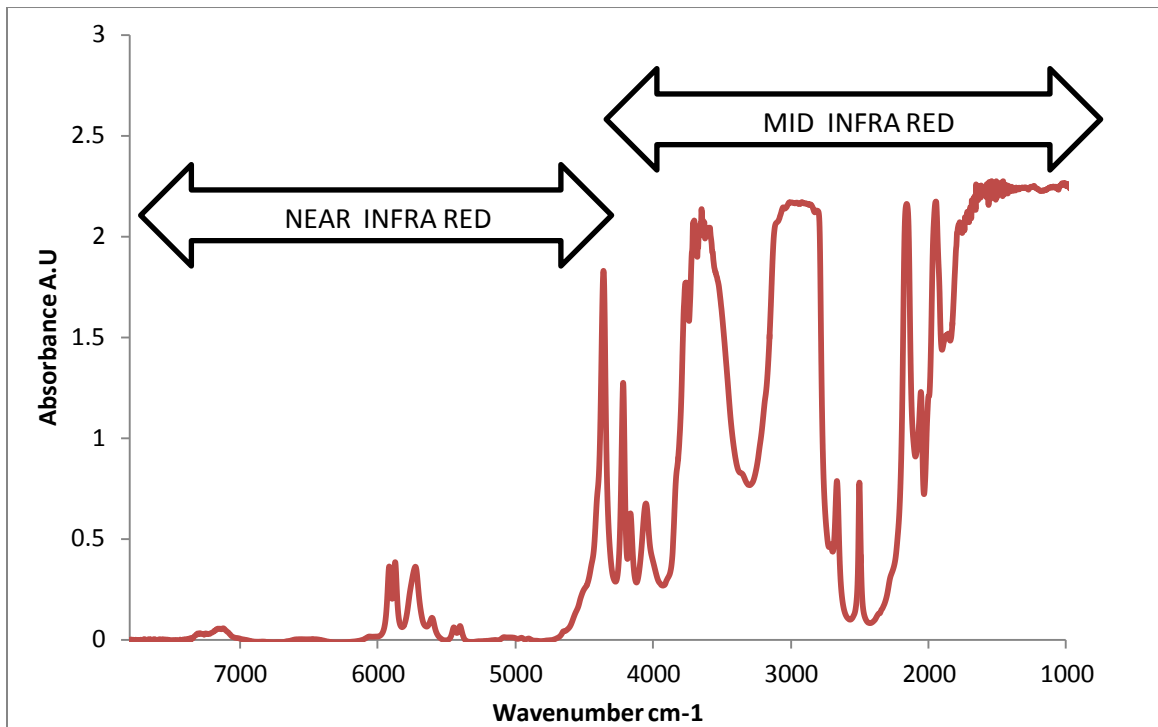
Figure 5.1: Infrared Spectra of a PDMS sample in the Near IR and Mid IR region

However it is important to note that, unlike the previous chapters, here the y axis is absorbance instead of transmittance. The reason for this shift is, to compare the achieved results with that of the literature especially in the area of food quality testing, the works

show absorbance. This does not change anything in the processing; transmission is just the inverse of absorbance in the logarithmic scale. In order to understand the performance of PDMS in the NIR region, experiments have been conceived with samples having characteristic absorbance peaks in NIR. Extra Virgin Olive Oil (EVOO) has been used as the sample and its characteristics have been studied both with the help of CaF_2 kit and a PDMS kit.

Based on the results it can be concluded that PDMS is in fact a suitable window material in the NIR region in lieu for CaF_2 kit. Experiment results have also been used to advance the concept of Critical Volume Ratio (CVR) which is explained in the further sections.

5.1 Summary of Experiments

The experiment procedure can be summarized as follows

- 2 slabs of PDMS with thickness of 4 mm each is fabricated in dimensions of the existing cell kit(ref section 2.2.2.1 and 2.3.4) and named (2X4)kit

- 2 slabs of PDMS with thickness of 2mm each is fabricated in dimensions of the existing cell kit(ref section 2.2.2.1 and 2.3.4) and named (2X2)kit

- Spacers of 100 µm, 190 µm, 400 µm 1000 µm and 2850 µm are arranged.

- The sample, Extra Virgin Olive Oil(EVOO) is loaded on a CaF_2 kit and its characteristic peaks are explored

- The EVOO sample is loaded on 2X4and 2X2 PDMS kits and then subjected to characterization

- A comparative analysis is done on the performance on both the PDMS Kits in the NIR and also in comparison with the CaF_2 kit

5.2   Materials and Methods

5.2.1   PDMS Fabrication

Commercially available PDMS polymer was mixed in ratio of 10:1 as described in the previous sections. The polymer was cured on a silicon wafer in an oven kept at 60ºC overnight. Two separate wafers were used for fabrication and slabs of thickness 2mm and 4mm thickness each were cut out in the dimensions of the CaF_2 window. These slabs were characterized in the NIR region for their peak absorbencies.

5.2.2   Spacers

The standard sizes of spacers available as accessories from Perkin Elmer™ are 100μm, 190μm, 400μm, 500μm and 2850μm. A 1000μm PDMS spacer was fabricated for the exclusive use in this work.

5.2.3   Setup

The original optical layout of the device is maintained as in the previous experiments (figures 2.14-2.16). The PDMS slabs are mounted in place of the original CaF_2 slabs in cell kit holder.

5.2.4   Sample

Extra Virgin Olive Oil (EVOO) has been chosen as the sample for this work due application reasons as well because of the advantages that it's easily available, is non-aqueous, has high fatty acid concentration, is stable at room temperature and is easy to handle. Extra Virgin Olive Oil (EVOO) was commercially procured from the local

market and was stored in room temperature in a cool and dry place away from direct sunlight.

5.2.5 *Experiments with the CaF₂ kit*

A sample of EVOO was placed in a 190μm spacer and was characterized using a CaF_2 cell kit. The scans were done in NIR (7800-4500 cm^{-1}). 8 scans were run for each trial with a resolution of 4 cm^{-1}. 3 runs each with the same specification were conducted to confirm the peaks. The peaks introduced by the fatty acid functional groups can be noted at 7185 cm^{-1},7078 cm^{-1} which are CH_3 second overtone and 5793 cm^{-1} and 5678 cm^{-1} which are CH_2 1st overtone. The results presented in the table 5.1 indicate the normalized values of the peaks expressed by EVOO and PDMS in the NIR region. The peaks were normalized with respect to 5793 cm^{-1} at 1.5 A.U. The peaks introduced (figure 5.2) by EVOO at 5793 cm^{-1} (EVOO-1), 5678 cm^{-1} (EVOO-2), 7078 cm^{-1} (EVOO-3), 7185 cm^{-1} (EVOO-4) are generic with any fatty acid family and the presence of these groups can indicate any vegetable oil specimen. Specialized data post processing steps like PLS are existent to understand the specific oil group. However, in this case, as the sample is already known, the peaks can be used as reliable data. The results (figure 5.2) have been compared with literature (figure 5.2) and in the table5.1

Experiments for Relative Absorbance Comparison	Absorbance/Wave number(± 5 cm^{-1})			
	7185 EVOO-4	7078 EVOO-3	5793 EVOO-1	5678 EVOO-2
LITERATURE [61]	0.24	0.24	1.50	0.9
CaF₂ KIT	0.3	0.29	1.50	1.03

Table 5.1: Comparison of CaF2 KIT with Literature for EVOO peaks
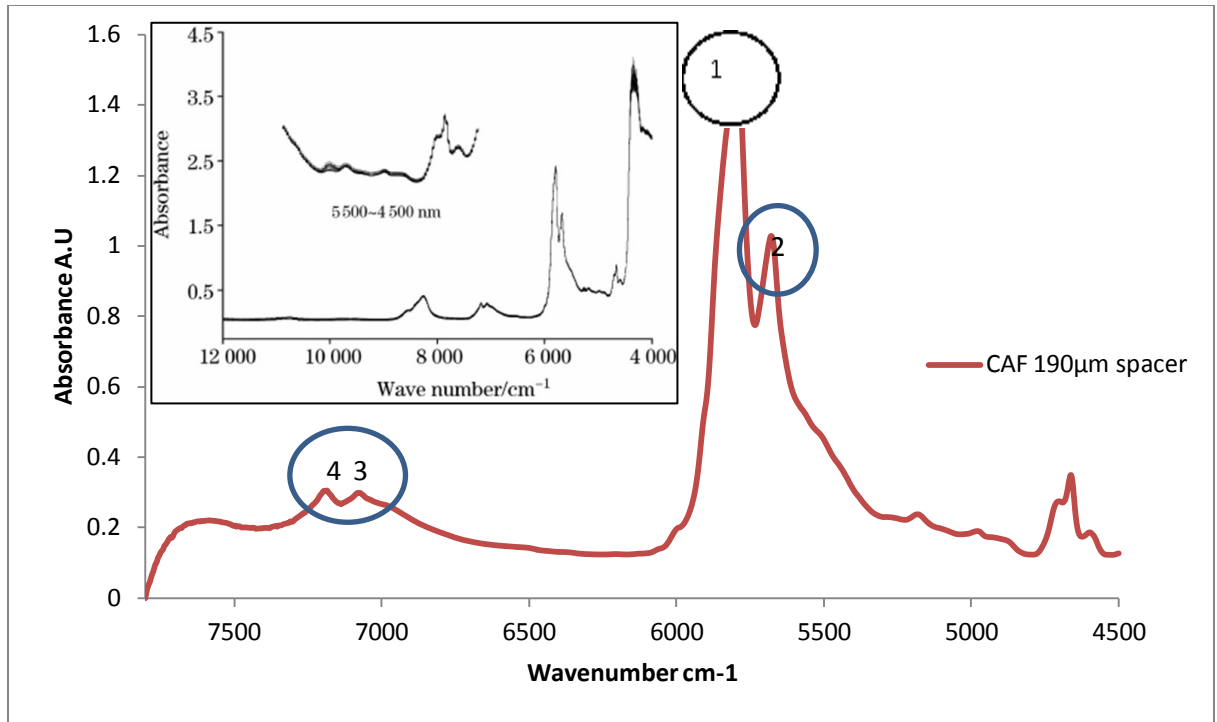
Figure 5.2: NIR Spectra of Olive oil in a CaF2 kit (insert shows the spectra from [70])

The results show good conformance with the literature for the peaks labeled 1, 2, 3 & 4. The results have been documented in table

5.2.6 *Experiments with PDMS 2X4 kit at 190 μm*

In order to understand the performance of the PDMS kit, a 2X4 kit with a sample thickness of 190μm was used to explore the effects of PDMS on the NIR spectra of EVOO.
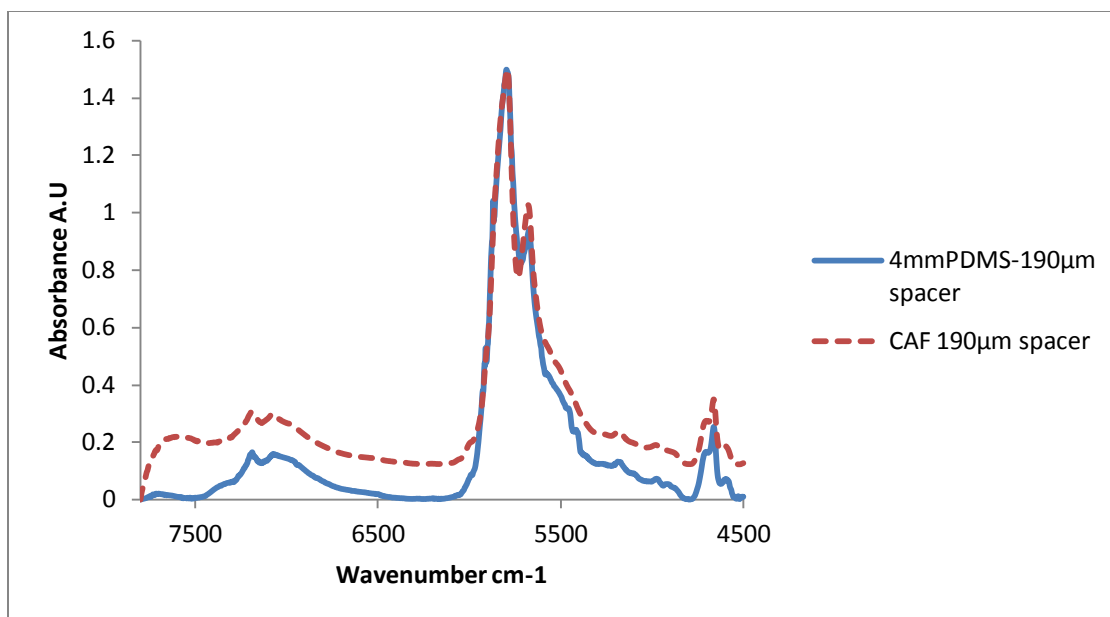
Figure 5.3: Comparison of EVOO NIR spectra in PDMS, CaF_2 kits

Experiments for Relative Absorbance Comparison	Absorbance/Wave number(± 5 cm^{-1})				
	7185	7078	5793	5678	5870(Peak of PDMS)
CaF$_2$ kit	0.3	0.29	1.50	1.03	NA
PDMS 4-190 kit	0.16	0.16	1.50	0.91	1.23

Table 5.2: Comparison of CaF_2 kit and PDMS 2X4-190 kit with EVOO peaks

The spectra of EVOO in 2X4 kit and CaF_2 kit is compared as above. Due to the inherent absorbance characteristics of PDMS in the NIR region in the 5900 cm^{-1} to 5500 cm^{-1} region, these peaks have a tendency to mask the peaks of CH_2 1st overtone of EVOO. Hence although a close correspondence can be noticed at 5793 cm^{-1} and 5678 cm^{-1} wave numbers by EVOO both in the 2X4 kit and CaF_2 kit, the interference produced by the PDMS artifacts' can be noticed in the region 5900 cm^{-1} to 5500 cm^{-1} at 5870 cm^{-1} with 1.23 AU.

In order to understand the effect of PDMS characteristics in EVOO spectra, further experiments were designed. The goal was to achieve the value for a Critical Volume Ratio (CVR) which will decide the minimum volume of sample needed for a given thickness of PDMS kit, in order that a particular sample characteristic is expressed equivalently as would have been in a CaF_2 kit. The highest spacer thickness available with the equipment is 2850μm. An experiment was designed with the said spacer on 2*4 kit and the results have been compared with CaF_2 kit with 190μm.

5.2.7   *Experiments with PDMS 2X4 kit at 2850 μm*

The results of the analysis of EVOO with a PDMS kit having a 2850 μm spacer are compared with the CaF_2 kit (figure 5.5, table 5.3). It can be noticed that a close correspondence is obtained in the peaks of EVOO as well as the PDMS peak in 5870 cm^{-1} is virtually nonexistent due to the masking of the peak by the EVOO peaks absorbance
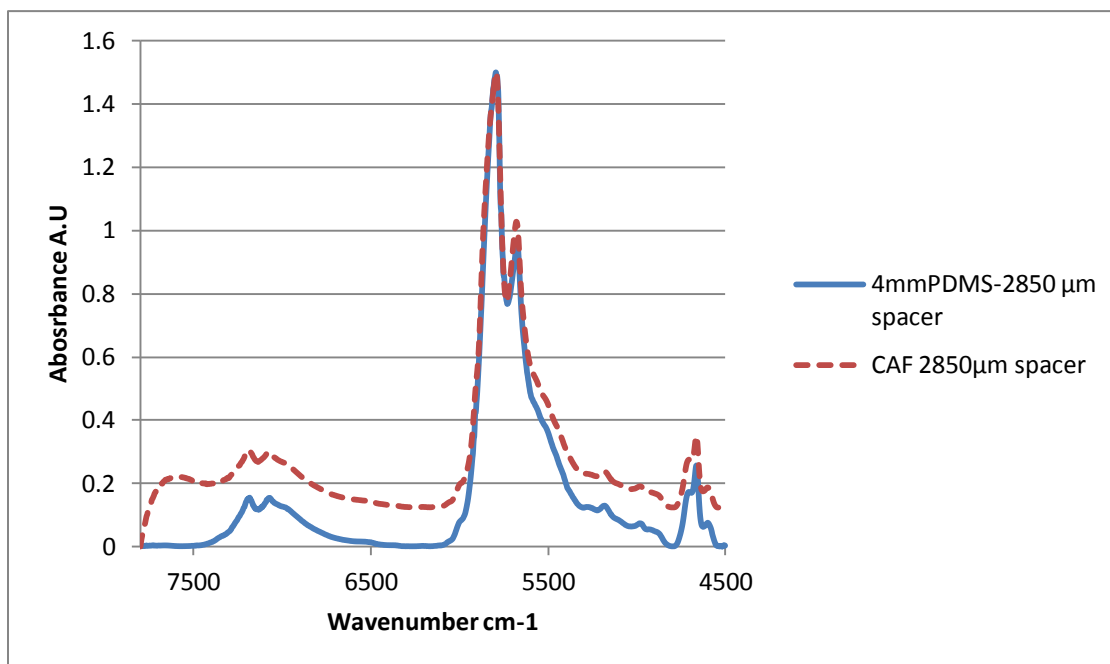
Figure 5.4: Comparison of EVOO NIR spectra in 2X4 2850 kit and CaF_2 kit

Experiments for Relative Absorbance Comparison	Absorbance/Wave number(± 5 cm^{-1})				
	7185	7078	5793	5678	5870(Peak of PDMS)
CaF$_2$ KIT	0.3	0.29	1.50	1.03	NA
PDMS 4-2850 KIT	0.15	0.16	1.50	0.97	None

Table 5.3: Comparison of CaF$_2$ kit with PDMS 2X4-2850 kit for EVOO peaks

A closer correspondence has been obtained compared to the previous set. However, more iterations with different spacer sizes are in order to arrive at the MINIMUM sample size required to achieve the result in Figure.5.3 for obtaining a CVR.

5.2.8   Experiments with PDMS 2X4 kit at 1000 µm

The spacer sizes in PDMS kit were reduced to about 1000 µm and the results compared with a CaF$_2$ kit (figure 5.6, table 5.4). Although there is correspondence obtained for EVOO peaks, the PDMS artifacts are introduced at 5870 cm^{-1}.
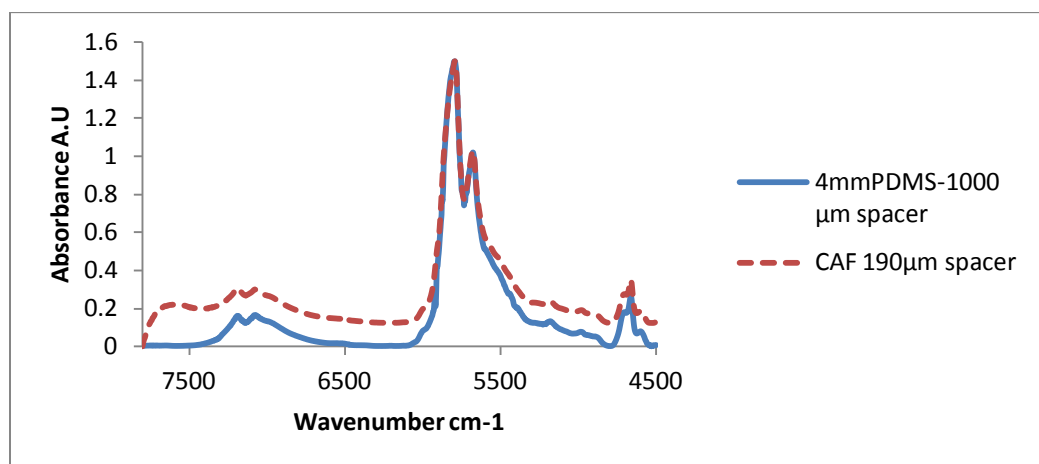
Figure 5.5: Comparison of EVOO NIR spectra in 2X4 1000 kit and CaF$_2$ kit

Experiments for Relative Absorbance Comparison	Absorbance/Wave number(± 5 cm-1)				
	7185	7078	5793	5678	5870(Peak of PDMS)
CaF$_2$ KIT	0.3	0.29	1.50	1.03	NA
PDMS 4-1000 KIT	0.16	0.16	1.50	1.02	0.77

Table 5.4: Comparison of CaF$_2$ kit with PDMS 2X4-2850 kit for EVOO peaks

Further trials are conducted with a 400 µm spacer in order to see if the results of 1000 µm can be repeated.

5.2.9   Experiments with PDMS 2X4 KIT at 400µm

The results of the analysis of a PDMS at 400 µm have been compared with the CaF$_2$ kit as in figure 5.7 and table 5.5
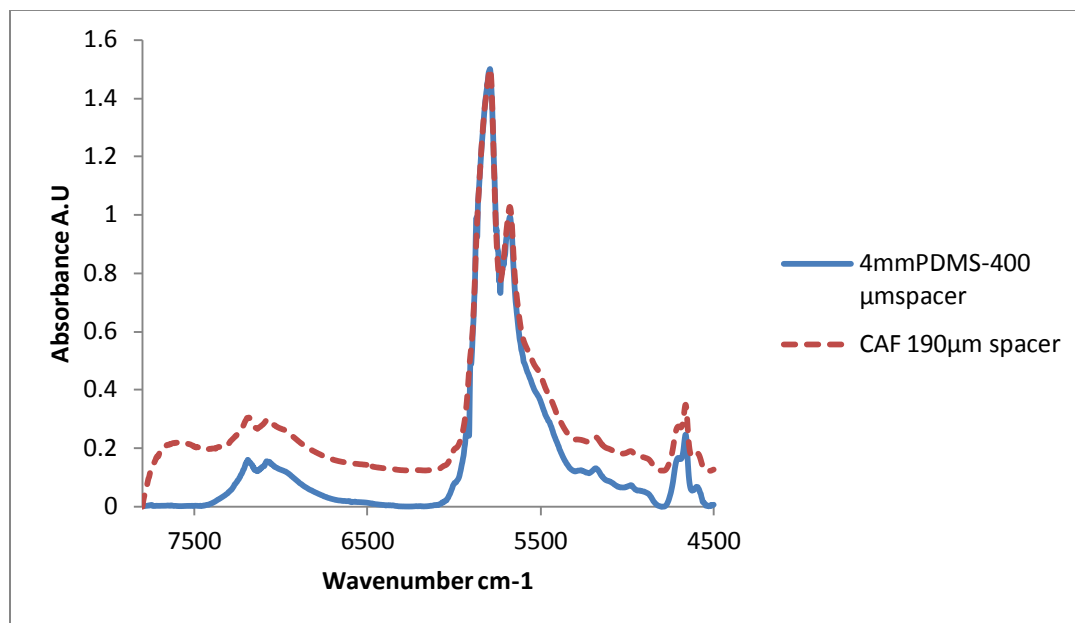

Figure 5.6: Comparison of EVOO NIR spectra in a 2X4-400 kit and CaF$_2$ kit

Experiments for Relative Absorbance Comparison	Absorbance/Wave number(± 5 cm^{-1})				
	7185	7078	5793	5678	5870(Peak of PDMS)
CaF$_2$ kit	0.3	0.29	1.50	1.03	NA
PDMS 4-400 kit	0.16	0.16	1.50	0.93	0.92

Table 5.5: Comparison of CaF$_2$ kit with PDMS 2X4-400 kit for EVOO peaks

It is observed from the Figure 5.5 that a close correspondence is observed with a PDMS kit and a CaF$_2$ kit at a 400 µm spacer thickness of sample. Any decrease in the sample size below this value for a 2X4 Kit could cause introduction of PDMS artifacts' as shown in for the results of 190 µm.

Hence for a PDMS 2X4 kit which has a total PDMS path length of 8000 µm requires a MINIMUM sample size of 400 µm for reliable detection of the sample characteristics. The CVR for EVOO in a 2X4 PDMS KIT is 400/8000 or 1:20 which shows that PDMS is 20 times less absorbent in the NIR region as compared to EVOO.

5.2.10 Comparison of the results of 2X4 PDMS kit with a 2X2 PDMS kit

In order to corroborate these results, a 2X2 kit was used with spacer thicknesses 100 µm and 190 µm and the results compared with 2X4 kit with spacers of 190 µm and 400 µm respectively. 2 different samples of EVOO were compared in the 2X2 and 2X4 kits as shown if Figure 5.8-5.9. The samples were examined in the area of EVOO peaks and in the region 5900 cm^{-1} to 5600 cm^{-1} where the characteristics of EVOO and PDMS are simultaneously expressed. The samples were scanned at 8 scans per run with a spectral resolution of 4 cm^{-1}. 3 runs were conducted to obtain conformance on the peaks. The spectral results of the samples loaded in both these kits were averaged and the results

indicate a close corroboration in the peaks expressed by PDMS as well as EVOO by both 2*2 and 2*4 kits, as shown in tables 5.6-5.7. The PDMS 2-100 kit (table 5.6) shows a higher AU value because of the higher absorbance of inherent PDMS artifacts' in the region masking the EVOO peaks.
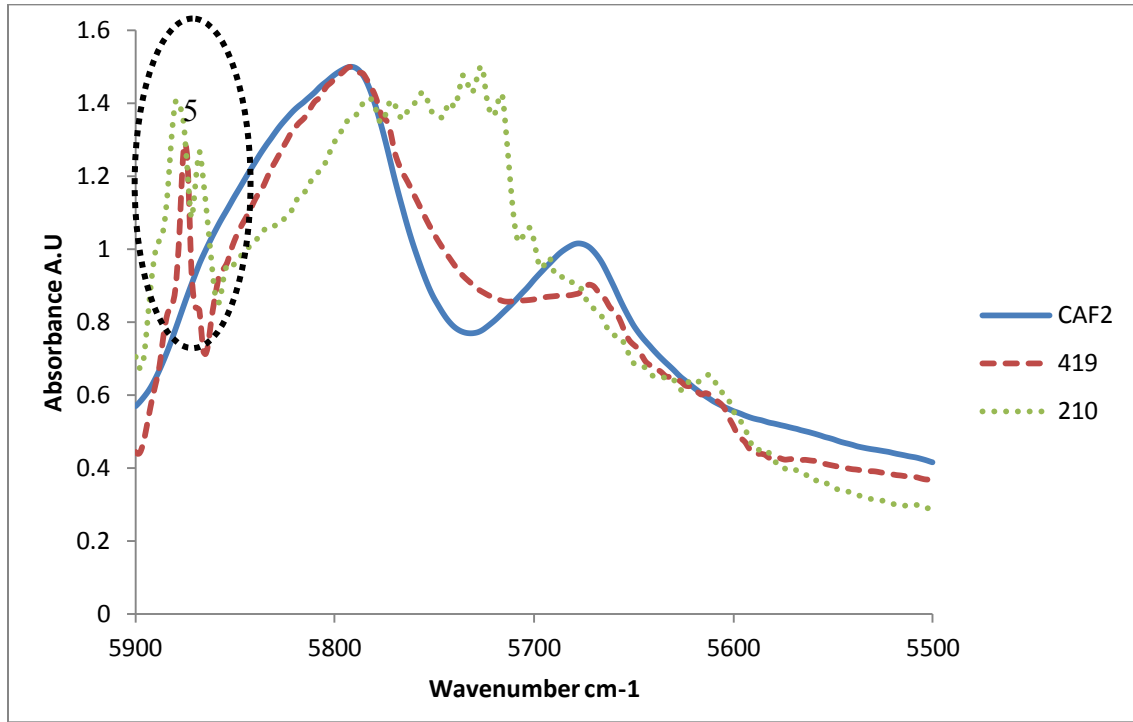
Figure 5.7: Comparison of Sample EVOO NIR spectra in 2X2 100, 2X4 190 kits and CaF$_2$ kit

Experiments for Relative Absorbance Comparison	Absorbance/Wave number(± 5 cm^{-1})				
	7185 (EVOO-4)	7078 (EVOO-3)	5793 (EVOO-1)	5678 (EVOO-2)	5870 (PDMS peaks)-5
CaF$_2$ kit	0.3	0.29	1.50	1.03	NA
PDMS 4-190 kit	0.16	0.16	1.50	0.91	1.23
PDMS 2-100 kit	0.22	0.23	1.50	1.13	1.25

Table 5.6: Comparison of CaF$_2$ kit with PDMS 2X4 -190, PDMS 2X2-100 kit for EVOO peaks
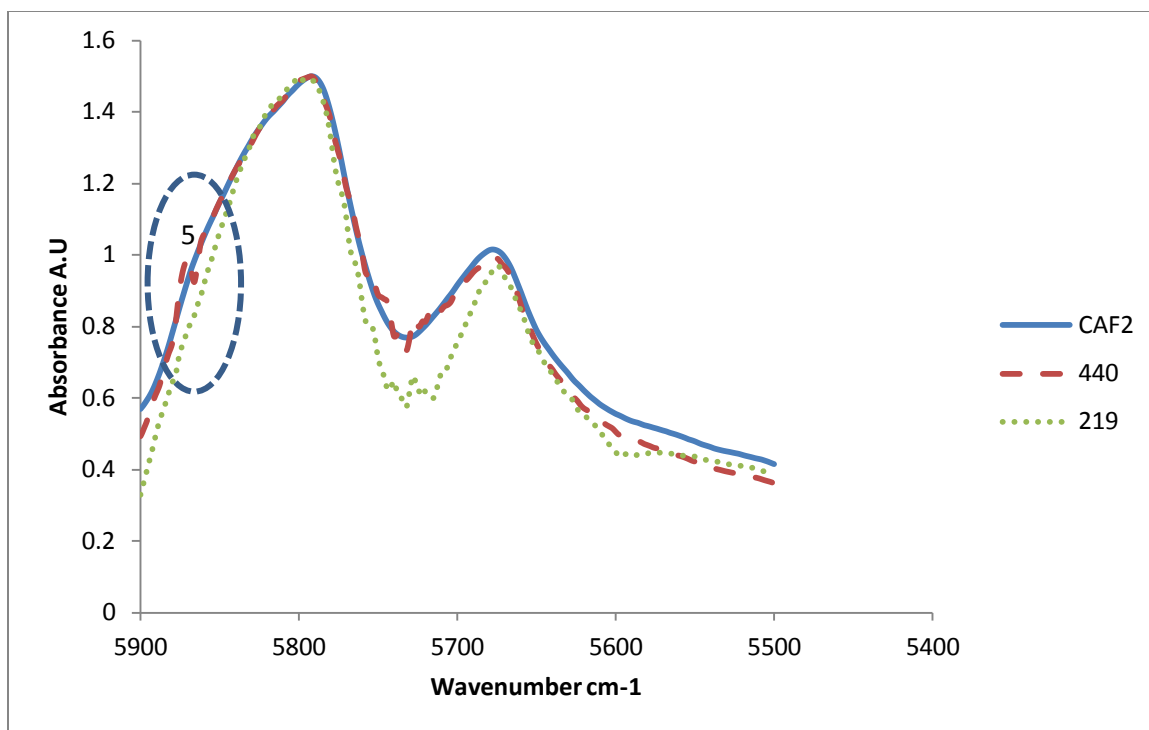
Figure 5.8: Comparison of Sample EVOO NIR spectra in 2X2-190, 2X4 -400 kits and CaF$_2$ kit

Experiments for Relative Absorbance Comparison	Absorbance/Wave number(± 5 cm^{-1})				
	7185 (EVOO-4)	7078 (EVOO-3)	5793 (EVOO-1)	5678 (EVOO-2)	5870 (PDMS peaks)-5
CaF$_2$ kit	0.3	0.29	1.50	1.03	NA
PDMS 4-400 kit	0.16	0.16	1.50	0.93	0.92
PDMS 2-190 kit	0.15	0.14	1.50	0.95	0.93

Table 5.7: Comparison of CaF$_2$ kit with PDMS 2X4-400 kit, PDMS 2X2-190 kit for EVOO peaks

This was also compared with the results of CaF$_2$ kit. This establishes that CVR is a scalable concept and the CVR of 1:20 for EVOO in the previous section can be equally applied in the 2X2 Kit. In order to further corroborate this concept, 2X2 kit with 2850 μm sample thickness was compared with CaF$_2$ Kit 190 μm sample. The results are shown in Figure 5.10
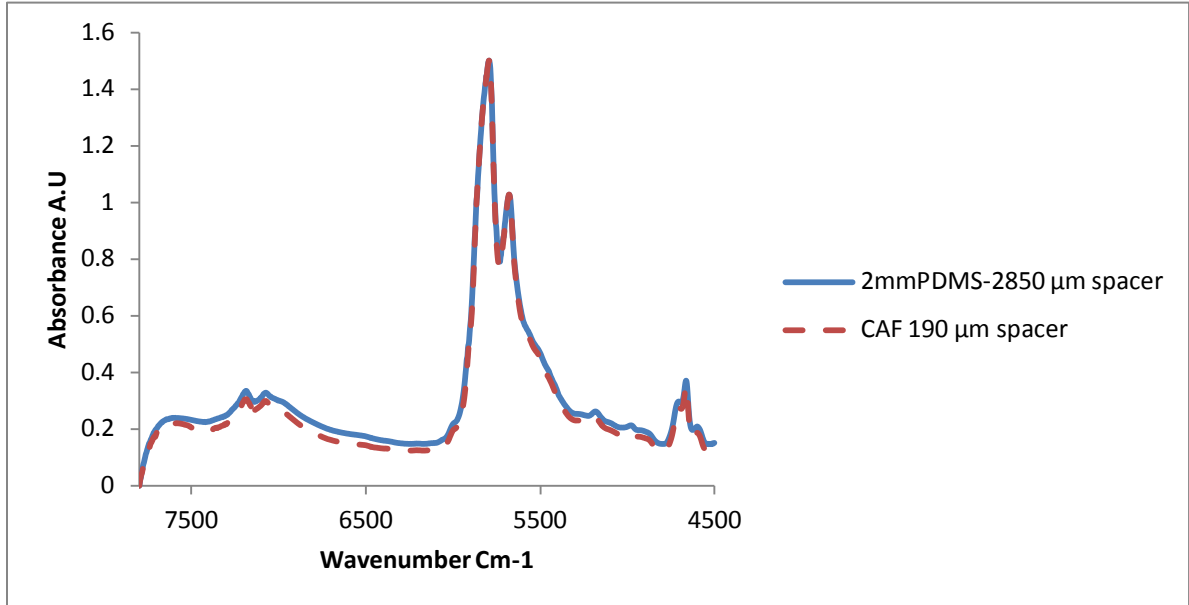
Figure 5.9: Comparison of EVOO NIR spectra of 2X2 2850 kit and CaF_2 kit

5.3 Establishing Proof of Concept in NIR

The results presented above can be summarized by figure 5-11 and table 5-8. It can be seen the closest correspondence to the results of EVOO peaks is obtained by a 2*4-2850 μm PDMS kit (figure 5.10-5.11). The concept of CVR can be extended in a 2*4 PDMS kit with a higher spacer size to obtain the same results as obtained in the 2*2 kit.

It can be concluded from the above results that a proof of concept for using PDMS in the NIR region for the detection of desired liquid state analyte can be established. Hence PDMS proves to be a suitable substitute for CaF_2 kit in the NIR region. These experiments could be extended to any analyte which has its characteristic peaks expressed in the NIR region. Once a suitable CVR is established, the PDMS kit can be used in lieu of the existing CaF_2 kit.
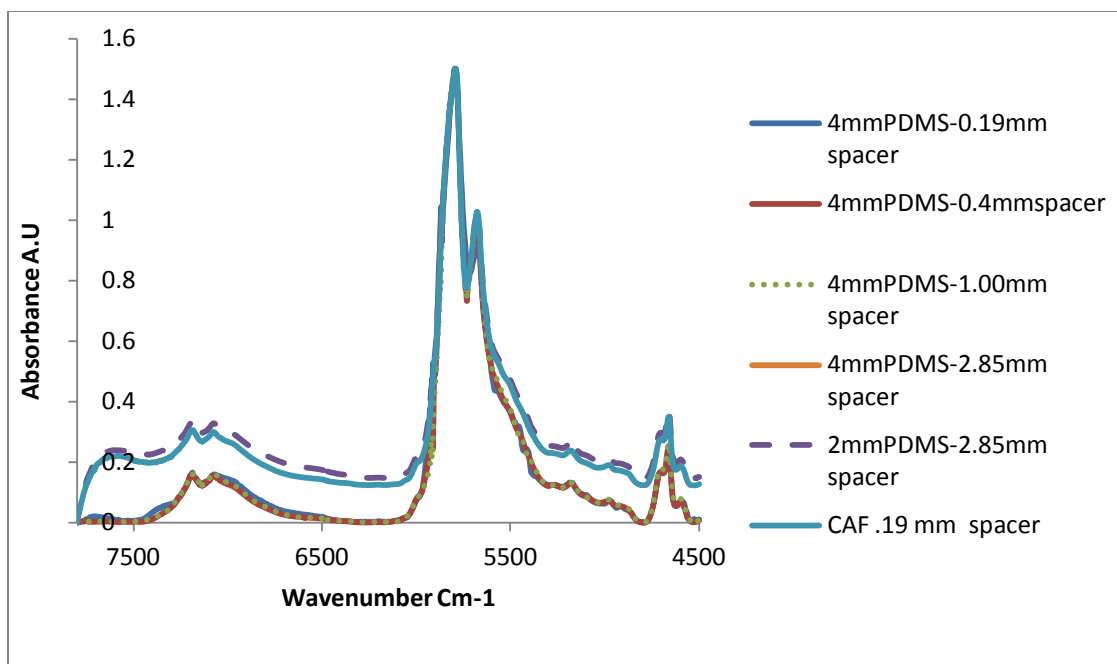
Figure 5.10: Comparative analysis of EVOO spectra in NIR -PDMS kits and CaF$_2$ kits

5.3.1 Results Summary

The results of the experiments have been summarized in the table 5.8 to understand the NIR Spectra of fatty acids in Olive Oil or the peaks for fatty acids in Olive oil introduced in the NIR region with CaF$_2$ kit and its comparison with the other PDMS kits.

5.4 Discussion of Results

Comparison of PDMS kit and CaF$_2$ kit and Analysis of the performance of both kits can be summarized as below

- PDMS kit introduces its own peaks in the region 5800 cm^{-1} to 5600 cm^{-1} .This masks the original olive oil peaks in the same region for small sample thickness like 100 µm.

- The peaks introduced by PDMS slowly disappear with the increase in sample size from about 100 μm to 2850 μm

- The same trend is noticed in 2X2mm and 2X4mm samples.

- At 2850 μm X 2mm the plot is closest to the characteristics presented by CaF_2 cell Kit.

- 4 mm X2850 μm provides comparable results, but with higher spacer thickness, these results can be improved.

Experiments for Relative Absorbance Comparison	Absorbance/Wave number(± 5 cm^{-1})				
	7185 (EVOO)	7078 (EVOO)	5793 (EVOO)	5678 (EVOO)	5870 (PDMS peaks)
LITERATURE [61]	0.24	0.24	1.50	0.9	NA
CaF$_2$ kit	0.3	0.29	1.50	1.03	NA
PDMS 4-190 kit	0.16	0.16	1.50	0.91	1.23
PDMS 4-400 kit	0.16	0.16	1.50	0.93	0.92
PDMS 4-1000 kit	0.16	0.16	1.50	1.02	0.77
PDMS 4-2850 kit	0.15	0.16	1.50	0.97	None
PDMS 2-100 kit	0.22	0.23	1.50	1.13	1.25
PDMS 2-190 kit	0.15	0.14	1.50	0.95	0.93
PDMS 2-2850 kit	0.33	0.33	1.50	1.03	None

Table 5.8: Comparison of the performance of CaF$_2$ Kit and PDMS Kits for EVOO peaks

5.4.1   Inference

The following points are inferred from the above summary

- There exists a Critical Volume Ratio(CVR) which is the minimum ratio of sample thickness(spacer thickness)/PDMS thickness(cumulative) which is needed for the kit to perform on par with a CaF_2 kit

- Identifying the CVR is crucial for any particular sample, CVR will vary for each sample and is a property of sample , if the absorbance values of Cell kit are fixed

- Qualitative spectrometry will require multiple trials to identify a CVR, but a quantitative spectrometer can identify the CVR in a single trial by prior calculations

- Lower the CVR, lesser the sample size required for optimum detection. The effect of prefabrication and post fabrication treatments (see section 4.1) affecting the CVR needs to be further investigated.

- There is a separate CVR for Mid IR spectroscopy and a separate CVR for NIR spectroscopy. CVRs for Mid IR spectroscopy could be typically lesser than CVRs for NIR spectroscopy , because of the fact that absorbencies are far stronger in Mid IR spectroscopy

5.5   Summary

In this chapter, an experimental approach to understand the utility of PDMS as a replacement window material for CaF_2 kit was pursued. Two different kits of PDMS were fabricated one with a 2mm slab thickness each (2 X 2mm) and other with a 4 mm slab thickness each (2X4 mm). Both these slabs were subjected to analysis with different sample volumes of EVOO. The 2X2 kit was subjected to samples with spacer thickness

of 100 µm, 190 µm and 2850 µm and the 2X4 kit was subjected to samples with 200 µm, 400 µm, 1000 µm and 2850 µm. Correspondence in peaks was observed for both the kits which were used for arriving at the proof of concept. A CVR of 1:20 (sample: PDMS thickness) has been arrived for EVOO.

The proof of concept being established, further trials can be conducted with different set of samples to generate a library of CVRs. The CVR established for EVOO in NIR for PDMS can be extrapolated for micro volume sample analysis. In the Mid IR region where PDMS has a narrow window of transmittance from wave numbers 2800 cm^{-1} to 2200 cm^{-1}, it can be used as a sample window for samples exhibiting characteristics in that region.

The CVR provides critical contribution in achieving the broad objective of fabricating a PDMS cell kit in lieu of the existing alkaline halide cell kit and enabling a microfluidic device.

CHAPTER 6.   CONCLUSION AND FUTUREWORK

6.1   Conclusion

In chapter 1, from a brief survey of the literature, the motivation and the objectives for the present work were defined. The motivation for this work is the need for a PDMS based micro device to facilitate low cost and rapid analysis in a FTIR spectrometer. Guided by these motivations, the broad objective of the thesis was defined so as to gain understanding about the optical characteristics of PDMS in an FTIR spectrometer and to understand the suitability of using PDMS as a window material in place of a CaF_2 cell. In order to achieve these objectives, the following tasks were designed and conducted as briefly summarized below.

In Chapter -2, experiments were designed to gain understanding of the design constraints introduced by the material selection (PDMS) and the inherent optical design as well as layout of the specific FTIR spectrometer (Spectrum BX™).The results of the experiments designed to extract these constraints which would be eventually used as design parameters for the desired PDMS Cell kit (device), were classified in to two categories of constraints (a) Constraints introduced by the material, (b) Constraints introduced by the FTIR spectrometer, Spectrum BX™. PDMS has higher transmittance in NIR and in Mid IR it introduces artifacts' which mask the peaks of any analyte. Also the effect of thickness on PDMS transmittance were identified, which showed that 4mm thick slabs of PDMS had lower transmittance compared to 1mm slabs. The design constraints introduced due to space available for placement of the device in the sample compartment and the effect of placing the device at different distances from the emitter were

understood, and it was found that the transmittance of the cell kit falls to about 50% at 60 mm from emitter and so it is ideal to place the device at the cell kit holder.

In Chapter-3, based on the understanding of the design parameters, a preliminary, tentative design for the device was arrived at and a suitable fabrication protocol was finalized. A high resolution transparency mask was printed, and an SU-8 mould was fabricated on a silicon wafer. The PDMS device was fabricated using soft lithography and bonded using uncured PDMS bonding technique. The device was subjected to preliminary testing with a solution of DIW. The results show close corroboration of the CaF_2 kit with the standard spectrum of DIW from NIST in the MIR region from about 3300 cm^{-1} to 3500 cm^{-1}. Also the results from the PDMS Kit match with that of the CaF_2 kit in the NIR region from about 7800 cm^{-1} to about 4500 cm^{-1}. Different techniques to improve the transmittance characteristics of PDMS in the MIR region are considered in Chapter- 4.

As a result of the non optimal performance of the device in the MIR region, few protocols common in published literature have been considered to effect a desired optical property modification of PDMS polymer in the MIR region in Chapter-4. Previous works suggest that certain treatments on PDMS polymer can affect its optical properties. These treatments have been classified as prefabrication and post fabrication treatments on the basis whether the treatment is carried out before or after the PDMS polymer fabrication process. In literature, certain prefabrication methodologies like using different curing agent ratios have shown an effect on optical transmittance on thin films of PDMS. Experiments have been designed to understand the viability of this approach and it has been found that as the thickness of the PDMS sample increases, the transmittance is not

widely affected by the change in the base: curing agent ratio of the polymer mix. Also a few experiment protocols involving heat treatment of the samples in an inert atmosphere were carried out. The results show that neither heat treatment nor base to curing agent ratio provided the desired effect in MIR transparency of PDMS. Further investigation with respect to changing chemical matrix of the polymer or other methods needs to be studied to improve the MIR transparency of the polymer without affecting its basic advantage which is rapid prototyping using soft lithography.

As a result of the inherent difficulties involved in enabling the MIR region in PDMS polymer through traditional optical transmittance modification approaches, experiments were done using Extra Virgin Olive Oil (EVOO), as their characteristic peaks are present in the NIR region, to establish a proof of concept in chapter- 5. The sample is investigated in the CaF_2 kit as well as the PDMS kit (2X2mm & 2X4mm). The peaks are plotted and correspondence studied. The proof of concept for the use of PDMS as a window material in the FTIR spectrometer is derived along with the concept of CVR. A CVR of 1:20 (sample: PDMS thickness) has been arrived for EVOO in the NIR region.

This concept can well be extended to the Mid IR region where PDMS has a transmittance window of 2800 cm^{-1} to 2200 cm^{-1} for samples exhibiting characteristics in those regions.

6.2   Contribution

The following summarizes the contribution from this work

- A preliminary understanding of design constraints of PDMS as an alternate window material in lieu of CaF_2.

- Established preliminary design, fabrication and testing protocols for PDMS micro device for replacing transmittance cell kit in a FTIR spectrometer.

- A brief study of approaches to enhance optical property of PDMS in Mid IR region has been attempted.

- A proof of concept on use of PDMS as a window material in NIR using EVOO as the analyte.

- A CVR has been arrived at for EVOO for use with PDMS base Cell kit, instead of the standard CaF_2 Cell kit.

6.3   Future Work

A preliminary understanding of the IR transmittance in the Mid IR and NIR regions has been achieved through a set of experiments. A proof of concept in the NIR region has been achieved with comparison of results in a CaF_2 kit and the PDMS kit. However, in the Mid IR region PDMS has shown artifacts because of it strong absorbance and the experiments in trying to improve its transmittance have not yielded consistent results. Following are areas which can be explored for future work.

1) Future work could be focused on devising innovative physical processes in order to improve the transmittance in the Mid IR.

2) Work needs to be done in customizing the device to adapt to biological applications including analysis of cell culture medium directly from a cell culture vessel and a micro incubator which has been described in detail in the thesis motivation (section 1.6).

3) In the NIR region, work can be pursued in refining the CVR concept with analysis of multiple samples from industrial, agricultural, food processing and pharmaceutical industries to prove the versatility of the device.

REFERENCES

(1) Smith C B. Quantitative Spectroscopy: Theory and Practice. First ed. California: Academic press; 2002.

(2) Everestinter Science Inc., Available at: http://www.everestinterscience.com /info/irtheory.htm. Accessed 04/08, 2012.

(3) Smith C B. Fundamentals of Fourier Transform Infrared Spectrscopy. Second ed. Florida: CRC Press; 2011.

(4) Stuart B. Infrared spectroscopy. : Wiley Online Library; 2004.

(5) Stuart B. Modern Infared Spectroscopy. First ed. Newyork: John Wiley & Sons; 1996.

(6) Jerry Workman Jr., Lois Weyer. Practical Guide to Interpretive Near- Infrared Spectrscopy. First ed. Florida: CRC Press; 2008.

(7) Analyical Spectroscopy. Available at: http://www.analyticalspectroscopy.net/ap3-8.htm. Accessed 04/08, 2012.

(8) Kemper MS, Magnuson EJ, Lowry SR, McCarthy WJ, Aksornkoae N, Watts DC, et al. Use of FT-NIR transmission spectroscopy for the quantitative analysis of an active ingredient in a translucent pharmaceutical topical gel formulation. The AAPS Journal 2001;3(3):81-85.

(9) Mao J, Xu J. Discrimination of herbal medicines by molecular spectroscopy and chemical pattern recognition. Spectrochimica Acta Part A: Molecular and Biomolecular Spectroscopy 2006;65(2):497-500.

(10) Dessipri E, Minopoulou E, Chryssikos GD, Gionis V, Paipetis A, Panayiotou C. Use of FT-NIR spectroscopy for on-line monitoring of formaldehyde-based resin synthesis. European polymer journal 2003;39(8):1533-1540.

(11) Ibarra JV, Munoz E, Moliner R. FTIR study of the evolution of coal structure during the coalification process. Org Geochem 1996;24(6-7):725-735.

(12) Jiang T, Xu K. FTIR study of ultradispersed diamond powder synthesized by explosive detonation. Carbon 1995;33(12):1663-1671.

(13) MacDonald H, Bedwell B, Gulari E. FTIR spectroscopy of microemulsion structure. Langmuir 1986;2(6):704-708.

(14) Maria SF, Russell LM, Turpin BJ, Porcja RJ. FTIR measurements of functional groups and organic mass in aerosol samples over the Caribbean. Atmos Environ 2002;36(33):5185-5196.

(15) Mendes LS, Oliveira FCC, Suarez PAZ, Rubim JC. Determination of ethanol in fuel ethanol and beverages by Fourier transform (FT)-near infrared and FT-Raman spectrometries. Anal Chim Acta 2003;493(2):219-231.

(16) Musto P, Martuscelli E, Ragosta G, Russo P. The curing process and moisture transport in a tetrafunctional epoxy resin as investigated by FT-NIR spectroscopy. High Perform Polymers 2000;12(1):155-168.

(17) Sorvaniemi J, Kinnunen A, Tsados A, Mälkki Y. Using partial least squares regression and multiplicative scatter correction for FT-NIR data evaluation of wheat flours. Lebensmittel-Wissenschaft und-Technologie 1993;26(3):251-258.

(18) Girolamo A, Lippolis V, Nordkvist E, Visconti A. Rapid and non-invasive analysis of deoxynivalenol in durum and common wheat by Fourier-Transform Near Infrared (FT-NIR) spectroscopy. Food Additives and Contaminants A 2009;26(6):907-917.

(19) Liu Y, Ying Y. Use of FT-NIR spectrometry in non-invasive measurements of internal quality of 'Fuji'apples. Postharvest Biol Technol 2005;37(1):65-71.

(20) Liu Y, Ying Y, Fu X, Lu H. Experiments on predicting sugar content in apples by FT-NIR technique. J Food Eng 2007;80(3):986-989.

(21) Liu Y, Ying Y, Yu H, Fu X. Comparison of the HPLC method and FT-NIR analysis for quantification of glucose, fructose, and sucrose in intact apple fruits. J Agric Food Chem 2006;54(8):2810-2815.

(22) Manley M, Van Zyl A, Wolf E. The evaluation of the applicability of Fourier transform near-infrared (FT-NIR) spectroscopy in the measurement of analytical parameters in must and wine. South African Journal for Enology and Viticulture 2001;22(2):93-100.

(23) Mlček J, Šustová K, Simeonovová J. Application of FT NIR spectroscopy in the determination of basic chemical composition of pork and beef. Czech J Anim Sci 2006;51:361-368.

(24) Rodriguez-Saona LE, Fry FS, McLaughlin MA, Calvey EM. Rapid analysis of sugars in fruit juices by FT-NIR spectroscopy. Carbohydr Res 2001;336(1):63-74.

(25) Sinija V, Mishra H. FT-NIR spectroscopy for caffeine estimation in instant green tea powder and granules. LWT-Food Science and Technology 2009;42(5):998-1002.

(26) Armenta S, Garrigues S, De la Guardia M. Determination of edible oil parameters by near infrared spectrometry. Anal Chim Acta 2007;596(2):330-337.

(27) Azizian H, Kramer JKG. A rapid method for the quantification of fatty acids in fats and oils with emphasis on trans fatty acids using Fourier transform near infrared spectroscopy (FT-NIR). Lipids 2005;40(8):855-867.

(28) Bendini A, Cerretani L, Di Virgilio F, Belloni P, Lercker G, Toschi TG. In‑process monitoring in industrial olive mill by means of FT-NIR. European Journal of Lipid Science and Technology 2007;109(5):498-504.

(29) Sinelli N, Cerretani L, Egidio VD, Bendini A, Casiraghi E. Application of near (NIR) infrared and mid (MIR) infrared spectroscopy as a rapid tool to classify extra virgin olive oil on the basis of fruity attribute intensity. Food Res Int 2010;43(1):369-375.

(30) Armenta S, Moros J, Garrigues S, De La Guardia M. The use of near-infrared spectrometry in the olive oil industry. Crit Rev Food Sci Nutr 2010;50(6):567-582.

(31) Kavdir I, Buyukcan MB, Lu R, Kocabiyik H, Seker M. Prediction of olive quality using FT-NIR spectroscopy in reflectance and transmittance modes. biosystems engineering 2009;103(3):304-312.

(32) Lerma-García M, Ramis-Ramos G, Herrero-Martínez J, Simó-Alfonso E. Authentication of extra virgin olive oils by Fourier-transform infrared spectroscopy. Food Chem 2010;118(1):78-83.

(33) Yang H, Irudayaraj J, Paradkar MM. Discriminant analysis of edible oils and fats by FTIR, FT-NIR and FT-Raman spectroscopy. Food Chem 2005;93(1):25-32.

(34) Galtier O, Dupuy N, Le Dréau Y, Ollivier D, Pinatel C, Kister J, et al. Geographic origins and compositions of virgin olive oils determined by chemometric analysis of NIR spectra. Anal Chim Acta 2007;595(1):136-144.

(35) Kasemsumran S, Kang N, Christy A, Ozaki Y. Partial Least Squares Processing of Near-Infrared Spectra for Discrimination and Quantification of Adulterated Olive Oils. Spectroscopy letters 2005;38(6):839-851.

(36) Duygu DY, Baykal T, Açikgöz İ, Yildiz K. Fourier Transform Infrared (FT-IR) Spectroscopy for Biological Studies (REVIEW). Gazi University Journal of Science 2010;22(3):117-121.

(37) Wood BR, Quinn MA, Burden FR, McNaughton D. An investigation into FTIR spectroscopy as a biodiagnostic tool for cervical cancer. Biospectroscopy 1996;2(3):143-153.

(38) Haris PI, Severcan F. FTIR spectroscopic characterization of protein structure in aqueous and non-aqueous media. J Molec Catal B 1999;7(1):207-221.

(39) Mariey L, Signolle J, Amiel C, Travert J. Discrimination, classification, identification of microorganisms using FTIR spectroscopy and chemometrics. Vibrational Spectroscopy 2001;26(2):151-159.

(40) Schmitt J, Beekes M, Brauer A, Udelhoven T, Lasch P, Naumann D. Identification of scrapie infection from blood serum by Fourier transform infrared spectroscopy. Anal Chem 2002;74(15):3865-3868.

(41) Fabian H, Lasch P, Naumann D. Analysis of biofluids in aqueous environment based on mid-infrared spectroscopy. J Biomed Opt 2005;10:031103.

(42) Mfoumou E. An Opto-Acoustic Approach to Biological Cell Proliferation Assessment. 2008.

(43) Bashir R. BioMEMS: state-of-the-art in detection, opportunities and prospects. Adv Drug Deliv Rev 2004;56(11):1565-1586.

(44) Fujii T. PDMS-based microfluidic devices for biomedical applications. Microelectronic Engineering 2002;61:907-914.

(45) James T, Mannoor MS, Ivanov DV. BioMEMS–Advancing the Frontiers of Medicine. Sensors 2008;8(9):6077-6107.

(46) Grayson ACR, Shawgo RS, Johnson AM, Flynn NT, Li Y, Cima MJ, et al. A BioMEMS review: MEMS technology for physiologically integrated devices. Proc IEEE 2004;92(1):6-21.

(47) Sasserath J, Fries D. Rapid Prototyping And Development Of Microfluidic And BioMEMS Devices. IVD Technology 2002;12.

(48) Ziaie B, Baldi A, Lei M, Gu Y, Siegel RA. Hard and soft micromachining for BioMEMS: review of techniques and examples of applications in microfluidics and drug delivery. Adv Drug Deliv Rev 2004;56(2):145-172.

(49) Liu C, Cui D, Chen X. Development of an integrated direct-contacting optical-fiber microchip with light-emitting diode-induced fluorescence detection. Journal of Chromatography A 2007;1170(1-2):101-106.

(50) Christen JB, Andreou AG. Design, Fabrication, and Testing of a Hybrid CMOS/PDMS Microsystem for Cell Culture and Incubation. Biomedical Circuits and Systems, IEEE Transactions on 2007;1(1):3-18.

(51) Franssila S. Introduction to microfabrication. : Wiley Online Library; 2004.

(52) Xia Y, Whitesides GM. Soft lithography. Annual review of materials science 1998;28(1):153-184.

(53) Wacker Inc. Available at: http://www.wacker.com/cms/en/products-markets/products/product.jsp?product=9499&country=CA&language=en Accessed April 29,2012

(54) Merschman SA, Lubbad SH, Tilotta DC. Poly (dimethylsiloxane) films as sorbents for solid-phase microextraction coupled with infrared spectroscopy. Journal of Chromatography A 1998;829(1):377-384.

(55) Chen K C, Wo A.M, Chen Y F. Transmission Spectrum of PDMS in 4-7micrometer Mid-IR Range for Characterisation of Protein Structure. NSTI 2006;Volume-2.

(56) Buffeteau T, Desbat B, Bokobza L. The use of near-infra-red spectroscopy coupled to the polarization modulation technique to investigate molecular orientation in uniaxially stretched polymers. Polymer 1995;36(22):4339-4343.

(57) Junkin M, Wong P. Probing cell migration in confined environments by plasma lithography. Biomaterials March 2011;Volume 32(Issue 7):1848–1855.

(58) Perkin Elmer. Spectrum BX Users Guide.

(59) Photolithography. Available at: http://tera.thoth.kr/blog/12742109. Accessed April 09, 2012.

(60) Dark and Light field Mask. Available at: http://www.cnf.cornell.edu/cnf_process_mask_patternprep.html. Accessed April 09, 2012.

(61) Michrochem MSDS. SU-8 2000 Permanent Epoxy Negative Photoresist.

(62) Eddings MA, Johnson MA, Gale BK. Determining the optimal PDMS–PDMS bonding technique for microfluidic devices. J Micromech Microengineering 2008;18:067001.

(63) NIST. Available at: http://webbook.nist.gov/cgi/cbook.cgi?ID=C7732185&Mask=80. Accessed April 9, 2012.

(64) Armani D, Liu C, Alum N. RE-CONFIGURABLE FLUID CIRCUITS BY PDMS ELASTOMER MICROMACHINING Twelfth IEEE International Conference on Micro Electro Mechanical Systems, 1999. MEMS '99. 1999(222 - 227).

(65) Mata A, Fleischman AJ, Roy S. Characterization of polydimethylsiloxane (PDMS) properties for biomedical micro/nanosystems. Biomed Microdevices 2005;7(4):281-293.

(66) Dow Corning Inc. Available at: http://www.dowcorning.com/content/publishedlit /Chapter12.pdf. Accessed April 9, 2012.

(67) Berdichevsky Y, Khandurina J, Guttman A, Loa Y H. UV/ozone modification of poly(dimethylsiloxane) microfluidic channels. Sensors and Actuators 2003;B(97 (2004)):402–408.

(68) Liu M, Sun J, Chen Q. Influences of heating temperature on mechanical properties of polydimethylsiloxane. Sensors and Actuators A: Physical 2009;151(1):42-45.

(69) Clarson S, Semlyen J. Studies of cyclic and linear poly (dimethyl-siloxanes): 21. High temperature thermal behaviour. Polymer 1986;27(1):91-95.

(70) Zhuang X, Qiang H, Zhang ZY, Zou MQ, Zhang XF. Quality analysis of olive oil and quantification detection of adulteration in olive oil by near-infrared spectrometry and chemometrics. Spectroscopy and Spectral Analysis 2010 Apr.;Apr(30(4)):933-6.